Atmospheric Chemistry of Traffic Related Compounds - Oxygenates and Aromatics

Platz, Jesper

Publication date:
2000

Document Version
Publisher's PDF, also known as Version of record

Risø-R-1170(EN)

Atmospheric Chemistry of Traffic Related Compounds

- Oxygenates and Aromatics -

Jesper Platz

Risø National Laboratory, Roskilde
January 2000

Abstract The atmospheric chemistry of dimethylether, dimethoxymethane, trimethoxymethane, cyclohexane, 1,4-dioxane, 1,3,5-trioxane and phenol have been studied in this work.

The present thesis gives an extended summary of nine papers given in Appendix A to Appendix I. Sections 1 to 3 contains Abstract, Danish summery, and Motivation. Section 4 describes the pulse radiolysis technique used at Risoe National Laboratory and the FTIR Smog-chamber technique used at Ford Motor Company. Sections 5 to 8 present results of absolute rate constants and UV absorption spectra obtained at Risoe. Sections 9 to 12 present results of relative rate constants and atmospheric degradations studies performed at Ford. Section 13 gives a conclusion. Some of the sections are in the following further described.

Section 5 reports rate constants for reactions between OH radicals and $CH_3OCH_2OCH_3$, $(CH_3O)_3CH$, 1,4-dioxane, and 1,3,5-trioxane and they are measured to $(4.9 \pm 1.9) \times 10^{-12}$, $(6.0 \pm 0.4) \times 10^{-12}$, $(11.6 \pm 0.8) \times 10^{-12}$, $(6.0 \pm 1.0) \times 10^{-12}$ cm^3 $molecule^{-1}$ s^{-1}, respectively. The obtained rate constants are 210-348% higher than expected using the Structure-Reactivity Relationship model suggested by Atkinson [1].

In section 6 UV absorption spectra of $(CH_3O)_2CHOCH_2(\bullet)$, $(CH_3O)_2CHOCH_2O_2(\bullet)$, c-$C_4H_7O_2(\bullet)$, (c-$C_4H_7O_2)O_2(\bullet)$, c-$C_3H_5O_3(\bullet)$, (c-$C_3H_5O_3)O_2(\bullet)$, c-$C_6H_{11}(\bullet)$, and c-$C_6H_{11}O_2(\bullet)$ radicals were recorded between (220-230) and (290-320) nm. They all show broad features with a typical maximum absorption cross section of approximately 6×10^{-18} cm^2 $molecule^{-1}$. UV absorption spectra of $C_6H_5(\bullet)$ and $C_6H_5O(\bullet)$ radicals were obtained between 220 - 575 nm and 220 - 400 nm, respectively. They both show a maximum absorption cross section of approximately 4×10^{-17} cm^2 $molecule^{-1}$ at approximately 245 nm.

In section 7 self-reactions and reactions with O_2 for $CH_3OCH_2(\bullet)$, $(CH_3O)_2CHOCH_2(\bullet)$, c-$C_4H_7O_2(\bullet)$, c-$C_3H_5O_3(\bullet)$, and c-$C_6H_{11}(\bullet)$ radicals were studied. Rate constants for the self-reactions are of the order of $3-4 \times 10^{-11}$ cm^3 $molecule^{-1}$ s^{-1}. This is approximately a factor of 4 higher than rate constants for reactions between the alkyl radicals and O_2. The reaction between $C_6H_5O(\bullet)$ radicals and O_2 is slow with an upper limit of 5×10^{-21} cm^3 $molecule^{-1}$ s^{-1}. Reaction between the $C_6H_5(\bullet)$ radical and NO show a rate constant of 2×10^{-11} cm^3 $molecule^{-1}$ s^{-1} where as reactions $C_6H_5O(\bullet)$ radicals and NO or NO_2 show rate constants of 2×10^{-11} and 2×10^{-12} cm^3 $molecule^{-1}$ s^{-1}, respectively.

In section 8 self-reactions of $(CH_3O)_2CHOCH_2O_2(\bullet)$, (c-$C_4H_7O_2)O_2(\bullet)$, and (c-$C_3H_5O_3)O_2(\bullet)$ radicals give rate constants which are a factor of 3 lower than self-reactions obtained for the corresponding alkyl radicals. Rate constants for the reactions between these alkyl peroxy radicals and NO or NO_2, together with the reactions between the c-$C_6H_{11}O_2(\bullet)$ radical and NO or NO_2 were reported. In all cases rate constants for NO_2 reactions are higher than the corresponding rate constants for NO reactions. Obtained rate constants were from $(9.5 \pm 1.5) \times 10^{-12}$ to $(1.3 \pm 0.3) \times 10^{-11}$ cm^3 $molecule^{-1}$ s^{-1}.

In section 9 a large number of relative rate constants with relation to experiments in the smog-chamber were reported.

In section 10 the atmospheric degradations of $CH_3OCH_2OCH_3$, $(CH_3O)_3CH$, c-C_6H_{12}, 1,4-dioxane, and 1,3,5-trioxane were studied. $CH_3OCH_2OCH_3$ give two major products, CH_3OCH_2OCHO and $CH_3OC(O)OCH_3$, arising from abstraction of H atoms placed at the primary and secondary carbon, respectively. $CH_3OC(O)OCH_3$ is the only product observed from $(CH_3O)_3CH$. The studies of 1,4-dioxane and 1,3,5-trioxane give only one product each $HC(O)OCH_2CH_2OCHO$ and $HC(O)OCH_2OCHO$, respectively.

Section 11 reports the atmospheric degradation of cyclohexane. The fate is competition between decomposition of the sixmembered ring and formation of cyclohexanone. The formation of cyclohexanone is a function of the O_2 concentration. At 1 atmosphere of air the yield of cyclohexanone is $39 \pm 3.9\%$ whereas $61 \pm 6.1\%$ of the oxidised cyclohexane decompose.

In section 12 the atmospheric fate of $C_6H_5O(\bullet)$ radical is reaction with NO or NO_2. The major product from the smog-chamber experiments is a $(C_6H_5O)_2$ compound. Using smog-chamber experiments, GC-MS, and quantum mechanical calculations of the structure of $(C_6H_5O)_2$ give that the formed $(C_6H_5O)_2$ is determined to be 4-phenoxyphenol.

ISBN 87-550-2673-7
ISBN 87-550-2674-5 (Internet)
ISSN ISSN 0106-2840

Information Service Department, Risø, 2000

Contents

Preface and Acknowledgement

The work in this thesis was performed Jan. 1996 - Jan. 1999 at Risoe National Laboratory, Denmark (24 months), and at the Science Research Laboratory at Ford Motor Company, Michigan, USA (7 months). The thesis includes kinetic of reactions involving dimethylether, dimethoxymethane, trimethoxymethane, 1,4-dioxane, 1,3,5-trioxane, cyclohexane, benzene, and phenol, and the atmospheric degradations of these compounds (except benzene) are studied. The results are obtained using a pulse radiolysis technique combined with UV-VIS absorption spectroscopy (Risoe) and a FTIR-smog chamber system (Ford).

During the period of this work I was lucky to collaborate with many excellent scientists and technicians from Russia, USA, and Europe. They all provided excellent help and great motivation during the work. Without this collaboration I would not be able to present this thesis. I am grateful for the help they provided. Especially I wish to thank Dr. Jens Sehested, my supervisor at Risoe National Laboratory Dr. Ole J. Nielsen, and my supervisor at Ford Motor Company Dr. Tim J. Wallington. Dr. Jens Sehested and Dr. Ole J. Nielsen introduced me to the pulse radiolysis system, during my M.Sc. work back in 1995. Their enthusiasm and always helpful manners have been outstanding. Dr. Tim J. Wallington taught me to operate the FTIR-smog chamber system. Dr. Tim J. Wallington has put his hole heart into the atmospheric science-group at Ford Motor Company. He has been an exceptional scientist to collaborate with, both during my stays at Ford, and also when the collaboration has been via fax, e-mail and phone. I also wish to thank him and his family for their great hospitality during my stays in USA (September 1996 and spring 1998). My supervisor at Odense University, Dr. Christian Lohse, has been a great help since 1994. He made the contact to Dr. Ole J. Nielsen. Through out the work Dr. Christian Lohse has supported me and I wish to thank him for his kindness. Humour and enthusiasm are keywords for all the people that have participated in The Risoe Group and I wish to thank Dr. Trine Møgelberg, Dr. Merete Bilde, Dr. Lene K. Christensen, and Thomas N. Stein for giving me a glorious time at Risoe.

I thank Dr. Trine Møgelberg and Dr. Jens Sehested for reading the proofs of this thesis.

I wish to thank Ford Motor Company and Risoe National Laboratory for financial support.

During my Ph.D. study my daughter Elisabeth and my wife Lene have been unbelievable by giving me lots of joy and support. Without their willingness to follow me to Ford Motor Company, USA, in the spring 1998 it would not have been possible for me to work in Dr. Tim J. Wallingtons group. During the hole period their patience have been outstanding.

Danish Summary

Atmosfærekemien af dimethylether, dimethoxymethan, trimethoxymethan, trimethoxymethan, cyclohexan, 1,4-dioxan, 1,3,5-trioxan og phenol er blevet studeret i dette arbejde.

Afhandlingen skal betragtes som et sammendrag af det egentlige Ph.D. arbejde. Arbejdet har resulteret i udgivelsen af ni artikler i internationale tidsskrifter. Appendix A til Appendix I indeholder disse ni artikler. Afsnittene 1 til 3 inderholder engelsk/dansk sammendrag af afhandlingen samt en motivation for Ph.D. projektet. Afsnit 4 beskriver puls radiolyse teknikken på Forskningscenter Risø samt FTIR Smog-kammer teknikken på Ford Motor Company. Afsnittene 5 til 8 er en præsentation af resultaterne af de absolutte hastighedskonstanter og UV absorption spektre der er bestemt på Risø. Afsnittene 9 til 12 præsenterer resultaterne for relative hastighedskonstanter og produktstudier udført på Ford. Afsnit 13 indeholder en konklusion. Et nærmere indhold af enkelte uddybes efterfølgende.

Afsnit 5 rapporterer hastighedskonstanter for reaktioner mellem OH radikalet og $CH_3OCH_2OCH_3$, $(CH_3O)_3CH$, 1,4-dioxan og 1,3,5-trioxan. Hastighedskonstanterne er fundet til $(4.9 \pm 1.9) \times 10^{-12}$, $(6.0 \pm 0.4) \times 10^{-12}$, $(11.6 \pm 0.8) \times 10^{-12}$, $(6.0 \pm 1.0) \times 10^{-12}$ cm^3 $molekyle^{-1}$ s^{-1}. De bestemte hastighedskonstanter ligger 210-348% højere en forventet når disse beregnes v.h.a. "Structure-Reactivity Relationship" modellen foreslået af Atkinson [1].

Afsnit 6 indeholder UV absorption spektre af $(CH_3O)_2CHOCH_2(\bullet)$, $(CH_3O)_2CHOCH_2O_2(\bullet)$, $c\text{-}C_4H_7O_2(\bullet)$, $(c\text{-}C_4H_7O_2)O_2(\bullet)$, $c\text{-}C_3H_5O_3(\bullet)$, $(c\text{-}C_3H_5O_3)O_2(\bullet)$, $c\text{-}C_6H_{11}(\bullet)$, og $c\text{-}C_6H_{11}O_2(\bullet)$ radikaler. Spektrene er optaget mellem (220-230) og (290-320) nm. De har alle brede absorptionsbånd typisk med et maximalt absorptionstværsnit på ca. 6×10^{-18} cm^2 $molekyle^{-1}$. UV absorption spektre af $C_6H_5(\bullet)$ og $C_6H_5O(\bullet)$ radikaler er optaget mellem henholdsvis 220 - 575 nm og 220 - 400 nm. De har begge et maximalt absorptionstværsnit på ca. 4×10^{-17} cm^2 $molekyle^{-1}$ ved omkring 245 nm.

Afsnit 7 rapporterer selv-reaktioner og reaktioner med O_2 for $CH_3OCH_2(\bullet)$, $(CH_3O)_2CHOCH_2(\bullet)$, $c\text{-}C_4H_7O_2(\bullet)$, $c\text{-}C_3H_5O_3(\bullet)$ og $c\text{-}C_6H_{11}(\bullet)$ radikaler. Hastighedskonstanter for selv-reaktionerne er 3-4 x 10^{-11} cm^3 $molecule^{-1}$ s^{-1}, hvilket er omkring 4 gange højere end hastighedskonstanterne for reaktioner mellem alkyl radikaler og O_2. Reaktionen mellem $C_6H_5O(\bullet)$ radikalet og O_2 er langsom med en øvre grænse på 5×10^{-21} cm^3 $molekyle^{-1}$ s^{-1}. Reaktion mellem $C_6H_5(\bullet)$ radikalet og NO har en hastighedskonstant 2×10^{-12} cm^3 $molekyle^{-1}$ s^{-1}, mens reaktioner mellem $C_6H_5O(\bullet)$ radikaler og NO eller NO_2 giver hastighedskonstanter på henholdsvis 2×10^{-11} og 2×10^{-12} cm^3 $molekyle^{-1}$ s^{-1}.

Afsnit 8 rapporterer selv-reaktioner af $(CH_3O)_2CHOCH_2O_2(\bullet)$, $(c\text{-}C_4H_7O_2)O_2(\bullet)$ og $(c\text{-}C_3H_5O_3)O_2(\bullet)$ radikaler. Hastighedskonstanterne er 3 gange lavere end selv-reaktionerne for de tilsvarende alkyl radikaler. Hastighedskonstanter for reaktioner mellem disse alkyl peroxy radikaler og NO eller NO_2 er bestemt tillige med reaktionerne mellem $c\text{-}C_6H_{11}O_2(\bullet)$ radikalet og NO eller NO_2. I alle tilfælde havde NO_2 reaktionen den højeste hastighedskonstant med værdier mellem $(9.5 \pm 1.5) \times 10^{-12}$ - $(1.3 \pm 0.3) \times 10^{-11}$ cm^3 $molecule^{-1}$ s^{-1}.

Afsnit 9 giver et stort antal relative hastighedskonstanter med relation til eksperimenterne i smog-kammeret på Ford.

Afsnit 10 beskriver den atmosfæriske nedbrydning af $CH_3OCH_2OCH_3$, $(CH_3O)_3CH$, $c\text{-}C_6H_{12}$, 1,4-dioxan og 1,3,5-trioxan. $CH_3OCH_2OCH_3$ giver to hovedprodukter CH_3OCH_2OCHO og $CH_3OC(O)OCH_3$ fra abstraktioner af H atomer fra henholdsvis det primære og det sekondære kulstof. $CH_3OC(O)OCH_3$ observeres som hovedprodukt fra nedbrydningen af $(CH_3O)_3CH$. 1,4-dioxan og 1,3,5-trioxan giver som hovedprodukt henholdsvis $HC(O)OCH_2CH_2OCHO$ og $HC(O)OCH_2OCHO$.

Afsnit 11 beskriver den atmosfæriske nedbrydning af cyclohexan. Nedbrydningen er en konkurrence mellem dekomponering og dannelsen af cyclohexanon. Dannelsen af cyclohexanon er en funktion af O_2 koncentrationen. I atmosfæren er udbyttet af cyclohexanon $39 \pm 3.9\%$ mens decomponeringen sker i et udbytte på $61 \pm 6.1\%$.

Afsnit 12 beskriver den atmosfæriske skæbne af $C_6H_5O(\bullet)$ radikalet der hovedsageligt er reaction med NO eller NO_2. Hovedproduktet i smog-kammer eksperimenterne var en $(C_6H_5O)_2$ forbindelse. V.h.a. smog-kammer forsøg, GC-MS, og kvantemekaniske af beregninger af strukturen af $(C_6H_5O)_2$ blev $(C_6H_5O)_2$ forbindelsen identificeret som 4-phenoxyphenol.

1 Motivation

1.1 The Global Climate

Is there evidence for global climate changes due to human impacts on the composition of the global atmosphere? If so - in what direction will these impacts change the global climate? Will the increased Greenhouse Effect cause an average global rise in the temperature? For several decades scientists have discussed and tried to give answers to these complex and serious questions. The scientific society has gathered lots of new information working in fields like for example ice cores and ocean sediments drillings, and atmospheric observations trying to shed light on these questions. The Greenhouse Effect is closely related to the atmospheric concentration of trace gases like CO_2. The CO_2 concentration has risen from a pre industrial level of approximately 280 ppm to a concentration of 360 ppm at the end of the millennium [2]. In their last report the Intergovernmental Panel of Climate Change (IPCC) has concluded that they saw evidence for a temperature rise caused by antropogenic activities [3]. This have led to international political concerns with respect to the global CO_2 emission. There are ongoing international attempts to control the CO_2 emission - latest in Kyoto, Japan, 1997 and in Buenos Aires, Argentina, 1998. In spite of these efforts, no binding international protocol has yet been achieved.

1.2 Traffic Related CO_2 Emission

Traffic is an essential source of the CO_2 emission to the atmosphere. 20% of the CO_2 emission in Denmark is emitted from domestic transport [4]. The lack of international agreements on CO_2 emission does not mean that there will be no restrictions on a more regional scale. For example, the European Commission has made an agreement with the European car industry to raise the energy efficiency of cars from an average of 12.7 km/l in 1995 to an average of 20 km/l before the year 2010. The energy efficiency of diesel based engines is approximately 15-20% higher than petrol based engines. A method of lowering the CO_2 emission from traffic is to switch from petrol to diesel based engines. In general diesel engines have higher particle and NO_x emissions than petrol engines. Some alternative diesel fuels produce less particles and less NO_x emissions and they have been investigated for years now. In 1995 the Danish company Haldor Topsoe and the American company Amoco proposed dimethylether, CH_3OCH_3, as a diesel substitute [5]. CH_3OCH_3 have several properties which makes it an attractive diesel fuel, see Appendix A. However CH_3OCH_3 boils at -25° C at 1 atm total pressure which make it difficult to handle using the conventional distribution net.

1.3 Collaboration Between Ford Motor Company and Risoe National Laboratory

Liquid ethers have become an interesting group of compounds suggested as diesel fuel alternatives and additives. A collaborative project between Ford Motor Company and Risoe National Laboratory, concerning the atmospheric chemistry of liquid ethers, was established in 1995. The aim of the project was to gather kinetic and atmospheric degradation data of ethers in general. Aromatic compounds is an other important class of traffic related chemicals and it was decided to incorporate benzene and phenol into this project.

My Ph.D. work was a part of this collaboration. The work was performed at Ford Motor Company (Michigan, USA) and at Risoe National Laboratory (Denmark). The work was performed in the period January 1996 to January 1999 under supervision of my supervisors Dr. O. J. Nielsen (Risoe), Dr. C. Lohse (Odense University), and Dr. T. J. Wallington (Ford). Obtained results are reported in nine papers published in international journals. They are presented in Appendix A to Appendix I. The aim of this thesis is to present a summary of these nine papers to give the reader a general view of the work. It should be mentioned here that only a few results from Appendix A and Appendix H are given in this report.

2 Experimental Setups at Risoe and Ford

At Risoe a pulse radiolysis system coupled with UV-VIS spectroscopy is used to obtain kinetic data and UV-VIS absorption spectra. At Ford a FTIR-smog chamber system is used to detect atmospheric degradation products, and to determine relative rate constants for reactions between organic compounds and Cl atoms or OH radicals. These experimental systems have been used intensively for decades and they are both described in details in the literature [6, 7, 8, 9]. The aim of this section is to give a short introduction of the Risoe and Ford setups.

Unless otherwise stated all experiments were performed at 296 ± 3 K and all uncertainties are two standard deviations. Standard error propagation methods were used where appropriate.

2.1 Pulse Radiolysis Experiments at Risoe

Pulse radiolysis setup

Figure **1** shows the pulse radiolysis system at Risoe National Laboratory. A Febetron 705 field emission accelerator is used to initiate gas phase reactions in a 1 litre stainless steel reactor. The Febetron delivers a 30 ns pulse of 2 MeV electrons. Interaction between electrons and the bath gas in the reactor, SF_6 or Argon, produce F atoms or exited Ar atoms (Ar*). In this work F atoms, Cl atoms or OH radicals were used to initiate gas phase reactions of organic compounds. These species were formed via the following reactions:

$$SF_6 \xrightarrow{2\ \text{MeV}\ e^-} F + \text{products} \qquad \textit{(1)}$$

$$F + HCl \longrightarrow HF + Cl \qquad \textit{(2)}$$

$$Ar \xrightarrow{2\ \text{MeV}\ e^-} Ar^* \qquad \textit{(3)}$$

$$Ar^* + H_2O \longrightarrow OH + H + Ar \qquad \textit{(4)}$$

At full radiolysis dose and a total pressure of 1 bar of SF_6 a yield of approximately 3×10^{15} molecule cm^{-3} F atoms is obtained. Pulse radiolysis (full dose) of a mixture of 15 mbar H_2O and 995 mbar Ar give an OH concentration of approximately 5×10^{13} molecule cm^{-3}. The radiolysis dose can be varied by insertion of stainless steel attenuators between the Febetron and the reactor. In this work delivered doses are given relative to the full dose. A gas inlet system, with five separate inlets, and the reactor were evaporated by a Alcatel 2008 A pump and a Varian Turbo-V 70 pump. The two pumps were controlled by a MKS Baratron 170 absolute membrane manometer and a Balzer TGP 306 manometer with detection limits of 10^{-2} and 10^{-4} mbar, respectively. A pulsed 150 W xenon arc lamp placed outside the reactor provided the analysing light. Three white type mirrors inside the reactor allows the path length of the analysing light to be 40, 80, 120, 160 or 200 cm.

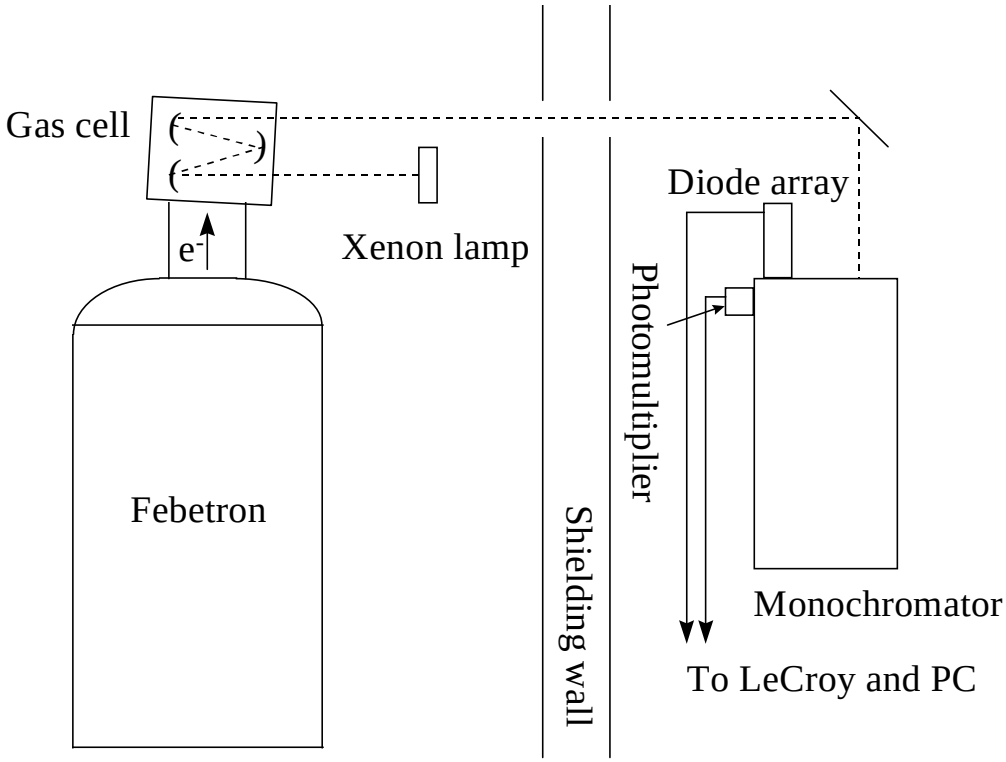

Figure 1. Pulse radiolysis setup at Risoe National Laboratory, Roskilde, Denmark.

Suprasil lenses are used to guide the analysing light from the xenon arc lamp to a McPherson grating monocromator with a focal length of 1 meter. Two different gratings, 1200 and 150 lines/mm, were used in this work, with optical resolutions of 0.8 and 6.4 nm/mm slit, respectively. Leaving the monocromator the analysing light was detected by a Hamamatsu photomultiplier or a OMA II diode array, digitised and transferred to a conventional PC. A combination of the 1200 lines/mm grating and the photomultiplier was used when time dependent absorption transients were obtained. The 150 lines/mm grating gives a optical window of approximately 100 nm. A combination of the 150 lines/mm grating and the diode array was used when UV-VIS absorption spectra were obtained.

Pulse radiolysis data handling

All obtained data are handled and stored on a conventional PC. First order rate constants and half lives are derived from three parametre fits to experimentally obtained absorption transients (formation or decay) using the following expression:

$$A(t) = (A_0 - A_\infty)\, exp(-k^{1st} t) + A_\infty \qquad (eq.\mathbf{1})$$

where A(t) is the observed absorbance at time t, A_0 is the absorbance at zero time, A_∞ is the absorbance at infinite time and k^{1st} is the first order rate constant. Second order decays from self-reactions of alkyl and alkyl peroxy radicals were obtained from fits using the following second order expression:

$$A(t) = (A_0 - A_\infty)/(1 + 2k^{2nd}(A_0 - A_\infty)t) + A_\infty \qquad (eq.\mathbf{2})$$

where k^{2nd} is the second order rate constant. Reported second order rate constants for self-reactions of alkyl peroxy radicals are reported to be observed rate constants because of potential influence from secondary chemistry.

Two computer programs, Chemsimul [10] and Acuchem [11], were used to provide numerical solutions to sets of differential equations of complex chemical systems. Concepts like lifetime and half life are used in this work. Lifetime is defined as the time for the concentration of a species to reach 1/e of the species initial concentration. Half life is defined as the time for the concentration of a species to reach half the concentration of the species initial concentration. For first order reactions the lifetime is $1/k^{1st}$ and the half life is $\ln 2/k^{1st}$. For second order reactions the half life is $1/2k^{2nd}[species]_0$, where $[species]_0$ is the initial concentration of the species.

Uncertainties associated with pulse radiolysis experiments

A number of possible complications such as formation of SF_5 radicals (formed via reaction (**1**)), wall reactions, and inhomogeneity of the electron beam in the reactor have earlier been discussed by Markert [12], Ellerman [6], and Sehested [7]. They find experimental uncertainties of a few percent due to these complications. These uncertainties lies within a typical experimental uncertainty of 10%. Other experimental complications can arise from small amounts of impurities in used chemicals, scattered light, and measured concentrations when small amounts of compounds are used.

2.2 FTIR-Smog Chamber Experiments at Ford Motor Company

FTIR-smog chamber setup

Figure **2** shows the FTIR-smog chamber setup at Ford Motor Company. The setup consist mainly of three parts; a gas handling system, a 2 m long and 140 litre Pyrex reaction chamber, and a

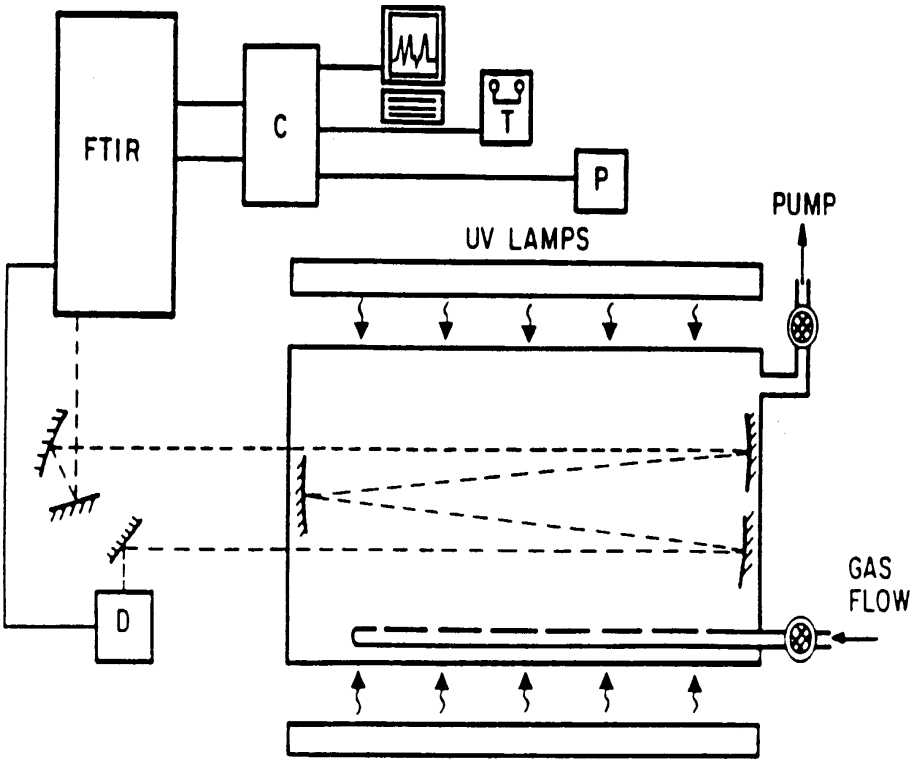

Figure 2. FTIR-Smog chamber setup at Ford Motor Company, Detroit, USA.

conventional FTIR detection system. The gas handling system consist of Pyrex lines and bulbs. It is pumped by a Franklin Electric (Model: 10 91 045 400) pump and controlled by a Baraton Type 122A absolute membrane manometer with a resolution of 1 x 10^{-3} Torr. Cl atoms and OH radicals initiate the gas phase reactions in the reaction chamber. The reaction chamber is surrounded by 22 GTE F40BLB fluorescent blacklamps to provide the light for the photochemical formation of Cl atoms or OH radicals via the following reactions:

$$Cl_2 \xrightarrow{h\nu} 2\,Cl \qquad (5)$$

$$CH_3ONO \xrightarrow{h\nu} CH_3O\bullet + NO \qquad (6)$$

$$CH_3O\bullet + O_2 \longrightarrow CH_2O + HO_2 \qquad (7)$$

$$HO_2 + NO \longrightarrow OH + NO_2 \qquad (8)$$

The path length of the analysing light in the reaction chamber is 28 m. The FTIR spectrometer (Mattson Instruments Inc. Sirius 100) operates with a spectral resolution of 0.25 cm^{-1}. Infrared spectra were derived from 32 co-added interferrograms, which gives a recording time of approximately 1.5 min. Obtained spectra were handled on a conventional PC. The setup can operate at a total pressure up to 760 Torr.

Uncertainties associated with the FTIR-smog chamber experiments

Obtained FTIR spectra were handled and stored on a conventional PC. The PC program WinFirst version 3.1 by Mattson Instruments was used to process the obtained spectra. In all cases, measured features were less than 0.7 absorption units and linearity between concentration and absorption was achieved. In each experiment complications due to photolysis and dark reactions in the cell were tested. Corrections to obtained data were made when necessary. In all cases potential uncertainties were estimated to be less than 10%.

3 Reactions Between OH Radicals and Ethers

3.1 Oxidation of Organic Compounds in the Troposphere

The majority of organic compounds released into the troposphere are initially oxidised through reaction with OH radicals [13] as shown in reaction (**9**).

$$RH + OH \longrightarrow R\bullet + H_2O \qquad (9)$$

Reactions between OH radicals and organic compounds have been studied for more than three decades to obtain the rate constants for this type of gas phase reactions [14]. OH rate constants have been measured using both absolute- and relative experimental techniques such as LP-LIF (Laser Photolysis - Laser Induced Fluorescence), FP-RF (Flash Photolysis – Resonance Fluorescence) PR-UV (Pulse Radiolysis – UV absorption) and RR (Relative Rate). Kwok and Atkinson have developed a Structure-Reactivity Relationship model (SAR) by using approximately 500 gas phase OH rate constants [1]. Approximately 90% of the estimated rate constants (using the SAR model) differs by less than a factor of two from the experimental obtained rate constants. Large disagreements between calculated and experimental rate constants were observed for halocarbons and polyethers. Few previous studies of polyethers and cyclopolyethers have been reported in the literature. A goal for this work was to measure rate constants for reactions between OH radicals and $CH_3OCH_2OCH_3$, $(CH_3O)_3CH$, 1,4-dioxane, and 1,3,5-trioxane. At Risoe the absolute rate constants were measured directly while at Ford a relative rate technique was used. Some of the rate constants obtained using the pulse radiolysis technique are still unpublished and the experiments will shortly be described here. Obtained rate constants using the relative rate experiments are described in Appendix B, C, and D.

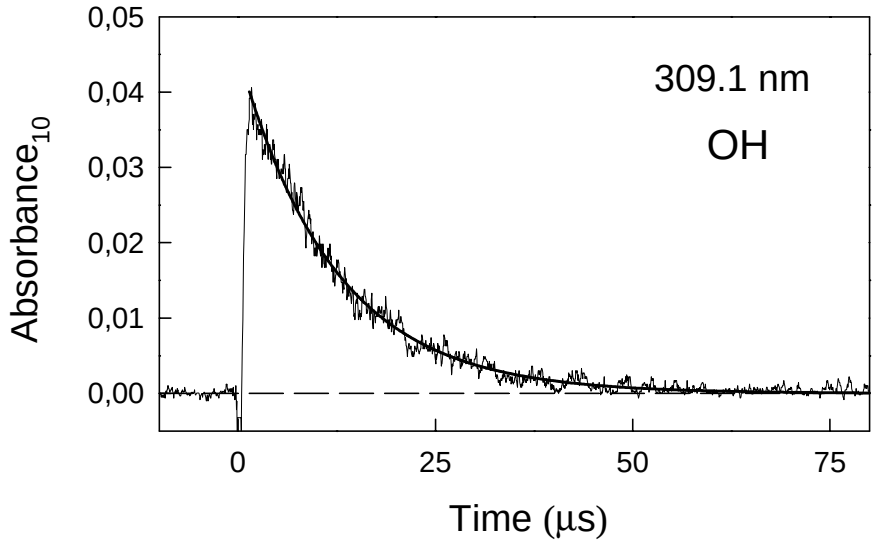

Figure 3. Transient absorbance at 309.1 nm following the pulsed radiolysis (maximum dose) of a mixture of 0.64 mbar of 1,3,5-trioxane, 13 mbar of H_2O, and 986 mbar of Ar. The UV path length was 120 cm and the temperature was 296 ± 2 K. The smooth line is a first-order decay fit (eq.1) to the experimental data.

3.2 OH Rate Constants Obtained at Risoe

Absolute rate constants for reactions between OH radicals and organic compounds have been studied extensively in the laboratory at Risoe using the pulse radiolysis technique [15,16,17]. Some of the results presented in this work are unpublished data. These unpublished experiments will in the following be described shortly using 1,3,5-trioxane as an example. Following pulsed radiolysis of a mixture of [1,3,5-trioxane] = 0.64 mbar, [H_2O] = 13.0 mbar, and [Ar] = 986 mbar at 309.1 nm a rapid rise in absorption followed by a slower decay was observed as shown in Figure **3**. The observed rise in absorption is due to formation of OH radicals via reaction (**4**). The rise is followed by a first order decay due to reaction between OH radicals and 1,3,5-trioxane, reaction (**10**).

$$Ar \xrightarrow{2\ MeV\ e^-} Ar^* \qquad \textit{(3)}$$

$$Ar^* + H_2O \longrightarrow OH + H + Ar \qquad \textit{(4)}$$

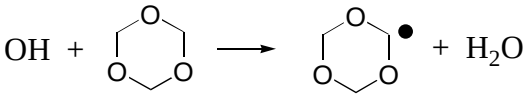

(10)

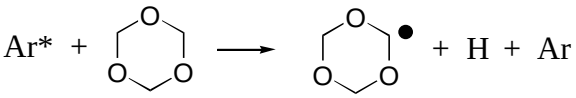

(11)

Ar* denotes metastable Argon atoms. To work under pseudo first order conditions with respect to OH radicals the 1,3,5-trioxane concentrations were kept at least 10 times that of OH radicals. To minimize interaction of Ar* with the 1,3,5-trioxane (reaction (**11**)) the H_2O concentrations were at least 10 times that of the 1,3,5-trioxane concentration. The decay shown in Figure **3** was fitted by a first order expression (eq.1) using a first order rate constant of 8.58 x 10^4 s^{-1}. Using different concentrations of 1,3,5-trioxane, transients were observed all showing different first order decays, which gave a series of first order rate constants. Similar experiments were performed for $(CH_3O)_3CH$ and 1,4-dioxane. Obtained first order rate constants were plotted as a function of the initial $(CH_3O)_3CH$, 1,4-dioxane, and 1,3,5-trioxane concentrations, respectively, as shown in Figure **4**. From linear least squares regression fits to the data in Figure **4** pseudo first order rate constants for the reaction between OH radicals and $(CH_3O)_3CH$, 1,4-dioxane, or 1,3,5-trioxane were obtained. All obtained results are shown in Table **1**. To avoid complication using this method, it is necessary that the formed alkyl radical in reaction (**9**) has a negligible absorption cross section compared to the absorption cross section of the OH radical at 309.1 nm. The formed alkyl radicals derived from reaction between OH radicals and $CH_3OCH_2OCH_3$ have a considerable absorption cross section at 309.1 nm and an alternative method was used to measure the rate constant between OH radicals and $CH_3OCH_2OCH_3$. This experiment was done at 280 nm where the absorption cross section of the OH radical is negligible, see Appendix B for details.

3.3 Atmospheric Lifetimes

The atmospheric lifetime of a compound with respect to OH radical oxidation is defined as $1/k_{compound+OH}[OH]$, where $k_{compound+OH}$ is the first order rate constant for the reaction between a compound and the OH radical, and [OH] is the global OH radical concentration. While the OH radical concentration in the atmosphere varies with location, time of day, season, and meteorological conditions, a reasonable 24 hour global average is (0.5-1.0) x 10^6 cm^{-3} [18, 19, 20]. Using an average

rate constant, calculated from the rate constants given in Table **1**, and a chosen OH concentration of 1 x 10^6 molecule cm^{-3}, atmospheric lifetimes between 25-94 hours were obtained for CH_3OCH_3, $CH_3OCH_2OCH_3$, $(CH_3O)_3CH$, 1,4-dioxane, and 1,3,5-trioxane, respectively, see Table **1**.

3.4 Comparison of OH Rate Constants for Polyethers

As shown in Table **1** different techniques have been used to obtain OH rate constants for CH_3OCH_3, $CH_3OCH_2OCH_3$, $(CH_3O)_3CH$, 1,4-dioxane, and 1,3,5-trioxane. No previous literature value was found for rate constant of the reaction between OH radicals and $(CH_3O)_3CH$.

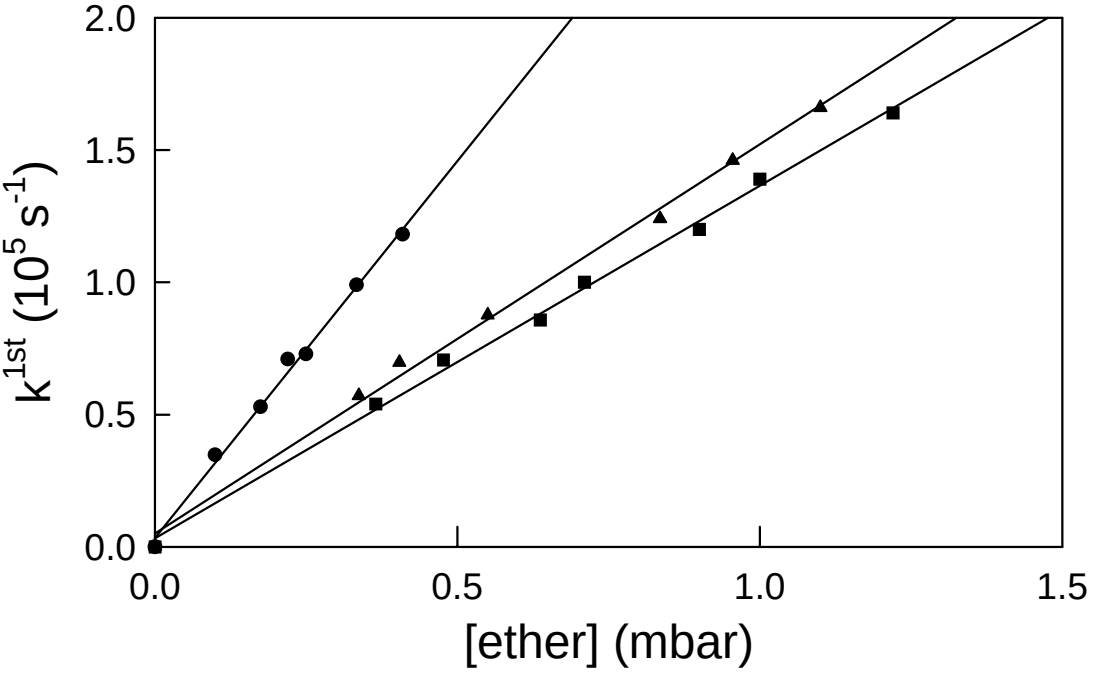

Figure 4. Pseudo first-order rate constants for reaction between OH radicals and 1,4-dioxane (circles), 1,3,5-trioxane (squares), or $(CH_3O)_3CH$ (triangles), following pulse radiolysis of mixtures of (1,4-dioxane, 1,3,5-trioxane or $(CH_3O)_3CH$)/H_2O/Ar. The monitoring wavelength was 309.1 nm and maximum radiolysis dose was used.

To compare the rate constants given in Table **1** average rate constants, with error limits that encompasses the extremes of the range, were calculated for each reaction using the data in Table **1**. Obtained values are $k_{OH+CH3OCH3}$ = (3.0 ± 0.9), $k_{OH+CH3OCH2OCH3}$ = (4.9 ± 1.5), $k_{OH+1,4\text{-dioxane}}$ = (11.2 ± 2.2), and $k_{OH+1,3,5\text{-trioxane}}$ = (5.9 ± 1.1) all in units of 10^{-12} cm^3 $molecule^{-1}$ s^{-1}. The uncertainties of these average rate constants are 19-30%. Calculating these rate constants using the SAR method given by Kwok and Atkinson [1] gives an overestimation of 210-348% for $(CH_3O)_3CH$, $CH_3OCH_2OCH_3$, 1,4-dioxane, and 1,3,5-trioxane compared to the obtained average values. The OH rate constant for CH_3OCH_3 was calculated to be 24% higher. Dagaut *et al.* [21] and Porter *et al.* [22] have in light of the discrepancy between the calculated SAR and the experimental obtained rate constants for polyethers and polyhydroxyethers developed the Group Reactivity (GR) model. The GR model can be used to calculate rate constants for reactions between OH radicals and polyether, polyhydroxy and polyhydroxyether compounds. The GR model predicts the rate constants better but there are still great differences between the calculated and the experimental values. An example is $k_{OH+1,4\text{-dioxane}}$ there is overestimated by 286%. The conclusion is that the understanding of these OH radical reactions still is incomplete. More work both experimentally and theoretically needs to be done if the final goal is good theoretical predictions of OH radical rate constants for this group of compounds.

Table 1. Gas phase rate constants for reactions between OH radicals and five different ethers measured at 295 ± 2 K and 1 atm. total pressure. Lifetimes are calculated using an average of the listed rate constants for each reaction and [OH] = 1 x 10^6 molecule cm^{-3}. a = 346 ± 3 K. App. = Appendix.

Compounds	Rate Constant (10^{-12} $cm^3 molecule^{-1} s^{-1}$)	Lifetime (hours)	Technique	Reference
CH_3OCH_3	3.5 ± 0.4	94	FP-RF	Perry *et al*. [23]
	3.0 ± 0.1		LP-LIF	Tully *et al*. [24]
	2.49 ± 0.2		FP-RF	Wallington *et al*.[25]
	2.82 ± 0.3		PR-UV	This work unpub.
$CH_3OCH_2OCH_3$	5.3 ± 1.0	57	RR	This work [App.B]
	4.6 ± 1.6 [a]		PR-UV	This work [App.B]
	4.9 ± 0.8		RR	Porter *et al*.[26]
	4.6 ± 0.1		PLP-LIF	Porter *et al*.[26]
$(CH_3O)_3CH$	6.0 ± 0.4	46	PR-UV	This work unpub.
Dioxane	11.6 ± 0.8	25	PR-UV	This work unpub.
	10.9 ± 0.5		FP-RF	Dagaut *et al*. [27]
	9.7 ± 0.7		RR	Porter *et al*.[26]
	12.6 ± 0.3		PLP-LIF	Porter *et al*.[26]
Trioxane	6.0 ± 1.0	47	RR	This work[App.D]
	5.4 ± 0.3		PR-UV	This work unpub.
	6.4 ± 0.2		PR-UV	Zabarnick *et al*.[28]

4 UV Absorption Spectra of Alkyl and Alkyl Peroxy Radicals

4.1 UV Absorption Spectra of Alkyl Radicals

UV absorption spectra of $(CH_3O)_2CHOCH_2(\bullet)$, c-$C_4H_7O_2(\bullet)$, and c-$C_3H_5O_3(\bullet)$ radicals.

UV absorption spectra of $(CH_3O)_2CHOCH_2(\bullet)$, c-$C_4H_7O_2(\bullet)$, and c-$C_3H_5O_3(\bullet)$ radicals were recorded in the range 220-320 nm using a OMA II diode array. The radicals were formed via reaction (**12**).

$$F + RORH \longrightarrow ROR\bullet + HF \qquad (12)$$

By using Lambert Beer´s law, equation (**eq.3**), it is possible to obtain the absolute absorption cross section (σ) in units of cm^2 $molecule^{-1}$ from the recorded absorbance.

$$A = l\,[x]\,\sigma \qquad (eq.3)$$

where A is the recorded absorbance, l is the path length of the analysis light in the reactor, [x] is the concentration of the radical species, and σ is the absorption cross section. To record the UV absorption spectrum of a specific alkyl radical, it is necessary to work under conditions where a known F atom concentration is converted stoichiometrically into alkyl radicals via reaction (**12**). Therefore the experimental conditions must be designed so that complications from second order radical-radical reactions such as reactions (**13**) and (**14**) are minimised. To find the optimal F atom concentration the maximum absorption of alkyl radicals, formed via reaction (**12**), needs to be measured as a function of the relative dose of F atoms. The results are shown in Figure **5**A. As seen from Figure **5**A there is a linear correlation between absorption and doses less than 42% of full dose, which gives that there is no complications from radical-radical reactions using less than 42% of full dose.

$$F + ROR\bullet \longrightarrow \text{products} \qquad (13)$$

$$RORO_2\bullet + RORO_2\bullet \longrightarrow \text{products} \qquad (14)$$

From the slopes of linear least squares regression fits to the low dose data in Figure **5**A absolute absorption cross sections at 250 nm were determine. Absorption cross sections were derived for $(CH_3O)_2CHOCH_2(\bullet)$, c-$C_4H_7O_2(\bullet)$, and c-$C_3H_5O_3(\bullet)$ radicals. Absolute absorption cross sections obtained in this work are listed in Table **2**. Using the obtained absolute absorption cross sections it is possible to scale the UV absorption spectra recorded by the OMA II diode array. Hereby the absolute UV absorption spectra are obtained. The UV absorption spectra are shown in Figure **6**. There is no UV absorption spectra of $(CH_3O)_2CHOCH_2(\bullet)$, c-$C_4H_7O_2(\bullet)$, and c-$C_3H_5O_3(\bullet)$ radicals reported in the literature to compare with the spectra shown in Figure **6**.

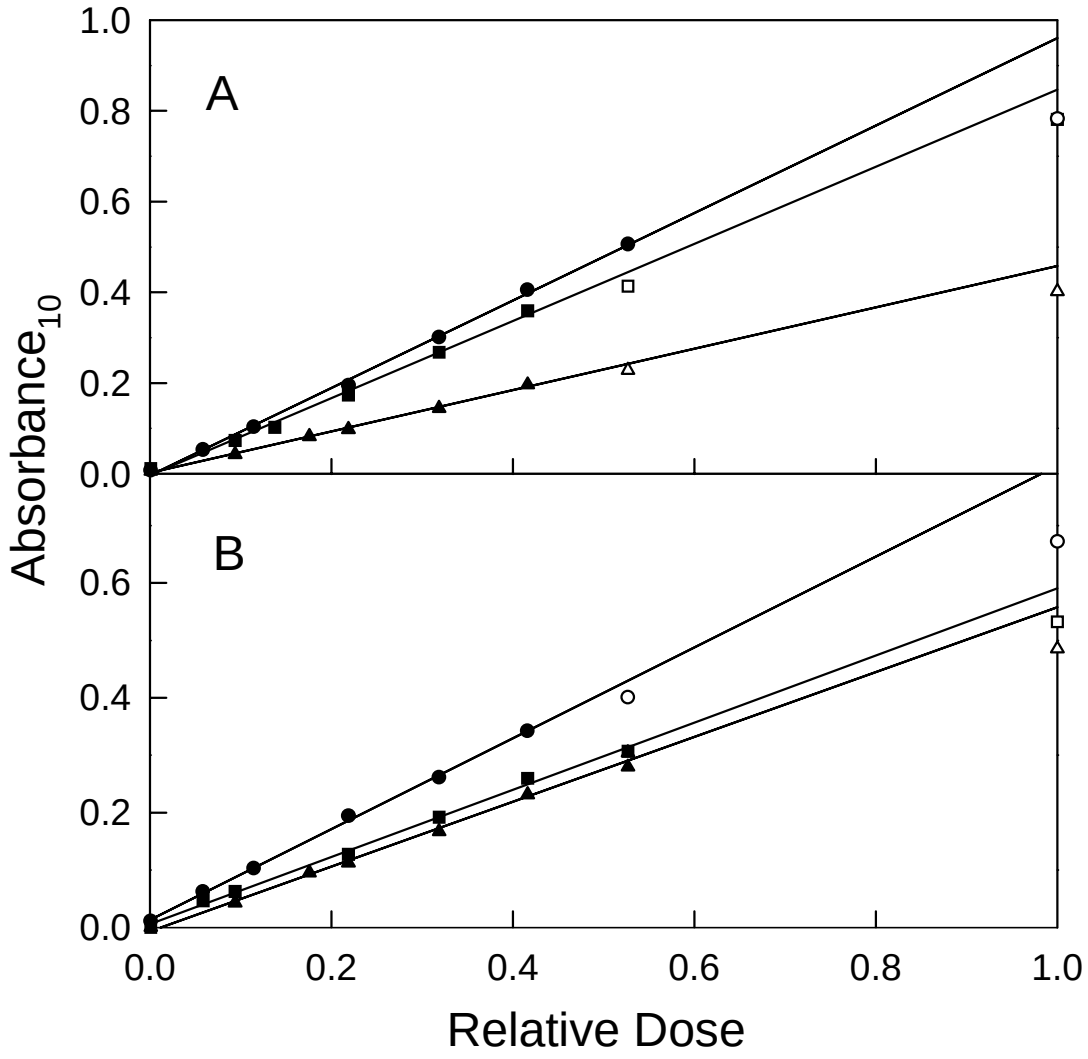

Figure 5. (A) Maximum transient absorbance at 250 nm following the pulse radiolysis of mixtures of 3 mbar 1,4-dioxane (circles), 3 mbar 1,3,5-trioxane (squares), or 5 mbar $(CH_3O)_3CH$ at 1000 mbar total pressure with SF_6 versus the radiolysis dose.
(B) Maximum transient absorbance at 250 nm (1,4-dioxane 240 nm) following the pulse radiolysis of mixtures of 3 mbar 1,4-dioxane and 20 mbar O_2 (circles), 3 mbar 1,3,5-trioxane and 40 mbar O_2 (squares), or 5 mbar $(CH_3O)_3CH$ and 20 mbar O_2 at 1000 mbar total pressure with SF_6 versus the radiolysis dose. The solid lines in A and B are linear least squares regression fits to the low dose data (solid symbols).

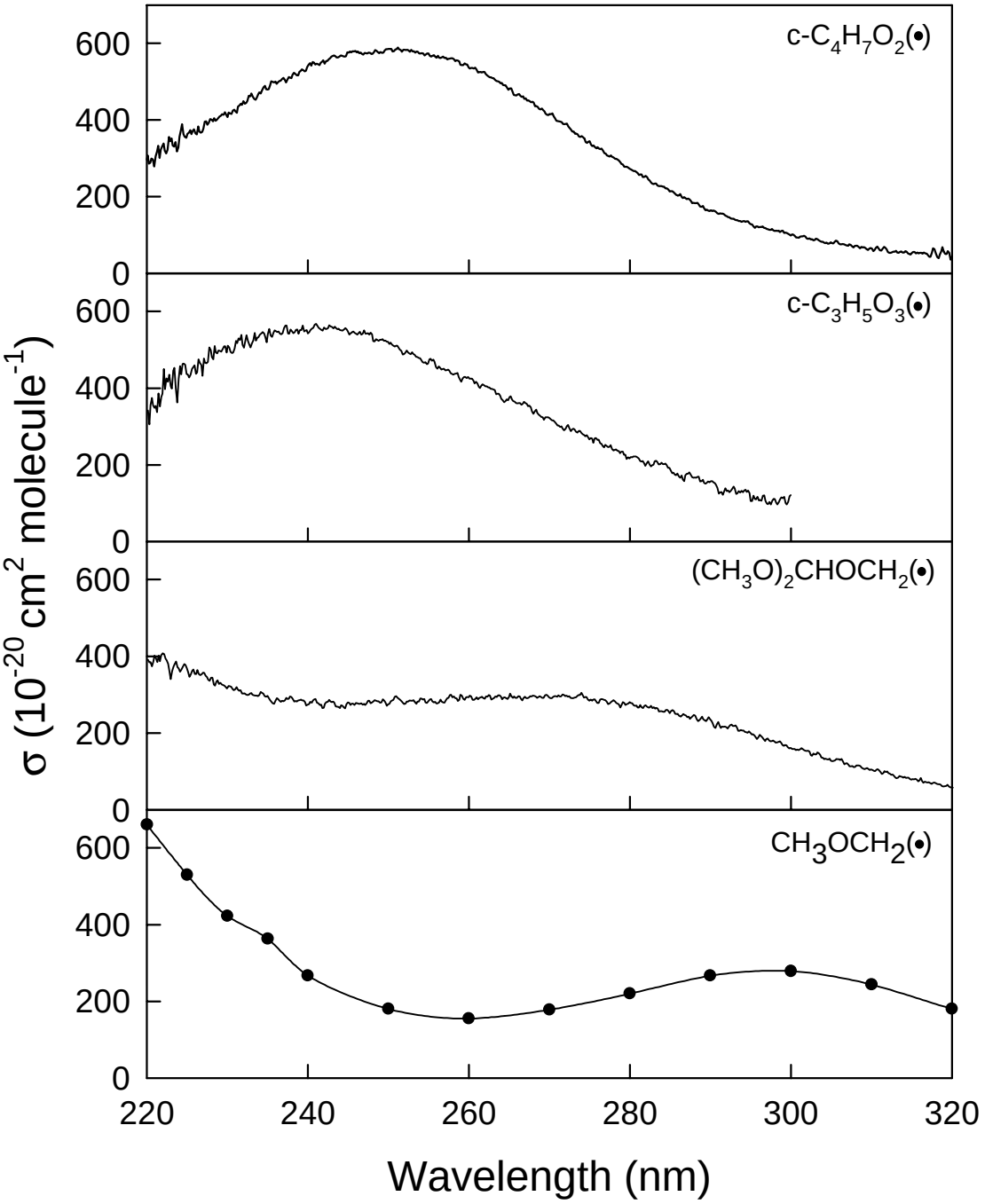

*Figure 6. UV absorption spectra of c-$C_4H_7O_2$(•), c-$C_3H_5O_3$(•), and $(CH_3O)_2CHOCH_2$(•) radicals recorded by a OMA II diode array. The UV absorption spectrum of the CH_3OCH_2(•) radical [**29**] is shown for comparison with the UV absorption spectrum of the $(CH_3O)_2CHOCH_2$(•) radical.*

Table 2. Absolute absorption cross sections obtained in this work.

Radical	**Wavelength** (nm)	**σ** (10^{-18} cm^2 $molecule^{-1}$)
$(CH_3O)_2HCOCH_2$	250	2.8 ± 0.5
$(CH_3O)_2HCOCH_2O_2$	250	3.5 ± 0.6
c-$C_4H_7O_2$	250	5.9 ± 0.6
(c-$C_4H_7O_2$)O_2	240	4.8 ± 0.8
c-$C_3H_5O_3$	250	5.2 ± 0.7
(c-$C_3H_5O_3$)O_2	250	3.7 ± 0.4
c-C_6H_{11}	250	7.0 ± 0.9
c-$C_6H_{11}O_2$	250	5.7 ± 0.6
C_6H_5	250	28 ± 5.8
C_6H_5O	235	38 ± 4.8

For comparison with the UV absorption spectrum of the $(CH_3O)_2CHOCH_2$(•) radical, the UV absorption spectrum of the CH_3OCH_2(•) radical [29] is given in Figure **6**. The shape and intensity of the CH_3OCH_2(•) and $(CH_3O)_2CHOCH_2$(•) radicals seem to be similar, except that the UV absorption spectrum of the $(CH_3O)_2CHOCH_2$(•) radical is blue shifted by 25-30 nm compared to the UV absorption spectrum of the CH_3OCH_2(•) radical. The maximum absorption and the shape of the UV spectra of c-$C_4H_7O_2$(•) and c-$C_3H_5O_3$(•) radicals are intense and broad. The UV absorption spectrum of the c-$C_3H_5O_3$(•) radical is blue shifted by 10-15 nm compared to the UV absorption spectrum of the c-$C_4H_7O_2$(•) radical.

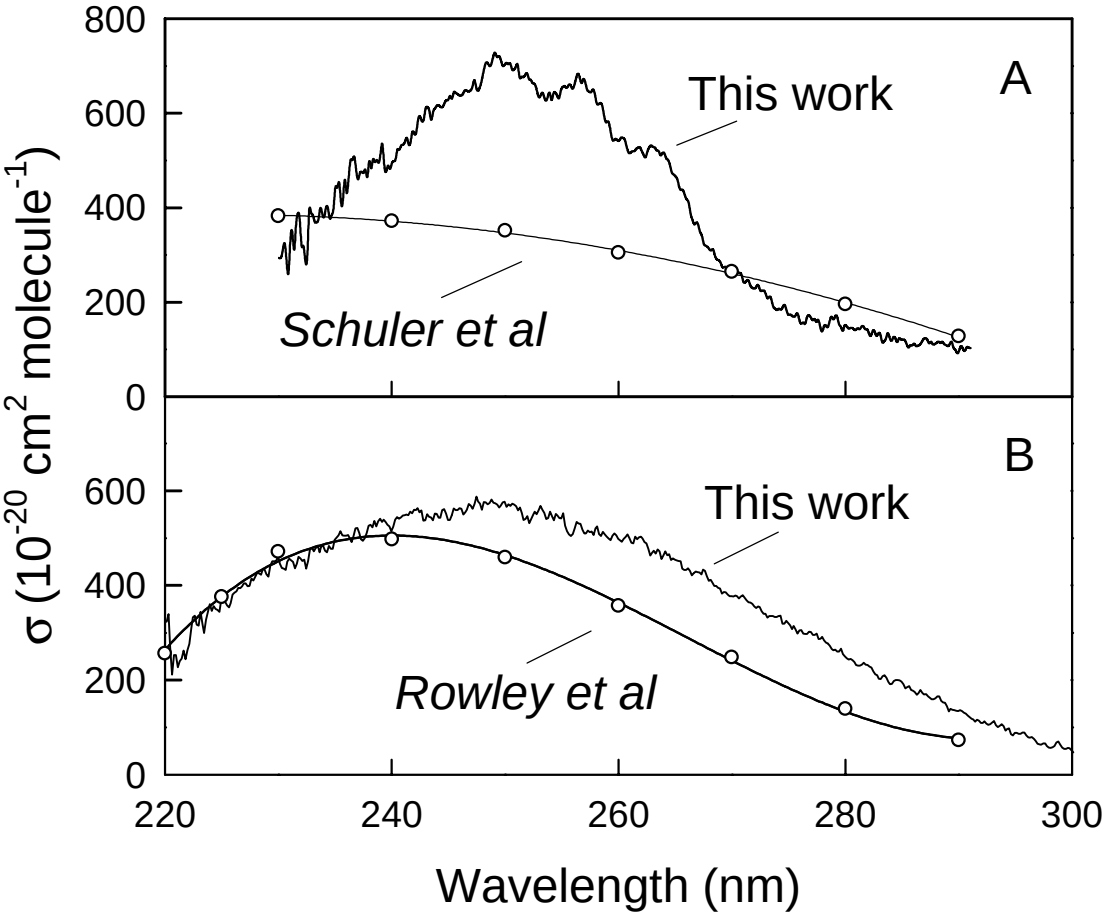

*Figure 7. (A) UV-absorption spectrum of the c-C_6H_{11}(•) radical reported by Schuler and Patterson [**30**] (circles), and measured herein (solid line).*
*(B) UV-absorption spectrum of the (c-C_6H_{11})O_2(•) radical reported by Rowley et al. [**47**] (circles) and measured in the present work (solid line).*

UV absorption spectrum of the c-C_6H_{11}(•) radical

The UV absorption spectrum of the cyclohexyl radical, c-C_6H_{11}(•), is shown in Figure **7**A. It is obtained using the same technique as described in section 6.1.1. As seen from Figure **7**A this highly symmetrical radical shows three small absorption maxima between 250-270 nm which may be indication of electronic vibrational fine structure. It is out of the scope for this work to determine this UV spectra with a higher resolution. It would be interesting for a future work to determine if this large symmetrical radical really has fine structure in the UV region. No gas phase UV absorption spectrum of the cyclohexyl radical is reported in the literature. Schuler *et al.* [30] have obtained a UV absorption spectrum of the cyclohexyl radical in liquid cyclohexane.

UV absorption spectrum of the C_6H_5(•) radical

The smallest aromatic alkyl radical is the phenyl radical, C_6H_5(•). The UV absorption spectrum of the C_6H_5(•) radical was recorded over the range 220-575 nm. No absorption was observed above 450 nm. The spectrum of C_6H_5(•) radicals in both the gas- [31, 36], liquid- [32], and solid phase [33,34,35] is reported in the literature. Previously no gas phase UV absorption spectrum of C_6H_5(•) radicals have been put on an absolute scale. C_6H_5(•) radicals were obtained via reaction (**15**) using pulse radiolysis of mixtures of [C_6H_6] = 1 mbar and [Ar] = 999 mbar.

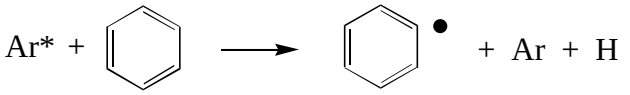

(15)

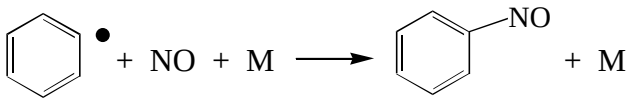

(16)

Ar* denote metastable Argon. The obtained Ar* concentration was of the order of 10^{14} molecule cm^{-3}. There is no direct way to determine the absolute Ar* concentration. As discussed by Ikeda *et al*. [36], $C_6H_5(\bullet)$ radicals react rapidly with NO to give nitrosobenzene. Nitrosobenzene absorbs strongly in the UV region with an absorption cross section at 270 nm of $\sigma(C_6H_5NO)_{270\ nm} = 3.82 \times 10^{-17}$ cm^2 $molecule^{-1}$ (average of references [37] and [38]). By pulse radiolysis of mixtures of C_6H_6/NO/Ar the observed maximum absorbance of nitrosobenzene, formed via reactions (**15**) and (**16**), was plotted as a function of the relative dose of Ar. An obtained slope from a linear least squares regression fit to the low dose data was scaled to the known $\sigma(C_6H_5NO)_{270\ nm} = 3.82 \times 10^{-17}$ cm^2 $molecule^{-1}$ and the yield of Ar* was obtained. From this indirectly determined Ar* yield the absolute absorption cross section of the $C_6H_5(\bullet)$ radical at 250 nm was determined to be $\sigma(C_6H_5(\bullet))_{250nm} = (2.75 \pm 0.58) \times 10^{-17}$ cm^2 $molecule^{-1}$. Two different techniques were used to record the UV absorption spectrum of $C_6H_5(\bullet)$ radicals, as seen from Figure **8**. First, the spectrum in the range 225-350 nm was mapped out using the photomultiplier system. Second, the diode camera was used to record the absorption in the range 225-575 nm. Both spectra were scaled to $\sigma\ (C_6H_5(\bullet))_{250nm} = (2.75 \pm 0.58) \times 10^{-17}$ cm^2 $molecule^{-1}$. The gas phase UV absorption spectrum was measured by Ikeda *et al*. [36]. This UV spectrum is not given on an absolute scale. Therefore the UV spectrum obtained by Ikeda *et al*. is scaled to $\sigma\ (C_6H_5(\bullet))_{250nm} = (2.75 \pm 0.58) \times 10^{-17}$ cm^2 $molecule^{-1}$. This spectrum is shown in Figure **8**. All three spectra shown in Figure **8** shows similar shapes.

UV absorption spectrum of the $C_6H_5O(\bullet)$ radical

Recently it has been shown that phenoxy radicals, $C_6H_5O(\bullet)$, are formed via reaction between Cl atoms and C_6H_5OH [39, 40, 41], reaction (**17**). In the laboratory at Risoe Cl atoms are formed via the reaction between F atoms and HCl, reaction (**2**). The UV absorption spectrum was recorded in the range 220-400 nm.

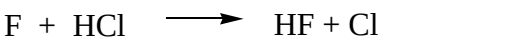

(2)

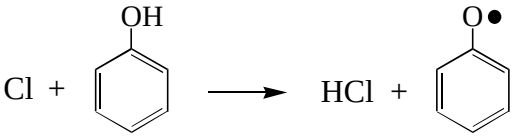

(17)

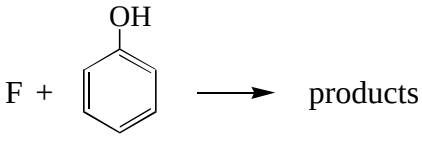

(**18**)

In this experiment mixtures of [C_6H_5OH] = 0.1 mbar, [HCl] = 20 mbar, and [SF_6] = 980 mbar was radiolyzed leading to a competition between reactions (**2**) and (**18**). It was calculated that under the experimental conditions approximately 89% and 11% of the formed F atoms reacted via reaction (**2**) and (**18**), respectively. F atoms generally react with aromatic compounds via two pathways; H atom abstraction and adduct formation giving $C_6H_5O(\bullet)$ radicals and F-C_6H_5OH adducts, respectively. Comparing the yields at 235 nm from pulse radiolysis of mixtures of $C_6H_5OH/HCl/SF_6$ and C_6H_5OH/SF_6 it was concluded that a substantial fraction (≈ 45%) of reaction (**18**) produce $C_6H_5O(\bullet)$ radicals and that the UV absorption spectra obtained using $SF_6/HCl/C_6H_5OH$ mixtures are free from significant complications associated with the formation of the F-C_6H_5OH adduct (see Appendix F for details). As seen from Figure **8** there is good agreement between the present result and the gas phase

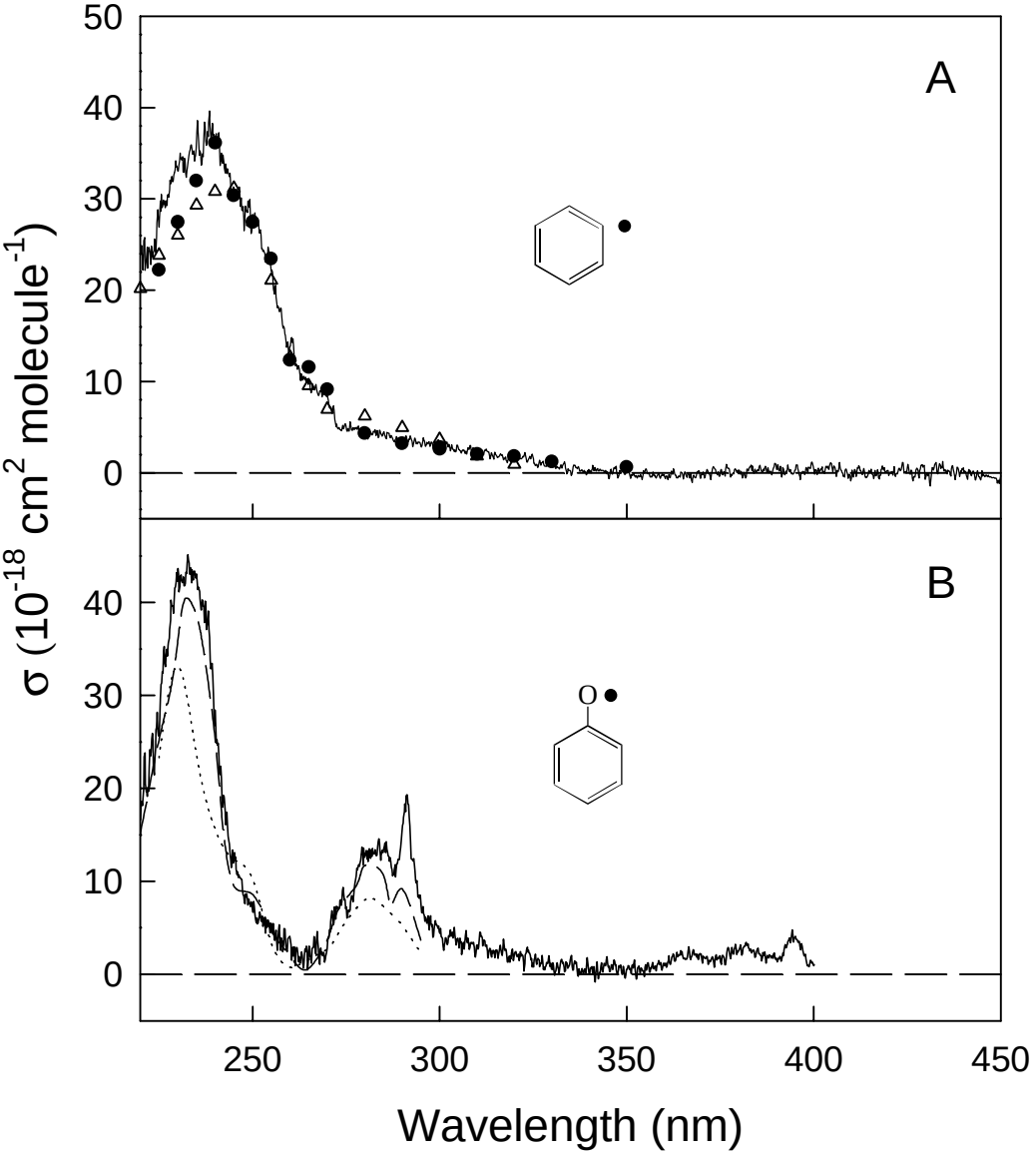

*Figure 8. (A) UV-visible absorption spectrum of the $C_6H_5(\bullet)$ radical, the circles are point by point determinations (this work) while the continuous spectrum is the average of 3 diode array spectra (this work). The triangles are the results of Ikeda et al. [**36**] scaled to $\sigma(C_6H_5(\bullet))_{250\ nm} = (27.5 \pm 5.8) \times 10^{-18}$ $cm^2\ molecule^{-1}$.*
*(B) UV-visible absorption spectrum of $C_6H_5O(\bullet)$ radical measured in the present work (solid), by Berho et al. [**40**] (dashed), and Kajii et al. [**42**] (dotted).*

spectra reported by Kajii et al.. [42], and Berho et al. Lesclaux [40]. Schuler et al. have obtained a phenoxy spectrum by pulse radiolysis of N_2O saturated aqueous solutions of C_6H_5OH [43], which has the same characteristic fine structure around 395 nm as the present spectrum. Very recently Sehested et al. [44] has obtained a phenoxy spectrum in the aqueous phase in the UV region and the spectral features are indistinguishable from those found in the present gas phase spectrum.

4.2 UV Absorption Spectra of Alkyl Peroxy Radicals

UV absorption spectra of $(CH_3O)_2CHOCH_2O_2(\bullet)$, $(c\text{-}C_4H_7O_2)O_2(\bullet)$, and $(c\text{-}C_3H_5O_3)O_2(\bullet)$ radicals

In the atmosphere alkyl radicals derived from ethers, react rapidly with O_2 (typical lifetime < 0.04 μs) to form alkyl peroxy radicals. UV absorption spectra of $(CH_3O)_2CHOCH_2O_2(\bullet)$, $(c\text{-}C_4H_7O_2)O_2(\bullet)$, and $(c\text{-}C_3H_5O_3)O_2(\bullet)$ radicals were recorded in the range 220-320 nm by using a diode array camera. The spectra are shown in Figure **9**. The studied peroxy radicals were obtained by pulse radiolysis of mixtures of ether/O_2/SF_6 via reactions (**12**) and (**19**).

$$F + RORH \longrightarrow ROR\bullet + HF \qquad (12)$$

$$ROR\bullet + O_2 + M \longrightarrow RORO_2\bullet + M \qquad (19)$$

$$F + O_2 + M \longrightarrow FO_2 + M \qquad (20)$$

In this experimental system there is a competition for F atoms between reactions (**12**) and (**20**). The FO_2 radical has a significant UV absorption below 260 nm [45]. To minimize the formation of FO_2 radicals the O_2 concentration must be kept to a minimum. On the other hand to minimize secondary radical-radical reactions like reaction between F atoms and alkyl radicals, reaction (**13**), the O_2 concentration needs to be as high as possible. Clearly the experimental conditions should be carefully designed to obtain the optimal oxygen concentration by taking the rate constants of reactions (**12**) and (**20**) into account. Recording of the UV absorption spectra were initiated 1-5 μs after the pulse radiolysis where all alkyl radicals were converted into alkyl peroxy radicals. The integration time was kept as short as possible (0.75-10 μs) to avoid complications from products formed via the self-reaction of alkyl peroxy radicals. As seen from Figure **9** the UV absorption spectra of $(CH_3O)_2CHOCH_2O_2(\bullet)$, $(c\text{-}C_4H_7O_2)O_2(\bullet)$, and $(c\text{-}C_3H_5O_3)O_2(\bullet)$ radicals are broad with absorptions maxima in the range 230-250 nm. There are no literature data to compare with these spectra. For comparison the UV absorption spectrum of the $CH_3OCH_2O_2(\bullet)$ radical is shown in Figure **9** [46]. The spectra of $(CH_3O)_2CHOCH_2O_2(\bullet)$ and $CH_3OCH_2O_2(\bullet)$ radicals are nearly identical. The shapes and intensities are typical for this class of compounds [46].

UV absorption spectrum of the $c\text{-}C_6H_{11}O_2(\bullet)$ radical

The UV absorption of the $c\text{-}C_6H_{11}O_2(\bullet)$ radical was recorded in the range 220-300 nm. Rowley *et al*. have reported an UV absorption spectrum of the $c\text{-}C_6H_{11}O_2(\bullet)$ radical. Both UV absorption spectra are shown in Figure **7**B. For reasons which are unclear, the spectrum measured in the present study is slightly (10%) more intense and is shifted to the red by approximately 10 nm when compared to that of Rowley *et al*. [47]. These spectra are similar to the spectra shown in Figure **9**.

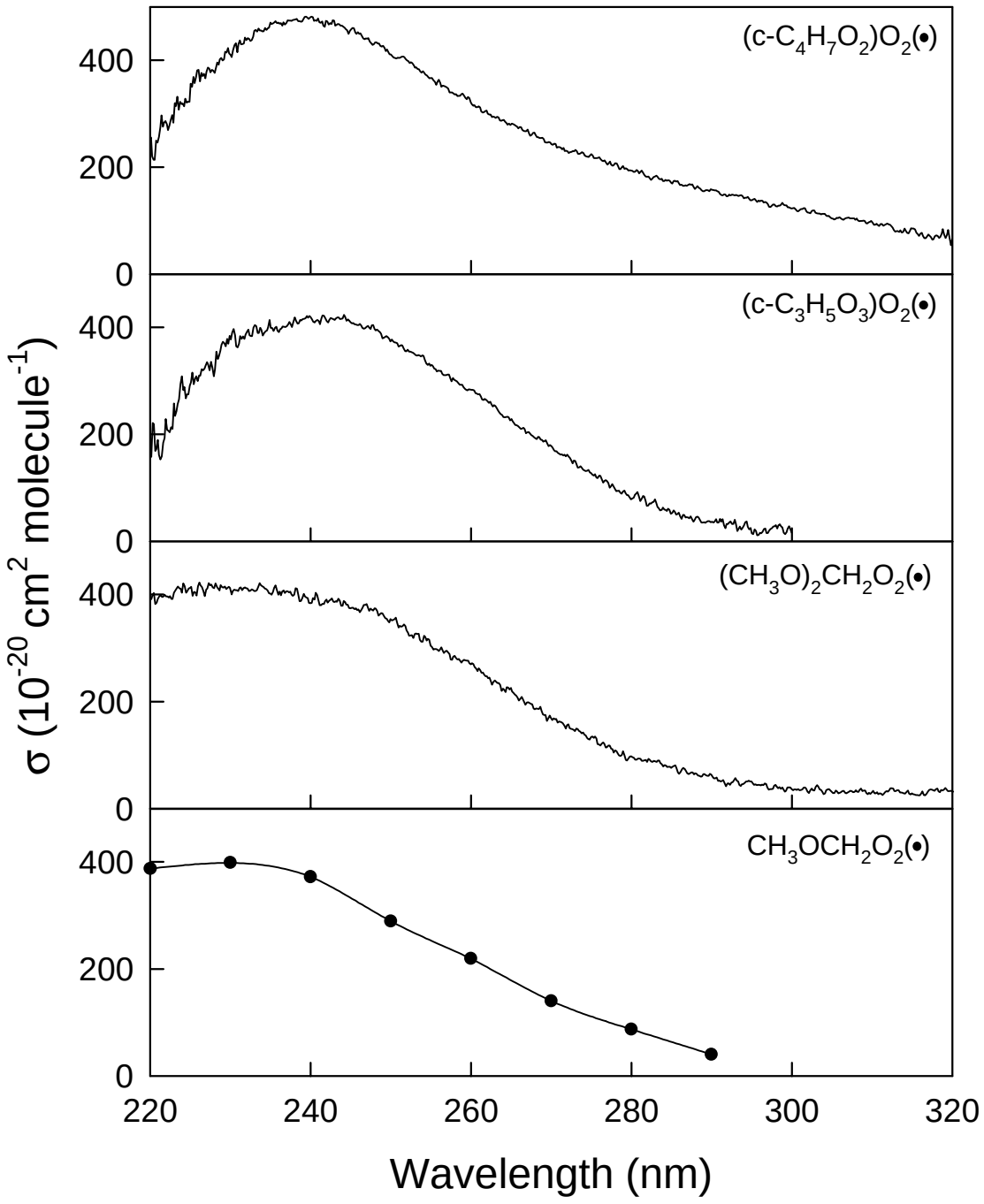

*Figure 9. UV absorption spectra of (c-$C_4H_7O_2$)O_2(•), (c-$C_3H_5O_3$)O_2(•), and $(CH_3O)_2CHOCH_2O_2$(•) radicals recorded by a OMA II diode array. The UV absorption spectrum of the $CH_3OCH_2O_2$(•) radical [**46**] is shown for comparison with the UV absorption spectrum of the $(CH_3O)_2CHOCH_2O_2$(•) radical.*

5 Reactions Involving Alkyl Radicals

5.1 Self-Reactions of Alkyl Radicals

Rate constants for self-reactions of $CH_3OCH_2(\bullet)$, $(CH_3O)_2CHOCH_2(\bullet)$, c-$C_4H_7O_2(\bullet)$, c-$C_3H_5O_3(\bullet)$, and c-$C_6H_{11}(\bullet)$ radicals have been measured. Following pulse radiolysis of mixtures of (CH_3OCH_3, $(CH_3O)_3CH$, c-$C_4H_8O_2$, c-$C_3H_6O_3$, or C_6H_{12})/SF_6 a rapid rise (< 3 μs) in absorption followed by a slower decay was observed. The rise is due to formation of alkyl radicals and the observed decay is ascribed to the self-reaction of alkyl radicals via reaction (**21**).

$$ROR\bullet + ROR\bullet \longrightarrow \text{products} \qquad \textit{(21)}$$

Different rates of decays were observed when the concentration of alkyl radicals was varied. Observed decays followed second-order kinetics and were well fitted using a second order expression:

$$A(t) = (A_0 - A_\infty)/(1 + 2k^{2nd}(A_0 - A_\infty)t) + A_\infty \qquad \textit{(eq.2)}$$

where A(t) is the measured absorption at time t, A_0 and A_∞ are the absorptions to time zero and infinite time, respectively. k^{2st} is equal to ($k_{selfreaction}$ ln10)/(σ(alkyl)l), where $k_{selfreaction}$ is the second-order rate constant for the observed self-reaction, σ(alkyl) is the absorption cross section of the alkyl radical at the monitoring wavelength, and l is the path length. Reciprocal half-lives (derived from the fits) are plotted as a function of A_0 as shown in Figure **10**. The slopes, of linear least squares regression fits to the data in Figure **10**, are equal to ($k_{selfreaction}$2ln10)/(σ(alkyl)L). Derived second-order rate constants for the self-reaction of alkyl radicals are $k_{CH3OCH2+CH3OCH2}$ = (4.1 ± 0.5), $k_{(CH3O)2CHOCH2+(CH3O)2CHOCH2}$ = (3.5 ± 0.6), $k_{c\text{-}C4H7O2+c\text{-}C4H7O2}$ = (3.3 ± 0.4), $k_{c\text{-}C3H5O3+c\text{-}C3H5O3}$ = (3.1 ± 0.6), and $k_{c\text{-}C6H11+c\text{-}C6H11}$ = (3.1 ± 0.4) all in units of 10^{-11} cm^3 $molecule^{-1}$ s^{-1}. The obtained rate constants are shown in Table **3**. As seen from Table **3** self-reactions of $(CH_3O)_2CHOCH_2(\bullet)$, c-$C_4H_7O_2(\bullet)$, c-$C_3H_5O_3(\bullet)$, and c-$C_6H_{11}(\bullet)$ radicals are equal within the uncertainties whereas the rate constant for $CH_3OCH_2(\bullet)$ radicals is approximately 25% higher. Hoyermann *et al*. [48] report a value of (2.5 ± 0.7) x 10^{-11} cm^3 $molecule^{-1}$ s^{-1} for the self-reaction of $CH_3OCH_2(\bullet)$ radicals. The reason of this discrepancy is unknown. An average rate constant of 3.3 x 10^{-11} cm^3 $molecule^{-1}$ s^{-1} is obtained from the rate constant given in Table **3** and the Hoyermann value. A rate constant of 3.3 x 10^{-11} cm^3 $molecule^{-1}$ s^{-1} fits well to the self-reaction rate constants obtained of this class of alkyl radicals. This combined with a small, but statistical significant, positive intercept in Figure **10** ($CH_3OCH_2(\bullet)$ panel) suggest that there could be a small unknown loss of $CH_3OCH_2(\bullet)$ radicals in this experiment. The kinetics of the self-reaction of cyclohexyl radicals has been studied previously by Schuler *et al.* [49]. For reasons which are unknown, the value reported by Schuler *et al.* is a factor of 16 times less than reported herein. There are no reported self-reaction rate constants to compare with the obtained rate constants for self-reactions of $(CH_3O)_2CHOCH_2(\bullet)$, c-$C_4H_7O_2(\bullet)$, and c-$C_3H_5O_3(\bullet)$ radicals.

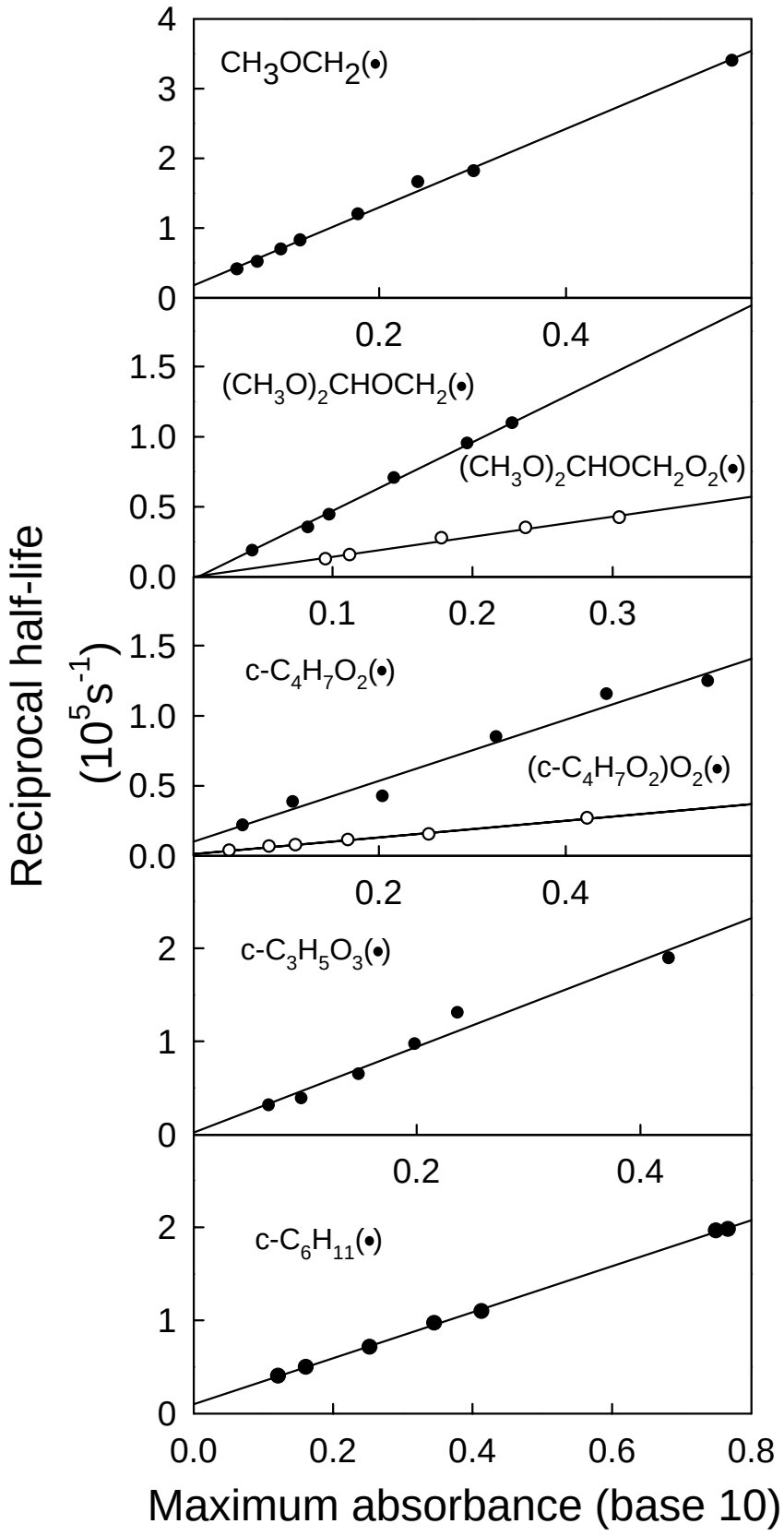

Figure 10. Plot of reciprocal half-life for self-reactions of a series of alkyl- and alkyl peroxy radicals as a function of the maximum absorbance.

5.2 Reactions between Alkyl Radicals and O_2

Reactions between $(CH_3O)_2CHOCH_2(\bullet)$, c-$C_4H_7O_2(\bullet)$, c-$C_3H_5O_3(\bullet)$, or c-$C_6H_{11}(\bullet)$ radicals and O_2

Rate constants for the association reactions between O_2 and $(CH_3O)_2CHOCH_2(\bullet)$, c-$C_4H_7O_2(\bullet)$, c-$C_3H_5O_3(\bullet)$, or c-$C_6H_{11}(\bullet)$ radicals have been measured. Pulse radiolysis of mixtures of $((CH_3O)_3CH$, c-$C_4H_8O_2$, c-$C_3H_6O_3$, or $C_6H_{12})/O_2/SF_6$ were used to study reaction (**19**). Examples of obtained absorption transients are shown as inserts in Figure **11**.

$$ROR\bullet + O_2 + M \longrightarrow RORO_2\bullet + M \qquad \textit{(19)}$$

Reactions rates between F atoms and organic compounds used in these experiments are typical of the order of 1 x 10^{-10} cm^3 $molecule^{-1}$ s^{-1} [50]. These reactions will form alkyl radicals. Alkyl radicals will under the used experimental conditions react with oxygen with rates of the order of 1 x 10^{-11} cm^3 $molecule^{-1}$ s^{-1}, see Table **3**. As expected, following pulse radiolysis of mixtures of $((CH_3O)_3CH$, c-$C_4H_8O_2$, c-$C_3H_6O_3$, or $C_6H_{12})/O_2/SF_6$ a rapid rise (< 0.1 μs) in absorption is observed. The rise in absorption is followed by a slower (complete within 5 μs) rise or decay. These observations were ascribed to a rapid formation of alkyl radicals followed by a slower formation of alkyl peroxy radicals. The formation of alkyl peroxy radicals will be observed as a rise in absorbance when $\sigma_{alkyl\ peroxy} > \sigma_{alkyl}$ and as a decay in absorbance when $\sigma_{alkyl\ peroxy} < \sigma_{alkyl}$. The used monitoring wavelength needs to be chosen where the absorption cross sections of the alkyl and the alkyl peroxy radicals are significantly different from each other. By varying the oxygen concentration different absorption transients were obtained. The formation of alkyl peroxy radicals were well fitted by first-order expressions and first-order rate constants were obtained from the fits. Obtained rate constants were plotted as a function of the oxygen concentration as shown in Figure **11**. As seen from Figure **11** the measured rate constants are not pressure dependent between 500 and 1000 mbar total pressure. Slopes of linear least squares regression fits to the data in Figure **11** gives pseudo first-order rate constants of $k_{(CH3O)2CHOCH2+O2} = (9.2 \pm 1.5)$, $k_{c\text{-}C4H7O2+O2} = (8.8 \pm 0.9)$, $k_{c\text{-}C3H5O3+O2} = (7.4 \pm 1.1)$, and $k_{c\text{-}C6H11} = (13 \pm 2)$ all in units of 10^{-12} cm^3 $molecule^{-1}$ s^{-1}, see Table **3**. As seen from Table **3** the rate constant for the reaction between $C_3H_5O_3(\bullet)$ radicals and O_2 is approximately half of the rate constant for reaction between c-C_6H_{11} radicals and O_2, where as the rate constants for the association reactions of $(CH_3O)_2CHOCH_2(\bullet)$ or c-$C_4H_7O_2(\bullet)$ radicals with O_2 lies in between these values. The following trend can be deduced from these data. Substitution of C atoms with O atoms in a six membered ring lower the rate constant between the corresponding alkyl radical and O_2. There is no reported value of the rate constant for reaction between c-C_5H_9O radical and O_2. It would be interesting for a future study to measure the rate constant between the c-C_5H_9O radical and O_2 together with a study of the association reactions of c-$C_5H_9(\bullet)$, c-$C_4H_7O(\bullet)$, and c-$C_3H_5O_2(\bullet)$ radicals with O_2. The measured rate constant for reaction between cyclohexyl radicals and O_2 is in excellent agreement with a value of (1.4 ± 0.2) x 10^{-11} cm^3 $molecule^{-1}$ s^{-1} measured by Wu *et al*. [51] in a previous gas phase study. In contrast, a value of (5.6 ± 1.0) x 10^{-12} cm^3 $molecule^{-1}$ s^{-1} has been measured in liquid cyclohexane by Bjellqvist and Reitberger [52].

Table 3. Rate constants measured in this work for reactions of alkyl and alkyl peroxy radicals. All in units of 10^{-11} cm^3 $molecule^{-1}$ s^{-1}.

Radicals	Self-reaction	O_2	NO	NO_2
CH_3OCH_2	4.1 ± 0.5			
$(CH_3O)_2CHOCH_2$	3.5 ± 0.6	0.92 ± 0.15		
$(CH_3O)_2CHOCH_2O_2$	1.3 ± 0.2		0.90 ± 0.12	1.0 ± 0.2
c-$C_4H_7O_2$	3.3 ± 0.4	0.88 ± 0.09		
(c-$C_4H_7O_2$)O_2	0.73 ± 0.12		1.2 ± 0.3	1.3 ± 0.3
c-$C_3H_5O_3$	3.1 ± 0.6	0.74 ± 0.11		
(c-$C_3H_5O_3$)O_2			0.58 ± 0.14	1.1 ± 0.2
c-C_6H_{11}	3.1 ± 0.4	1.3 ± 0.2		
(c-C_6H_{11})O_2			0.67 ± 0.09	0.95 ± 0.15
C_6H_5			2.1 ± 0.2	
C_6H_5O		< 5 x 10^{-10}	0.19 ± 0.02	0.21 ± 0.02

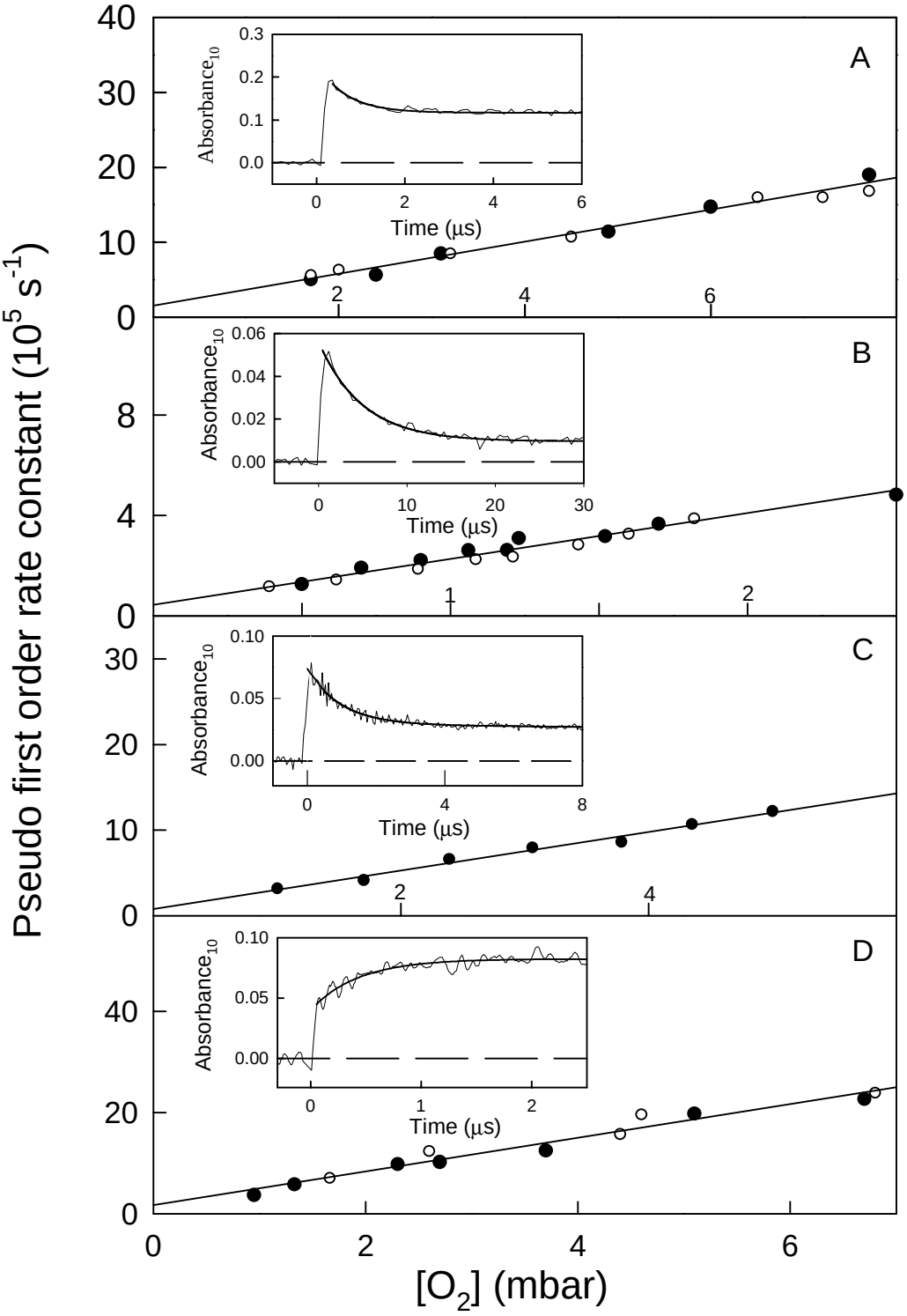

Figure 11. Pseudo first-order rate constants for reactions between O_2 and c-$C_4H_7O_2$(•) (A), c-$C_3H_5O_3$(•) (B), $(CH_3O)_2CHOCH_2$(•) (C), and c-C_6H_{11}(•) radicals (D) as a function of the O_2 concentration. Open - and closed symbols are obtained in 500 and 1000 mbar of SF_6 diluent, respectively. The inserts show experimental obtained absorption transients.

Reaction between $C_6H_5O(\bullet)$ radicals and O_2

The reaction between $C_6H_5O(\bullet)$ radicals and O_2 is a very slow reaction. It was not possible to measure this reaction using an absolute technique. Taking the uncertainties into account FTIR studies at Ford Motor Company showed no reaction between formed $C_6H_5O(\bullet)$ radicals and O_2 (even in pure O_2). Using the Acuchem chemical kinetic program [53] an upper limit of $k_{C6H5O(\bullet)+O2}<5.0 \times 10^{-21}$ cm^3 molecule^{-1} s^{-1} was established for this reaction, see Appendix F for details.

5.3 Reaction of $C_6H_5(\bullet)$ Radicals with NO

In a polluted urban troposphere $C_6H_5(\bullet)$ radicals react rapidly with NO to give C_6H_5NO via reaction (**16**). Phenyl radicals were in these experiments formed via two different reactions (**15**) and (**22**). The rate constant of reaction (**16**) is measured in this work following the formation of C_6H_5NO due to pulse radiolysis of mixtures of C_6H_6/NO/Ar or C_6H_5I/NO/Ar. An example of a typical absorption transient is shown in Figure **12**A.

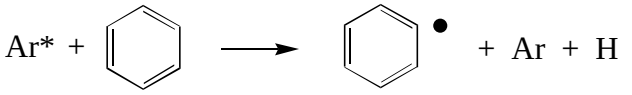

(15)

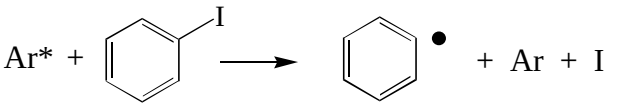

(22)

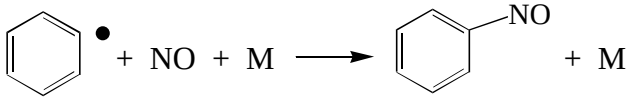

(16)

From the slope obtained by a linear least squares regression fit to the data in **Figure 12**A a rate constant of $(2.09 \pm 0.15) \times 10^{-11}$ cm^3 molecule^{-1} s^{-1} was obtained. This value is twice the value measured for other NO reactions in this work, see Table **3**. It has been shown recently that $C_6H_5(\bullet)$ radicals add to C_6H_5NO to give $(C_6H_5)_2NO(\bullet)$ (biphenyl nitroxide) radical with a rate of 9.1×10^{-12} cm^3 molecule^{-1} s^{-1} [54]. To avoid complications from formation of biphenyl nitroxide the NO concentration was always more than 50 times bigger than the concentration of $C_6H_5(\bullet)$ radicals. The rate constant for reaction (**16**) is pressure independent between 200-1000 mbar of Ar. This result is in good agreement with the values of $(1.97 \pm 0.13) \times 10^{-11}$ and $(1.87 \pm 0.16) \times 10^{-11}$ reported by Yu and Lin [55, 56] but in disagreement with the value of $(1.08 \pm 0.2) \times 10^{-11}$ cm^3 molecule^{-1} s^{-1} reported by Preidel and Zellner [57].

5.4 Reactions of $C_6H_5O(\bullet)$ Radicals with NO or NO_2

The kinetics of the reactions of phenoxy radicals with NO or NO_2, reactions (**23**) and (**24**), were studied in this work, by monitoring the decay in absorption at 235 nm (attributed to phenoxy radicals) following the pulse radiolysis of mixtures of SF_6/HCl/C_6H_5OH/NO or SF_6/HCl/C_6H_5OH/NO_2. The reaction between Cl atoms and C_6H_5OH, reaction (**17**), was used as the source of $C_6H_5O(\bullet)$ radicals. An example of an experimentally obtained absorption transient is shown in **Figure 12**B.

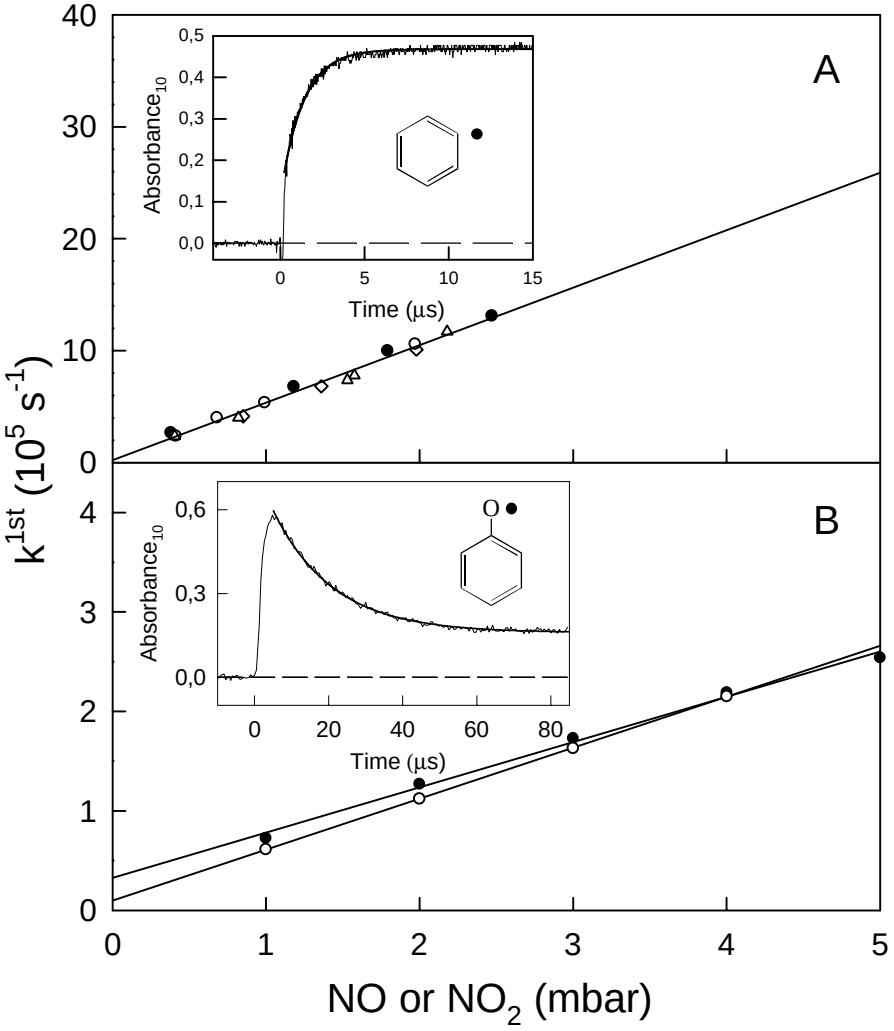

Figure 12. (A) Plot of the pseudo first-order rate constants for formation of C_6H_5NO, k^{1st}, versus [NO]. The formation of C_6H_5NO was monitored at either 270 nm (triangles) or 300 nm (circles) after pulsed radiolysis of mixtures of 10 mbar C_6H_6, 0.41-2.18 mbar of NO, and 990 mbar of Ar (open symbols) and 1 mbar of C_6H_5I and 0.38-2.47 mbar of NO, in 999 mbar of Ar (filled symbols). The open diamonds were obtained with 10 mbar of C_6H_6 and 0.85-1.98 mbar of NO with Ar added to give a total pressure of 200 mbar. The insert shows a typical transient obtained using a mixture containing 1.53 mTorr of NO, the UV path length was 160 cm, the smooth curve is a pseudo first order fit which gives $k^{1st} = 7.37 \times 10^5\ s^{-1}$.
(B) Pseudo first order rate constants for reaction of $C_6H_5O(\bullet)$ radicals with NO (open circles) or NO_2 (closed circles) following pulsed radiolysis of $SF_6/HCl/C_6H_5OH/(NO$ or $NO_2)$ mixtures versus [NO] or $[NO_2]$, respectively. The insert shows first-order fit to a transient at 235 nm observed following pulsed radiolysis (dose = 22% of maximum) of mixture containing of 0.1 mbar C_6H_5OH, 20 mbar HCl, 980 mbar SF_6, and 1.0 mbar of NO.

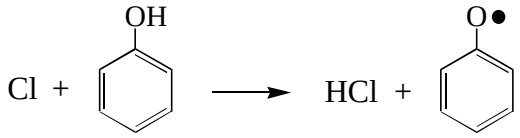

(17)

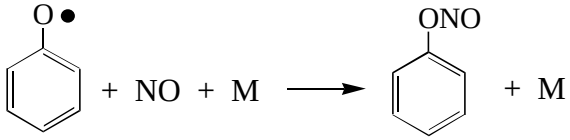

(23)

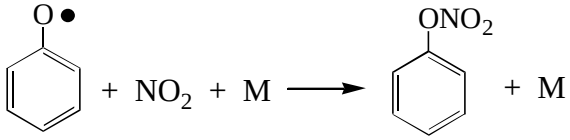

(24)

The decay rate of the absorbance at 235 nm increased linearly with the NO/NO_2 concentration. It seems reasonable to ascribe the decay of absorbance to the loss of phenoxy radicals via reactions (**23**) and (**24**). The residual absorption in the insert in **Figure 12**B is ascribed to UV absorption by C_6H_5ONO. While there are no reported measurements of the UV absorption spectrum of $C_6H_5ONO_2$, Berho *et al*. [41] have reported $\sigma(C_6H_5ONO) = 5.0 \times 10^{-18}$ cm^2 molecule^{-1} at 240 nm. All experimental traces followed pseudo first order kinetics. The pseudo first order loss rates for the $C_6H_5O(\bullet)$ radicals derived from the fits are plotted versus the concentrations of NO and NO_2, respectively. The data are shown in **Figure 12**B. From the slopes, obtained by linear least squares regression fits to the experimental data in **Figure 12**B, values of $k_{C6H5O+NO} = (1.88 \pm 0.16) \times 10^{-12}$ and $k_{C6H5O+NO2} = (2.08 \pm 0.15) \times 10^{-12}$ cm^3 molecule^{-1} s^{-1} were obtained. The small positive y-axis intercept in **Figure 12**B may reflect the contribution of self-reaction to loss of $C_6H_5O(\bullet)$ radicals. The obtained rate constant for reaction (**23**) are in excellent agreement with the reported value of 1.7×10^{-12} cm^3 molecule^{-1} s^{-1} by Berho and Lesclaux [41]. It is interesting to note that the reaction between phenyl radicals and NO is approximately 10 times faster than the reaction between phenoxy radicals and NO or NO_2. There are no literature data for the rate constant of reaction (**24**) to compare with the present rate constant.

6 Reactions Involving Alkyl Peroxy Radicals

6.1 Self-reactions of Alkyl Peroxy Radicals

Kinetics for the self-reactions between $(c\text{-}C_4H_7O_2)O_2(\bullet)$ or $(CH_3O)_2CHOCH_2O_2(\bullet)$ radicals have been measured using pulse radiolysis of mixtures of $(c\text{-}C_4H_8O_2$ or $(CH_3O)_3CH)/O_2/SF_6$. The experimental technique used was the same as the one described in section 5.1.

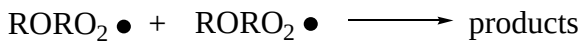

(25)

The experimental data are shown in Figure **10**. By linear least squares regression fits to the data values of $k_{obs\ (c\text{-}C4H7O2)O2+(c\text{-}C4H7O2)O2} = (7.3 \pm 1.2) \times 10^{-12}$ and $k_{obs\ (CH3O)2CHOCH2O2+(CH3O)2CHOCH2O2} = (1.3 \pm 0.2) \times 10^{-11}$ cm^3 molecule^{-1} s^{-1} were obtained. In both experiments alkoxy radicals where formed as a product in reaction (**25**). Degradation of alkoxy radicals generates in these experimental systems "other alkyl peroxy" radicals, which may have influence on obtained self-reaction rate constants. It was not possible to correct for complications due to "other alkyl peroxy" radicals and obtained self-reaction rate constants are given as observed values. Compared to the self-reaction of $c\text{-}C_4H_7O_2(\bullet)$ and

$(CH_3O)_2CHOCH_2(\bullet)$ radicals the obtained rate constants are a factor three lower. There are no previous literature values to compare with these results.

6.2 Reactions between Alkyl Peroxy Radicals and NO

Rate constants for reactions between $(CH_3O)_2CHOCH_2O_2(\bullet)$, $(c\text{-}C_4H_7O_2)O_2(\bullet)$, $(c\text{-}C_3H_5O_3)O_2(\bullet)$, or $c\text{-}C_6H_{11}O_2(\bullet)$ radicals and NO were measured. These reactions proceeds via two reaction channels, reactions (**26**a) and (**26**b).

$$RORO_2\bullet + NO \longrightarrow RORO\bullet + NO_2 \qquad \textit{(26a)}$$

$$RORO_2\bullet + NO + M \longrightarrow RORONO_2 + M \qquad \textit{(26b)}$$

NO_2 has a significant absorption cross section (6.01×10^{-19} cm^2 $molecule^{-1}$) at 400 nm [58]. By following the formation of NO_2 formed from pulse radiolysis of mixtures of ($(CH_3O)_3CH$, $c\text{-}C_4H_8O_2$, $c\text{-}C_3H_6O_3$ or C_6H_{12})/O_2/NO/SF_6 the rate of the overall reaction (**26**) can be measured. This technique has been used extensively at the Risoe laboratory [59, 60]. An example of an experimentally obtained absorption transient is shown in the insert in Figure **13**. By varying the NO concentration absorption transients were obtained. To obtain first-order rate constants the absorption transients were fitted using a first-order expression. The first-order rate constants were plotted as a function of the NO concentration, see Figure **13**. By linear least squares regression fits to the experimental data in Figure **13**, pseudo first-order rate constants were obtained from the slopes; $k_{(CH3O)2CHOCH2O2+NO} = (9.0 \pm 1.2) \times 10^{-12}$, $k_{(c\text{-}C4H7O2)O2+NO} = (1.2 \pm 0.3) \times 10^{-11}$, $k_{(c\text{-}C3H5O3)O2+NO} = (5.8 \pm 1.4) \times 10^{-12}$, $k_{c\text{-}C6H11O2+NO} = (6.7 \pm 0.9) \times 10^{-12}$ cm^3 $molecule^{-1}$ s^{-1}.

There are no previous reported literature values to compare with these results. Two types of complications, having influence on the experiments done in this work, will be addressed here. First, if the rate of the self-reaction, reaction (**25**), is of the same order or faster than the rate of reaction (**26**) then reaction (**25**) will be important at low NO concentrations. The rate constants for the self-reactions of $(CH_3O)_2CHOCH_2O_2(\bullet)$ and $(c\text{-}C_4H_7O_2)O_2(\bullet)$ radicals were measured in this work. These self-reactions were found to be of the same order as the rate constants for the reactions between $(CH_3O)_2CHOCH_2O_2(\bullet)$ or $(c\text{-}C_4H_7O_2)O_2(\bullet)$ radicals and NO, see Table **3**. Presumable this pattern is the same for the $(c\text{-}C_3H_5O_3)O_2(\bullet)$ radicals. Under these circumstances first-order rate constants obtained from the fits are overestimated at low NO concentrations. This will give a small positive intercept as seen in Figure **13**. Secondly, the NO_2 yield calculated from the maximum absorption can be observed to be more than 100% of that expected if all F atoms were converted into alkyl peroxy radicals and all alkyl peroxy radicals reacted via reaction (**26**a). In the case of the reaction between NO and $(c\text{-}C_4H_7O_2)O_2(\bullet)$ radicals the observed NO_2 yield was 90-130%. This observation suggest that there must be at least one additional reaction channel producing NO_2 under the used experimental conditions. A possible explanation could be that the $(c\text{-}C_4H_7O_2)O(\bullet)$ radical, formed in reaction (**26**a), decompose to give other alkyl radicals. These alkyl radicals will react with O_2 to give alkyl peroxy radicals, which then will react with NO to give NO_2. Fits to the experimental obtained absorption transients will then give first-order rate constants which are underestimated compared to the real rate constant of reaction (**26**). When complications related to positive intercepts or yields higher than 100% of NO_2, were observed, the experimental transients were modelled using computer modelling programs, Chemsimul [10] or Acuchem [11]. See Appendix C and G for details.

Studying the reaction between the $c\text{-}C_6H_{11}O_2(\bullet)$ radical and NO, a rate constant of 6.7×10^{-12} cm^3 $molecule^{-1}$ s^{-1} was obtained. Rowley *et al*. have reported a rate constant of 4.15×10^{-14} cm^3 $molecule^{-1}$ s^{-1} for the self-reaction of $c\text{-}C_6H_{11}O_2(\bullet)$ radicals. This rate constant is more than 150 times slower than the measured rate constant value of 6.7×10^{-12} cm^3 $molecule^{-1}$ s^{-1}. Therefore there will be no complication from the self-reaction of the $c\text{-}C_6H_{11}O_2(\bullet)$ radical. The obtained NO_2 yield was less than 100%. No significant intercept was observed from a linear least squares regression fit to the

c-$C_6H_{11}O_2$(•) radical data (diamonds), see Figure **13**A. This is in good agreement with no complications from the self-reaction of c-$C_6H_{11}O_2$(•) radicals and decomposition of the c-$C_6H_{11}O$(•) radical leading to more than a 100 percent yield of NO_2.

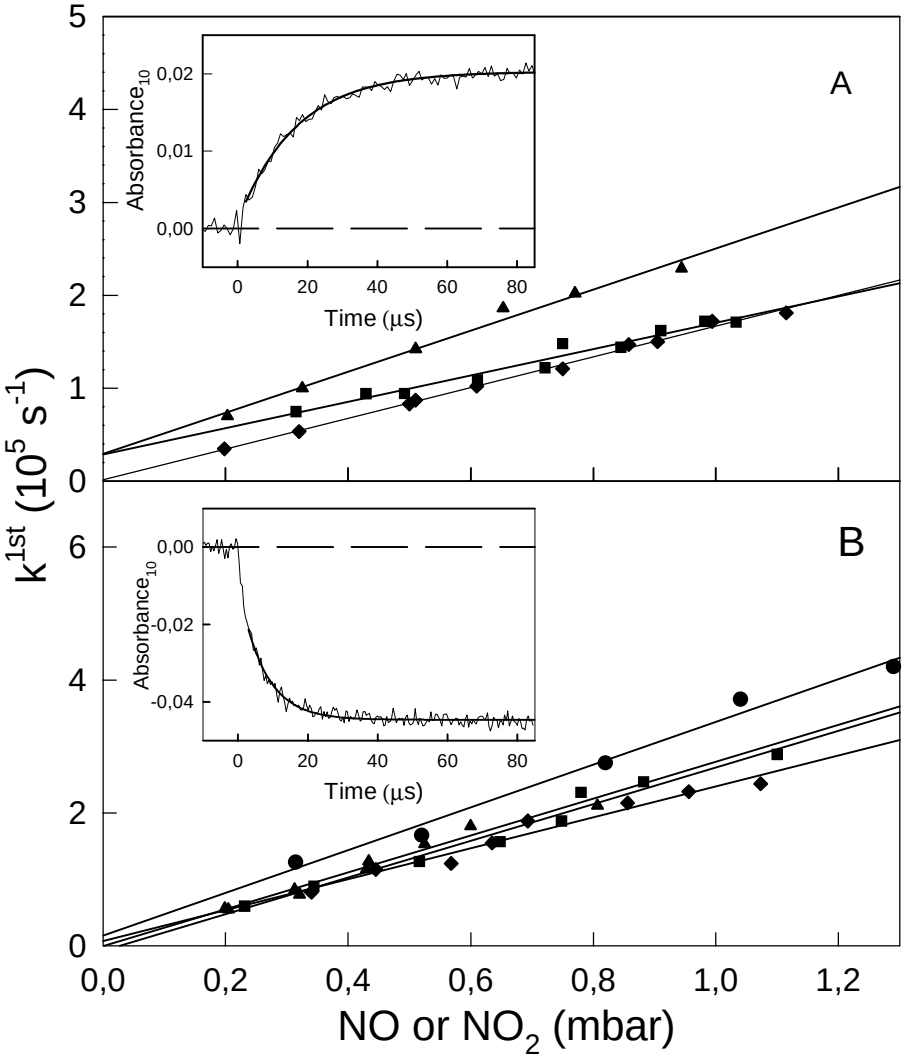

Figure 13. (A) Pseudo first-order rate constants for reactions between NO and (c-$C_3H_5O_3$)O_2(•) (squares), $(CH_3O)_2CHOCH_2O_2$(•) (triangles), and c-$C_6H_{11}O_2$(•) radicals (diamonds) versus the NO concentration. The insert shows the transient absorbance at 400 nm observed following pulsed radiolysis (dose = 22% of maximum, path length 200 cm) of a mixture of 0.40 mbar NO, 10 mbar cyclohexane, 10 mbar O_2, and 980 mbar SF_6.
(B) Pseudo first-order rate constants for reactions between NO_2 and (c-$C_4H_7O_2$)O_2(•) (circles), (c-$C_3H_5O_3$)O_2(•) (squares), $(CH_3O)_2CHOCH_2O_2$(•) (triangles), and c-$C_6H_{11}O_2$(•) radicals (diaomonds) versus the NO_2 concentration. The insert shows the transient absorbance at 400 nm observed following pulsed radiolysis (dose = 42% of maximum, path length 160 cm) of a mixture of 0.64 mbar NO_2, 10 mbar cyclohexane, 10 mbar O_2, and 980 mbar SF_6.

6.3 Reactions between Alkyl Peroxy Radicals and NO_2

Pulse radiolysis of mixtures of ($(CH_3O)_3CH$, c-$C_4H_8O_2$, c-$C_3H_6O_3$, C_6H_{12})/O_2/NO_2/SF_6 were used to measure rate constants for reactions between $(CH_3O)_2CHOCH_2O_2(\bullet)$, (c-$C_4H_7O_2$)$O_2(\bullet)$, (c-$C_3H_5O_3$)$O_2(\bullet)$, or c-$C_6H_{11}O_2(\bullet)$ radicals and NO_2. The decay of NO_2, via reaction (**27**), was followed using 400 nm as the monitoring wavelength. A typical absorption transient is shown in the insert in Figure **13**B.

$$RORO_2\bullet + NO_2 \longrightarrow \text{products} \qquad \textit{(27)}$$

Observed decays were fitted using a first-order expression and first-order rate constants (obtained from the fits) were plotted as a function of the NO_2 concentration. See Figure **13**B. In all cases the experimental transients were well described using the first-order expression (**eq.1**). The slopes from linear least squares regression fits, to the data in Figure **13**B, give pseudo first-order rate constants values of $k_{(CH3O)2CHOCH2O2+NO2} = (1.0 \pm 0.2) \times 10^{-11}$, $k_{(c\text{-}C4H7O2)O2+NO2} = (1.3 \pm 0.3) \times 10^{-11}$, $k_{(c\text{-}C3H5O3)O2+NO2} = (1.1 \pm 0.2) \times 10^{-11}$, $k_{c\text{-}C6H11O2+NO2} = (9.5 \pm 1.5) \times 10^{-12}$ cm^3 $molecule^{-1}$ s^{-1}. The rate constants obtained in this work are all within the uncertainties equal with an average value of 1.1×10^{-11} cm^3 $molecule^{-1}$ s^{-1}. They are all higher compared to the rate constants for reactions between the $(CH_3O)_2CHOCH_2O_2(\bullet)$, (c-$C_4H_7O_2$)$O_2(\bullet)$, (c-$C_3H_5O_3$)$O_2(\bullet)$, or c-$C_6H_{11}O_2(\bullet)$ radicals and NO, see Table **3**. There are no previously reported values to compare with these results.

7 Relative Rate Measurements

The relative rate measurement method is used to determine an unknown rate constant of a reaction relative to a well determined rate constant for a reference reaction. This relative method has been used for more than a decade at Ford Motor Company. The FTIR smog chamber system is used to study reactions between Cl atoms, F atoms or OH radicals and organic compounds [61]. The relative rate method is easy to operate and complications due to impurities does not normally have influence on the experiment. A disadvantage is that the rate constant is not determined directly.

$$Cl + \text{Reactant} \longrightarrow \text{Products} \qquad \textit{(28)}$$

$$Cl + \text{Reference} \longrightarrow \text{Products} \qquad \textit{(29)}$$

The experiments in this part of the work were done by irradiation of mixtures of Cl_2/reactant/reference at 1 atm. total pressure and at 296 ± 2 K. Assuming that the solely fate of reactant and reference is reactions (**28**) and (**29**), that reactant or reference is not reformed during the experiment and that the Cl atoms reach a steady state concentration, $[Cl]_{ss}$, it follows that:

$$\ln([\text{Reactant}]_t/[\text{Reactant}]_{t0}) = -k_{28}\,[Cl]_{ss}\,t \qquad \textit{(eq.4)}$$

$$\ln([\text{Reference}]_t/[\text{Reference}]_{t0}) = -k_{29}\,[Cl]_{ss}\,t \qquad \textit{(eq.5)}$$

where t and t0 refers to time of irradiation and starting time, respectively. Combining equations (**eq.4**) and (**eq.5**) gives:

$$ln([Reactant]_t/[Reactant]_{t0}) = k_{28}/k_{29}\, ln([Reference]_t/[Reference]_{t0}) \quad (eq.\mathbf{6})$$

From the slope of a plot of $ln([Reactant]_t/[Reactant]_{t0})$ versus $ln([Reference]_t/[Reference]_{t0})$ and the known rate constant (k_{29}) for the reference reaction it is possible to determine an rate constant (k_{28}) for the studied reaction. An example of a relative rate experiment is shown in Figure **14**. To avoid complications from secondry reactions more than one reference was used to determine the unknown rate constant. The $[Reactant]_0/[Reference]_0$ ratio was varied by more than a factor of two. Results obtained in this work are shown in Table **1** and Table **4**.

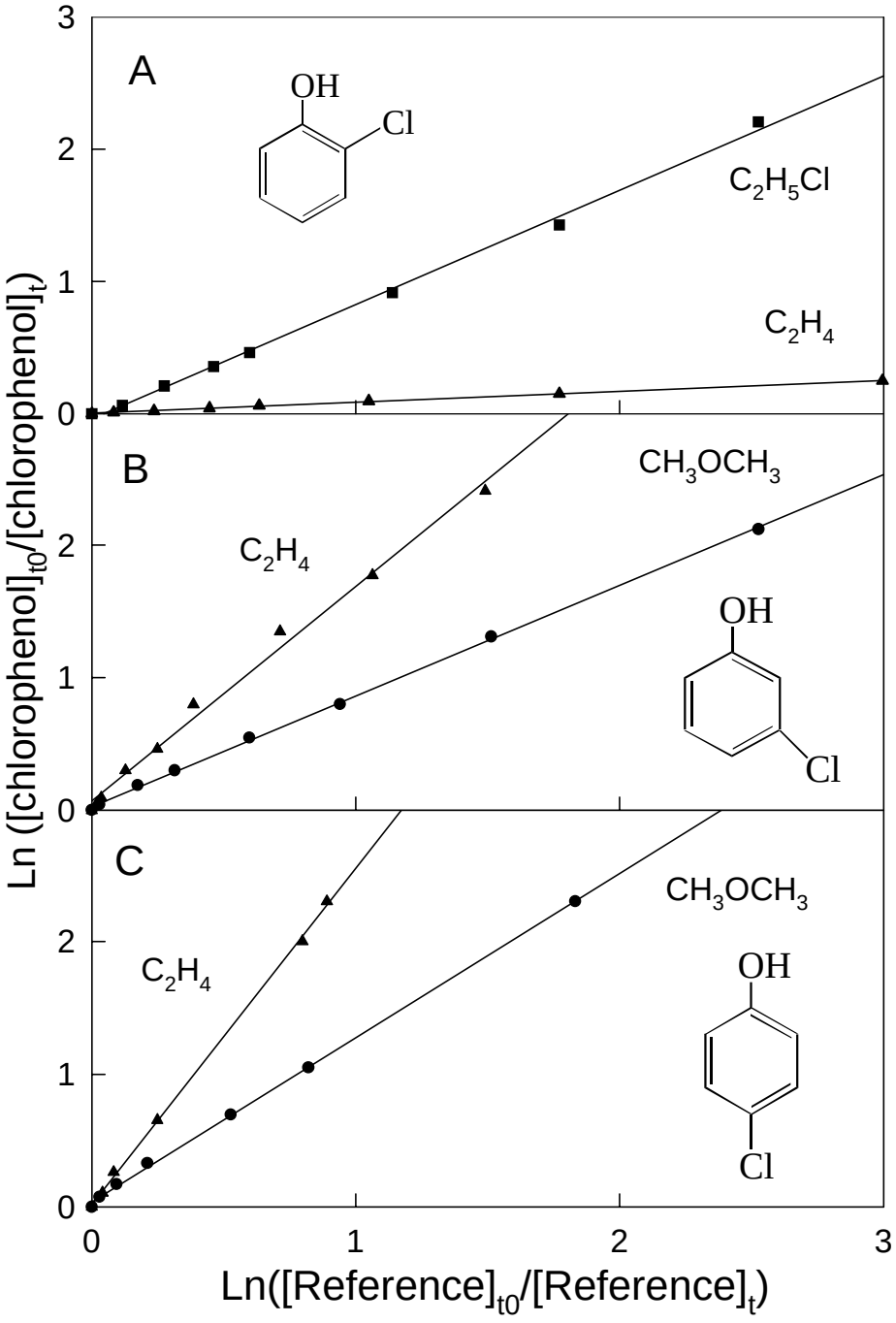

Figure 14. (A) Decay of 2-chlorophenol versus C_2H_5Cl (squares) and C_2H_4 (triangles), (B) 3-chlorophenol and (C) 4-chlorophenol versus C_2H_4 (triangles) and CH_3OCH_3 (circles) when mixtures of these compounds were exposed to Cl atoms in 700 Torr total pressure at 296 ± 2 K.

Table 4. Rate constants for reactions between Cl atoms and organic compounds measured in this work. The rate constants in the left second column are average rate constants of the obtained rate constants using different references.

Reactant	Rate Constant	Reference Compounds				
		CD_4	C_2H_4	C_3H_6	$(CH_3)_2O$	C_2H_5Cl
CF_2ClH	*0.17±0.01*	*0.17±0.01*				
C_6H_5OH	1.94±0.39		1.91±0.13	2.07±0.26	1.84±0.13	
2-chlorophenol	0.08±0.02		0.08±0.01			0.07±0.01
3-chlorophenol	1.56±0.14		1.53±0.11		1.58±0.11	
4-chlorophenol	2.37±0.21		2.37±0.19		2.36±0.20	
Benzoquinone	1.94±0.28		1.91±0.13		1.96±0.26	

Reactant	Rate Constant	Reference Compounds			
		CH_3OH	C_2H_4	n-C_4H_{10}	$(CH_3)_2O$
1,4-dioxane	1.95±0.25		1.90±0.1		2.0±0.2
1,3,5-trioxane	0.99±0.09	0.96±0.05	1.02±0.06		1.12±0.06
$CH_3OCH_2OCH_3$	1.35±0.15			1.4±0.1	1.3±0.1

Reactant	Rate Constant	Reference Compounds			
		CH_4	CH_3Cl	c-$C_3H_6O_3$	C_2H_4
$(HC(O)O)_2CH_2$	*5.1±0.9*	*5.4±0.5*	*4.8±0.6*		
$(CH_3O)_3CH$	1.53±0.16			1.54±0.15	1.52±0.10

All in units of 10^{-12} cm^3 $molecule^{-1}$ s^{-1}. Italic in units of 10^{-14} cm^3 $molecule^{-1}$ s^{-1}.

8 Atmospheric Fate of Dimethoxymethane, Trimethoxymethane, 1,4-Dioxane and 1,3,5-Trioxane

The FTIR-smog Chamber System at Ford Motor Company, USA, was used in this work to study the atmospheric fate of a series of ethers. The atmospheric fate of alkoxy radicals derived from the atmospheric oxidation of $CH_3OCH_2OCH_3$, $(CH_3O)_3CH$, c-$C_4H_8O_2$, and c-$C_3H_6O_3$ was determined, for details see Appendix B, G, C, and D, respectively. Alkoxy radicals were obtained via reactions (**30**), (**19**), and (**26**a) by irradiation's of mixtures of ($CH_3OCH_2OCH_3$, $(CH_3O)_3CH$, c-$C_4H_8O_2$, or c-$C_3H_6O_3$)/Cl_2/O_2/NO at 296 ± 2 K and total 700 Torr total pressure with O_2, N_2 or Air as diluent.

$$Cl + RORH \longrightarrow ROR\bullet + HCl \qquad (30)$$

$$ROR\bullet + O_2 + M \longrightarrow RORO_2\bullet + M \qquad (19)$$

$$RORO_2\bullet + NO \longrightarrow RORO\bullet + NO_2 \qquad (26a)$$

An example of a FTIR spectra obtained by irradiation of a mixture of 1,3,5-trioxane/Cl_2/NO/O_2/N_2 is shown in Figure **15**. Experimental conditions are given in the figure text.

8.1 Atmospheric fate of $CH_3OCH_2OCH_2O(\bullet)$ and $CH_3OCH(O(\bullet))OCH_3$ radicals

The initial atmospheric oxidation of $CH_3OCH_2OCH_3$ is H atom abstraction by the OH radical to give $CH_3OCH_2OCH_2(\bullet)$ and $CH_3OCH(\bullet)OCH_3$ radicals. These radicals will in the atmosphere be converted to $CH_3OCH_2OCH_2O(\bullet)$ and $CH_3OCH(O(\bullet))OCH_3$ radicals via reactions (**19**) and (**26**a). Methoxymethyl formate (CH_3OCH_2OCHO) and dimethyl carbonate ($CH_3OC(O)OCH_3$) were observed as the two major products associated with the degradation of $CH_3OCH_2OCH_2O(\bullet)$ and $CH_3OCH(O(\bullet))CH_3$ radicals, respectively. As seen from Figure **16** the yield of $CH_3OC(O)OCH_3$ was independent of the partial O_2 pressure over the range 5.6-600 Torr. This gives that two reaction channels can contribute to the formation of $CH_3OC(O)OCH_3$.

$$CH_3OCH(O\bullet)OCH_3 + O_2 \longrightarrow CH_3OC(O)OCH_3 + HO_2 \qquad (31)$$

$$CH_3OCH(O\bullet)OCH_3 + M \longrightarrow CH_3OC(O)OCH_3 + H + M \qquad (32)$$

In contrast to the yield of $CH_3OC(O)OCH_3$ the yield of CH_3OCH_2OCHO was sensitive to the O_2 concentration. As shown in Figure **16** the yield of CH_3OCH_2OCHO does not approach zero at the lowest O_2 concentration. Such behaviour suggest that there are at least two reaction channels by which CH_3OCH_2OCHO is formed; one is dependent upon O_2, the other is not.

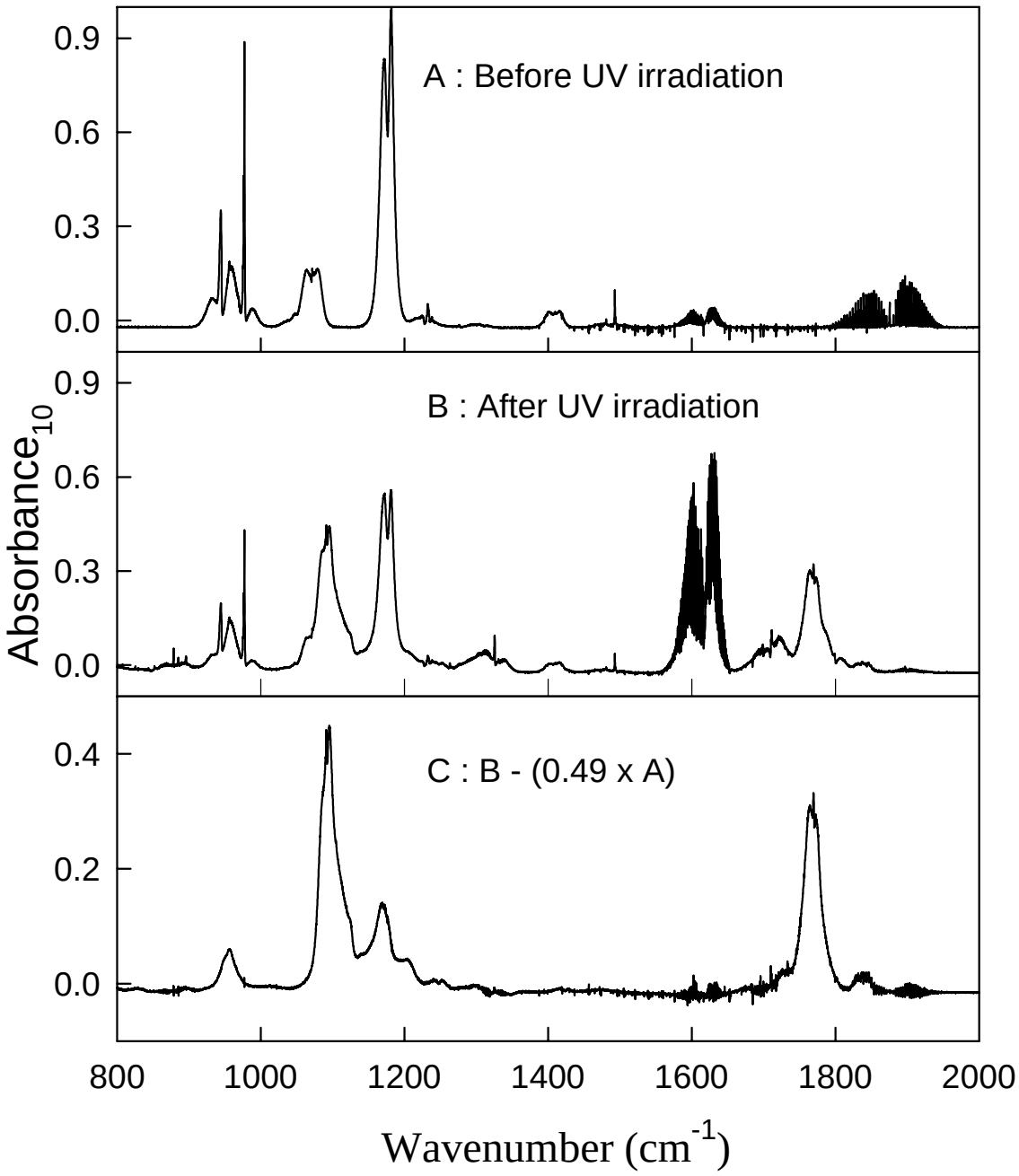

Figure 15. IR spectra acquired before (A) and after (B) a 30 second irradiation of a mixture of 8.0 mTorr of 1,3,5-trioxane, 87 mTorr of Cl_2, 12 mTorr of NO, and 592 Torr of O_2 in 700 Torr total pressure of N_2 diluent. During the irradiation 51% of the 1,3,5-trioxane was consumed. Subtraction of features attributable to 1,3,5-trioxane, NO, NO_2, $ClNO$, $ClNO_2$, $HONO$, $HONO_2$, and HO_2NO_2 from panel B gives panel C. The IR features at 957, 1091, 1168, and 1769 cm^{-1} in panel C are assigned to methylene glycol diformate, $HC(O)OCH_2OC(O)H$.

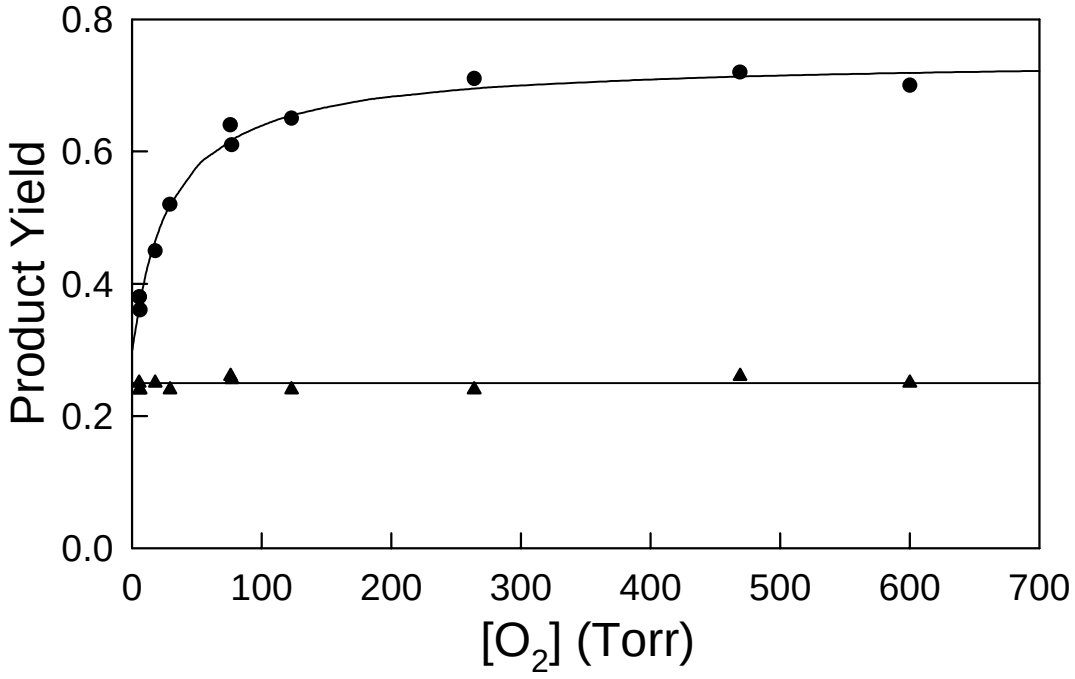

Figure 16. Observed yields of methoxymethyl formate (circles) and dimethyl carbonate (triangles) versus the O_2 partial pressure. The curve through the methoxymethyl formate data is a fit to the experimental data. The line through the dimethyl carbonate data reflects a constant yield of 0.25.

$$CH_3OCH_2OCH_2O\bullet + M \longrightarrow CH_3OCH_2OCOH + H + M \qquad \textbf{(33)}$$

$$CH_3OCH_2OCH_2O\bullet + O_2 \longrightarrow CH_3OCH_2OCOH + HO_2 \qquad \textbf{(34)}$$

$$CH_3OCH_2OCH_2O\bullet \longrightarrow \text{other products} \qquad \textbf{(35)}$$

The expected dependence of the yield of CH_3OCH_2OCHO on the O_2 partial pressure can be expressed as:

$$Y(CH_3OCH_2OCHO) = Y(CH_3OCH_2OCH_2O\bullet)\left(\frac{(\frac{k_{34}}{k_{33}})[O_2]+1}{(\frac{k_{34}}{k_{33}})[O_2]+1+(\frac{k_{35}}{k_{33}})}\right) \qquad \textit{(eq. 7)}$$

where $Y(CH_3OCH_2OCH_2O(\bullet))$ is the molar yield of $CH_3OCH_2OCH_2O(\bullet)$ radicals in the system and k_{33}, k_{34}, and k_{35} are rate constants for reactions (**33**), (**34**), and (**35**), respectively. The above expression was fitted to the data in Figure **16** with three parameters varied simultaneously: k_{34}/k_{33}, k_{35}/k_{33}, and $Y(CH_3OCH_2OCH_2O(\bullet))$. The obtained fit is shown in Figure **16**. A value of $0.74 \pm 0.05 = Y(CH_3OCH_2OCH_2O(\bullet))$ was obtained from the fit. This value is in good agreement with an expected value of 0.75 ± 0.02 obtained from a yield of 0.25 ± 0.02 of $CH_3OC(O)OCH_3$. Using the obtained values of k_{34}/k_{33}, k_{35}/k_{33} it was calculated that at 298 K and in the presence of 1 atm of air reactions (**33**)-(**35**) account for $7 \pm 3\%$, $84 \pm 4\%$, and $9 \pm 5\%$, respectively. So far the initial oxidation reaction in these experiments was reaction between Cl atoms and $CH_3OCH_2OCH_3$. In the atmosphere the initial

oxidation of $CH_3OCH_2OCH_3$ is reaction with the OH radical. An experiment using OH radicals instead of Cl atoms was performed. A yield of 0.24 ± 0.02 of $CH_3OC(O)OCH_3$ was obtained, indicating that the relative importance of H atom abstraction from the two possible sites in $CH_3OCH_2OCH_3$ is directly proportional to the number of different C-H bonds.

8.2 Atmospheric Fate of $(CH_3O)_3CO(\bullet)$ and $(CH_3O)_2CHOCH_2O(\bullet)$ Radicals

The $(CH_3O)_3CO_2(\bullet)$ and $(CH_3O)_2CHOCH_2O_2(\bullet)$ radicals formed during the oxidation of $(CH_3O)_3CH$ will react with NO via reaction (**26**a) to give two different alkoxy radicals, the $(CH_3O)_3CO(\bullet)$ and the $(CH_3O)_2CHOCH_2O(\bullet)$ radical. When the oxidation of $(CH_3O)_3CH$ is initiated by reaction with OH radicals it was determined that the ratio $(CH_3O)_3CO(\bullet)/(CH_3O)_2CHOCH_2O(\bullet)$ was 1/9. This ratio was obtained by comparing the rate constant for reactions between OH radicals and CH_3OCH_3, $CH_3OCH_2OCH_3$, $(CH_3O)_3CH$ and $(CH_3O)_4C$ and the reactivity of a single -OCH_3 group. The rate constant values are listed in Table **1**. During the time of the experiment a significant part (30%) of the $(CH_3O)_3CH$ was hydrolysed to give CH_3OCHO. After correction of formation of CH_3OCHO a yield of 81 ± 10% of $(CH_3O)_2CO$ was observed from the fate of the two alkoxy radicals. The $(CH_3O)_3CO(\bullet)$ radical is expected to eliminate $CH_3O(\bullet)$ radicals via reaction (**36**) to give $(CH_3O)_2CO$, whereas $(CH_3O)_2CHOCH_2O(\bullet)$ radicals form $(CH_3O)_2CO$ via reaction (**37**) and (**38**).

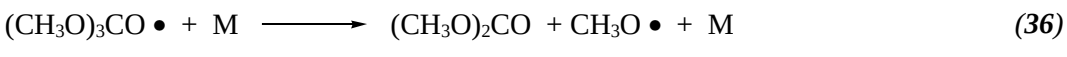

(36)

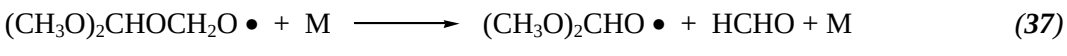

(37)

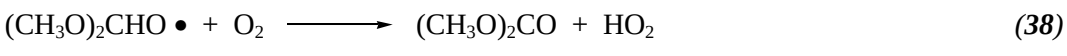

(38)

The fate of the remaining 19% of the $(CH_3O)_3CH$ is unknown.

8.3 Atmospheric Fate of $(c\text{-}C_4H_7O_2)O(\bullet)$ and $(c\text{-}C_3H_5O_3)O(\bullet)$ Radicals

When 1,4-dioxane and 1,3,5-trioxane are oxidised in the atmosphere $(c\text{-}C_4H_7O_2)O(\bullet)$ and $(c\text{-}C_3H_5O_3)O(\bullet)$ radicals will be formed. There are two possible fates for both radicals: reaction with O_2 forming a lactone and HO_2, reactions (**39**) and (**40**), or breaking up the 6 membered ring forming a new radical, reactions (**41**) and (**42**).

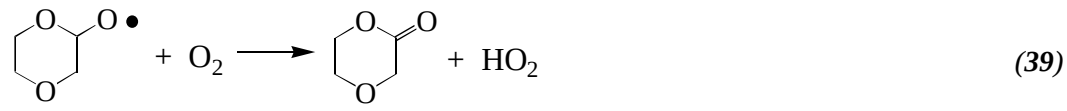

(39)

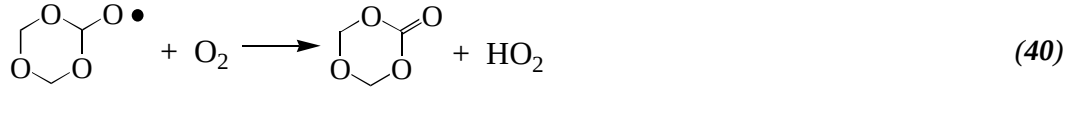

(40)

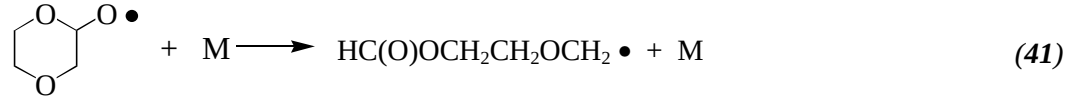

(41)

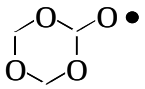

+ M ⟶ HC(O)OCH$_2$OCH$_2$O • + M *(42)*

HC(O)OCH$_2$CH$_2$OCHO (ethylene glycol diformate) and HC(O)OCH$_2$OCHO (methylene glycol diformate) were the only carbon containing product in the 1,4-dioxane and 1,3,5-trioxane experiments, respectively. No evidence for formation of lactones were observed. Under the experimental conditions used HC(O)OCH$_2$CH$_2$OCHO is obtained from the HC(O)OCH$_2$CH$_2$OCH$_2$O(•) radical via reactions (**43**)-(**45**).

HC(O)OCH$_2$CH$_2$OCH$_2$ • + O$_2$ + M ⟶ HC(O)OCH$_2$CH$_2$OCH$_2$O$_2$ • + M *(43)*

HC(O)OCH$_2$CH$_2$OCH$_2$O$_2$ • + NO ⟶ HC(O)OCH$_2$CH$_2$OCH$_2$O • + NO$_2$ *(44)*

HC(O)OCH$_2$CH$_2$OCH$_2$O • + O$_2$ ⟶ HC(O)OCH$_2$CH$_2$OCHO + HO$_2$ *(45)*

The formation of HC(O)OCH$_2$CH$_2$OCHO was not dependent on the O$_2$ concentration between 5.2 and 595 Torr O$_2$. As mentioned in section 8.1 it is not possible to exclude the reaction where the HC(O)OCH$_2$CH$_2$OCH$_2$O(•) radical dissociates to give HC(O)OCH$_2$CH$_2$OCHO and a H atom. Nese *et al*. [62] have studied the behaviour of the alkoxy radical (c-C$_4$H$_7$O$_2$)O(•) in oxygenated aqueous solutions and report that decomposition via reaction (**41**) is the dominant fate of (c-C$_4$H$_7$O$_2$)O(•) radicals in such systems. The present result obtained in the gas phase is entirely consistent with those reported by Nese *et al*. [62] obtained from a similar study in the liquid phase.

The formation of HC(O)OCH$_2$OCHO from the HC(O)OCH$_2$OCH$_2$O(•) radical is dependent on the O$_2$ concentration under ~100 Torr of O$_2$. A plot of the yield of HC(O)OCH$_2$OCHO versus O$_2$ concentration (similar to Figure **16**) gives a intercept of approximately 0.7. This suggest that there must be at least two channels giving HC(O)OCH$_2$OCHO, one is depending on oxygen the other is not. By a fit to the data it was established that in 1 atmosphere of air 96% of oxidised 1,3,5-trioxane gives HC(O)OCH$_2$OCHO, see Appendix D for details.

9 Atmospheric Fate of Cyclohexane

The atmospheric fate of cyclohexane has been studied by Aschmann *et al.* [63] and Tagagi *et al.* [64]. There is great discrepancy between the reported results (9 - 16% nitrate yield formed via reaction (**46**b)). The goal of this part of the work was to measure the nitrate yield formed via reaction (**46**b) and to determine the rate constant ratio k_{48}/k_{47}. To achieve this goal experiments were conducted using flash photolysis of mixtures of c-C$_6$H$_{12}$/Cl$_2$/O$_2$/N$_2$ in 700 Torr total pressure at 296 ± 2 K. In the atmosphere c-C$_6$H$_{11}$(•) radicals are formed via H atom abstraction by the OH radical. This alkyl radical rapidly adds O$_2$ (lifetime of 15 ns) to give the c-C$_6$H$_{11}$O$_2$(•) radical. There are two reaction channels for reactions between the c-C$_6$H$_{11}$O$_2$(•) radical and NO.

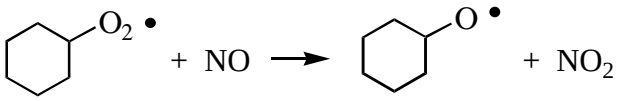

(**46**a)

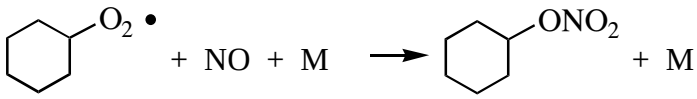

(46b)

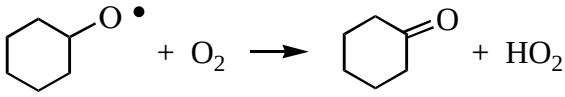

(47)

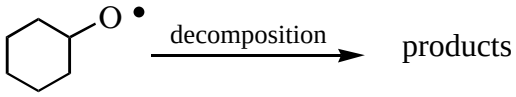

(48)

The c-$C_6H_{11}O(\bullet)$ radical formed via reaction (**46**a) has two possible fates, reactions (**47**) and (**48**). Cyclohexanone was observed as a significant product in these experiments. Aschmann *et al*. have shown the existence of $HC(O)(CH_2)_5ONO_2$, $HC(O)(CH_2)_4CHO$, and $HC(O)CH_2CH(OH)CH_2CH_2CHO$ formed after decomposition of the alkoxy radical. These products have never been quantified. Experiments were performed using $[O_2]$ = 50-595 Torr. The cyclohexanone yield increased with increasing O_2 concentration reflecting a competition between reactions (**47**) and (**48**) for the available cyclohexoxy radicals produced in reaction (**46**a). For the experiment using $[O_2]$ = 595 Torr the cyclohexanone yield is 70%. The dominant fate of cyclohexoxy radicals is reaction with O_2 and complications caused by nitrates formed subsequent to the decomposition of cyclohexoxy radicals should be of minor importance. The c-$C_6H_{11}ONO_2$ yield was estimated using an integrated absorption cross section for the IR band centred at 1281 cm^{-1} of 2.7 x 10^{-17} cm $molecule^{-1}$ (average of values reported in [65], see Appendix I). Figure **17** shows c-$C_6H_{11}ONO_2$ formation versus c-C_6H_{12} loss (corrected for the formation of a small amount of c-$C_6H_{11}O_2NO_2$ via reaction between c-$C_6H_{11}O_2(\bullet)$ radical and NO_2) from experiments conducted using $[O_2]$ = 595 Torr. A linear least squares regression fit of the data in Figure **17** gives $k_{46b}/(k_{46a} + k_{46b}) = 0.197 \pm 0.010$. Incorporating an estimated uncertainty of 15% in the integrated cross section of 2.7 x 10^{-17} gives $k_{46b}/(k_{46a} + k_{46b}) = 0.197 \pm 0.031$. It should be noted that this approach overestimates the branching ratio because of the possible contribution of nitrates formed subsequent to decomposition of the cyclohexoxy radicals via reaction (**48**). This point is addressed at the end of this section.

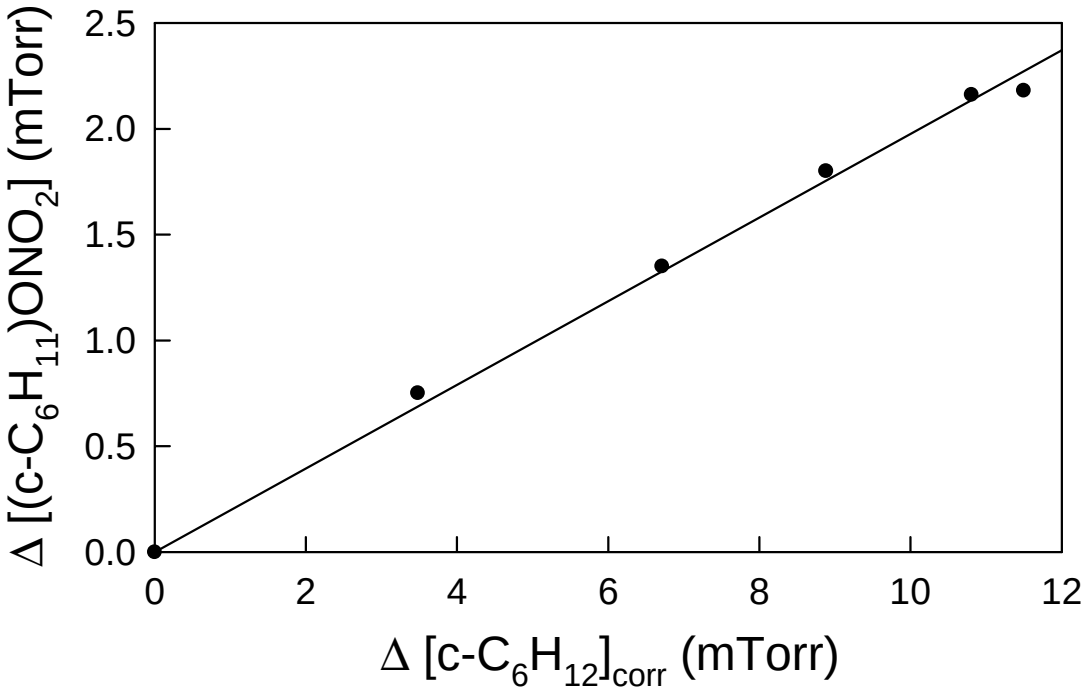

Figure 17. Yield of (c-C_6H_{11})ONO_2 following the UV irradiation c-C_6H_{12}/Cl_2/NO/O_2/N_2 mixtures as a function of the c-C_6H_{12} loss (corrected for formation of (c-C_6H_{11})O_2NO_2) at constant total pressure (700 or 750 Torr) and 296 ± 2K. The fit through the data is a linear least squares regression which gives a (c-C_6H_{11})ONO_2 yield of 19.7 ± 0.1%.

Reactions (**47**) and (**48**) compete for the cyclohexoxy radicals produced in reaction (**46**a). Defining α as the yield of cyclohexoxy radicals from reaction (**46**), $\alpha = k_{46a}/(k_{46a} + k_{46b})$, then the molar yield of cyclohexanone, Y(c-$C_6H_{10}O$), can be expressed as:

$$Y(c-C_6H_{10}O) = \alpha \times \left(\frac{k_{47}[O_2]}{(k_{48}[O_2] + k_{48})} \right) \qquad \textit{(eq.8)}$$

and

$$\frac{1}{Y(c-C_6H_{10}O)} = \frac{1}{\alpha} \times \frac{k_{48}}{k_{47}} \times \frac{1}{[O_2]} + \frac{1}{\alpha} \qquad \textit{(eq.9)}$$

Where k_{47} and k_{48} are rate constants for reactions (**47**) and (**48**). Cyclohexanone yields at different O_2 concentrations were obtained from linear least squares regression fits of plots of cyclohexanone formations versus c-C_6H_{12} consumptions. Figure **18** shows a plot of 1/Y(c-$C_6H_{10}O$) versus 1/[O_2]. The filled circles in Figure **18** are results from the present work. The open circle in Figure **18** is the cyclohexanone yield observed during cyclohexane oxidation in air reported by Aschmann *et al.* [63]. The fit shown in Figure **18** is a linear least squares regression fit to both data sets giving an intercept of $1/\alpha = 1.11 \pm 0.15$ and a slope of $(1/\alpha) \times (k_{48}/k_{47}) = 279 \pm 20$ Torr, hence $k_{48}/k_{47} = 251 \pm 47$ Torr. Quoted errors in k_{48}/k_{47} include uncertainties in both the slope and the intercept. There is no literature data to compare with this result.

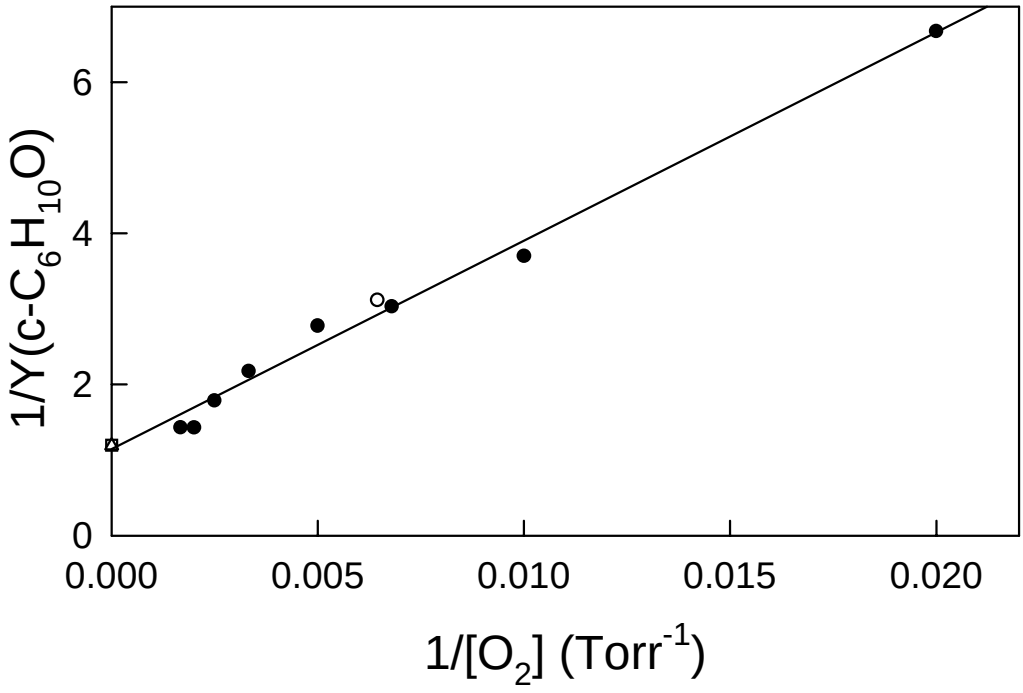

*Figure 18. Reciprocal yield of cyclohexanone following the UV irradiation of c-C_6H_{12}/Cl_2/NO/O_2/N_2 mixtures as a function of the reciprocal oxygen concentration at a total pressure of 700 or 750 Torr and 296 ± 2K. Closed circles are data obtained in this work. The open circle is taken from Aschmann et al. [**63**]. The open triangle and square are the limiting cases calculated using a (c-C_6H_{11})ONO_2 yield of 0.16 (this work) and 0.156 (Aschmann et al. [**63**]).*

At this point it is appropriate to return to the estimation of $k_{46a}/(k_{46a} + k_{46b}) = 0.197 \pm 0.031$ above and consider the likely impact of the formation of nitrates formed subsequently to decomposition of the cyclohexoxy radicals. Using k_{48}/k_{47} = 251 Torr it follows that in the presence of 595 Torr of O_2, 30% of the cyclohexoxy radicals will decompose via reaction (**48**) while the remaining 70% will react with O_2. Based upon the literature data base for hexyl peroxy and pentyl peroxy radicals [66] it is likely that 10-20% of the peroxy radicals formed following reaction (**47**) will react with NO to give nitrates. Correcting for the formation of such nitrates $k_{46b}/(k_{46a} + k_{46b}) = 0.16 \pm 0.04$, where the quoted error includes uncertainties associated with the correction procedure. This result is in good agreement with the value $k_{46b}/(k_{46a} + k_{46b}) = 0.156 \pm 0.017$ reported by Aschmann *et al* [63] but somewhat higher than that $k_{46b}/(k_{46a} + k_{46b}) = 0.09 \pm 0.04$ reported by Tagagi *et al*. [64]. The open triangle and square in Figure **18** are the limiting cases calculated using values of $k_{46b}/(k_{46a} + k_{46b}) = 0.16$ (derived above) and 0.156 [63]. This is consistent with expectations based upon extrapolation of cyclohexanone yields observed using experiments with $[O_2]$ = 50-592 Torr. At 296 K and one atmosphere of air, 61% of the c-$C_6H_{11}O(\bullet)$ radical decompose and 39% react to give cyclohexanone. It is interesting to compare this result with the atmospheric fate of 1,4-dioxane and 1,3,5-trioxane given in section 8.3. No evidence of formation of lactones were found in these studies suggesting that the fate of the (c-$C_4H_7O_2$)$O(\bullet)$ and (c-$C_3H_5O_3$)$O(\bullet)$ radicals allways is decomposition of the six membered ring.

10 Atmospheric Fate of $C_6H_5O(\bullet)$ Radicals

The aim of this part of the work was to provide information concerning the likely atmospheric fate of $C_6H_5O(\bullet)$ radicals. To obtain this goal smog chamber experiments were performed at Ford Motor Company. $C_6H_5O(\bullet)$ radicals were obtained by irradiation of C_6H_5OH/Cl_2 at 700 Torr total pressure and at 296 ± 2 K, as discussed in section 6.1.4.

10.1 Fate of $C_6H_5O(\bullet)$ Radicals Formed in the Smog Chamber at Ford

When studying the fate of the $C_6H_5O(\bullet)$ radicals in the smog chamber two facts need to be considered. First; reaction between $C_6H_5O(\bullet)$ radicals and O_2 is extremely slow ($k_{C6H5O(\bullet)+O2} < 5 \times 10^{-21}$ cm^3 molecule^{-1} s^{-1}, see section 7.2.2). Second; dark reaction (in the smog chamber) between C_6H_5OH and Cl_2 given ortho- and para chlorophenol with a rate of $k_{C6H5OH+Cl2} \leq 1.9 \times 10^{-20}$ cm^3 molecule^{-1} s^{-1}, see Appendix F for details. Figure **19** shows examples of FTIR spectra obtained in this study. The spectra were obtained before and after irradiation of a mixture of C_6H_5OH/Cl_2. The product spectrum in panel C Figure **19** represents features attributable to an unknown product(s) "X". Given that reaction with O_2 is unimportant, a number of other possibilities for the source of the unknown compound(s) "X" in the smog chamber experiments are considered:

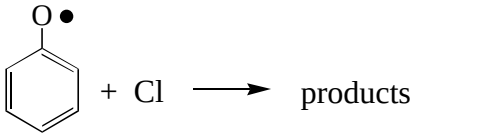

(49)

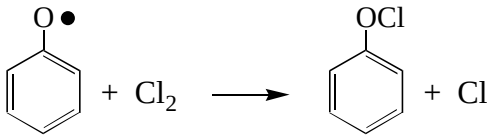

(50)

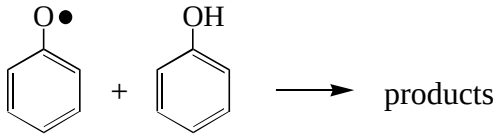

(51

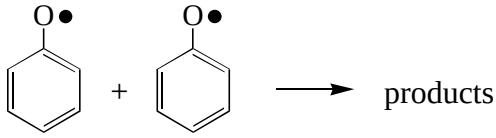

(52

Reaction of Cl atoms with C_6H_5OH proceeds at a rate of $k_{C6H5OH+Cl} = (1.93 \pm 0.36) \times 10^{-10}$ cm^3 molecule^{-1} s^{-1} (see Table 4). For low consumption's (< 20%) of C_6H_5OH reaction (**49**) will not play any significant role, but the concentration of "X" was observed to increase linearly over the entire range of C_6H_5OH consumption's used (17 to 85%). This concludes that reaction (**49**) is not the source of "X".

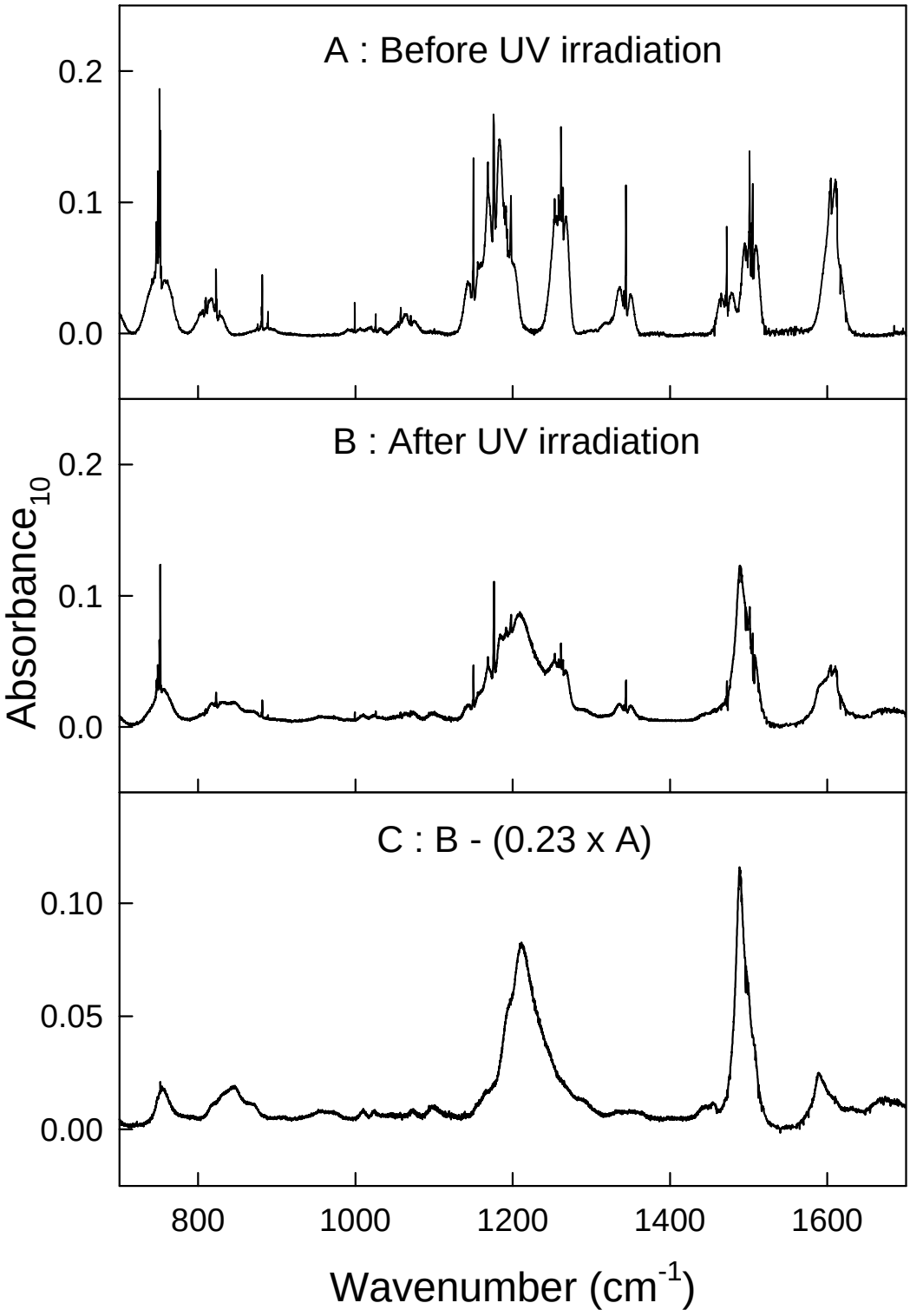

Figure 19. IR spectra acquired before (A) and after (B) a 60 second irradiation of a mixture of 5.5 mTorr of C_6H_5OH and 44 mTorr of Cl_2 in 700 Torr total pressure of O_2 diluent. During the irradiation 73% of the C_6H_5OH was consumed. Subtraction of features attributable to C_6H_5OH and chlorophenol from panel B gives panel C. The IR features in panel C are ascribed to the product of the self-reaction of $C_6H_5O(\bullet)$ radicals.

To establish whether "X" could be the phenyl hypochlorite (C_6H_5OCl), formed via reaction of $C_6H_5O(\bullet)$ radicals with Cl_2, W. F. Schneider used electronic structure calculations to estimate the thermodynamics of reaction (**50**). The result of the calculations gave reaction (**50**) to be endothermic by 32 kcal mol^{-1} at 298 K. Given the highly unfavourable thermodynamics of reaction (**50**) it is concluded that this reaction is unimportant in the system and "X" is not C_6H_5OCl.

The product(s) "X" must arise, then, from either the self-reaction of $C_6H_5O(\bullet)$ radicals or their reaction with C_6H_5OH. It is unlikely that these two pathways can be distinguished based on the identity of "X". Two other pieces of evidence argue against reaction (**51**), however. First, Berho and Lesclaux have reported the results of a study of the kinetics of the $C_6H_5O(\bullet)$ radical self-reaction in the presence of 3-12 mTorr of phenol [40]. The loss of $C_6H_5O(\bullet)$ radicals followed second order kinetics and was insensitive to variation of the phenol concentration suggesting reaction (**51**) is of negligible importance. Second, Buth *et al.* [39] monitored the loss of phenol in the presence of Cl atoms in a discharge flow study of reaction between Cl atoms and C_6H_5OH. Variation of the initial phenol concentration over the range 0.2-3.7 mTorr had no discernible impact on the measured value of this reaction, suggesting, but not proving, that reaction (**51**) is not significant.

It is most likely, then, that the product(s) "X" arise from the self-reaction of $C_6H_5O(\bullet)$ radicals. In considering the possible products of reaction (**52**), the electronic structure of $C_6H_5O(\bullet)$ radicals can be represented as an admixture of three principle resonance structures, which are expected to dominate in determining self-reaction products.

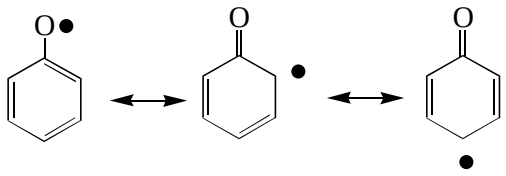

Density functional calculations predict Mulliken spin densities of 0.40, 0.27, and 0.36 electrons at the phenoxy oxygen, ortho, and para carbon positions, respectively. In contrast, the meta position has a Mulliken spin density of only –0.10 electrons. Assuming the most probable products of the self-reaction to be those arising from dimerization of the phenoxy radical at these radical centers, then 3! = 6 products are possible, which are shown below. It seems most likely that "X" is one, or some combination of, these six species.

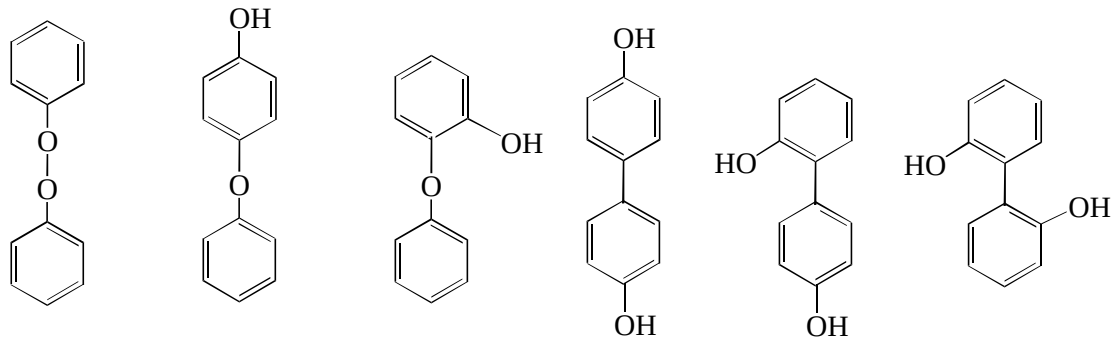

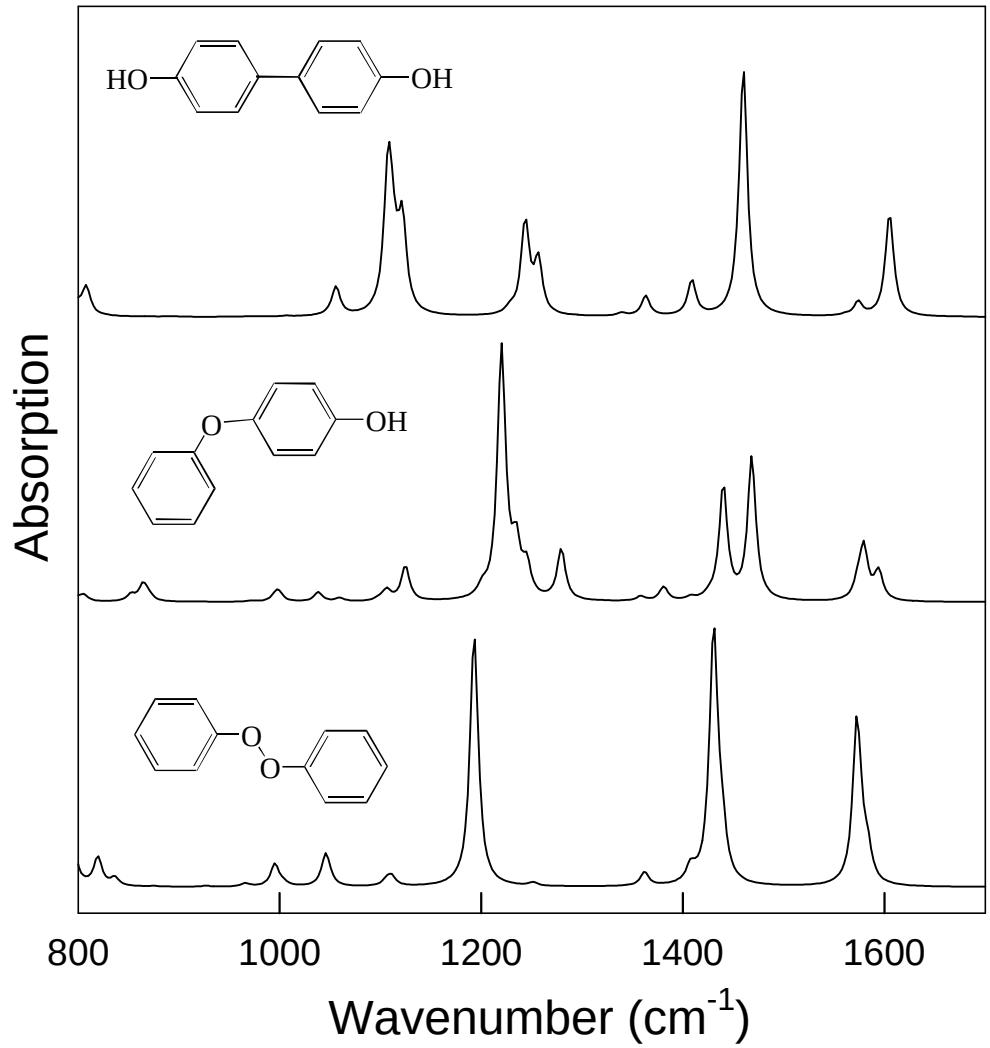

Figure 20. LSDA calculated vibrational spectra of three possible products of phenoxy radical self-reaction. Frequencies scaled by 0.97, and bands artificially broadened by 10 cm^{-1}.

Density functional theory was used to investigate the structures, energetics, and vibrational spectra of the biphenyl peroxide and a representative ether (4-phenoxyphenol) and biphenyl (4,4′-biphenol). Calculated (LDA) vibrational spectra for these three isomers is shown in Figure **20**. Even though, the experimental spectrum of the unknown "X", have broad and featureless bands the consistency between the experimental and calculated spectre is remarkable. Unfortunately it is not possible to identify "X" on the basis of its vibrational spectrum, except for that it likely includes some combination of the six self-reaction products suggested above.

Calculations of the energetics of formation of the three phenoxy radical dimers give

$2\ C_6H_5O(\bullet) \rightarrow C_6H_5OOC_6H_5$ $\quad \Delta H°_{298} = +2.2\ kcal\ mol^{-1}$

$2\ C_6H_5O(\bullet) \rightarrow 4\text{-}C_6H_5OC_6H_4OH$ $\quad \Delta H°_{298} = -51.3\ kcal\ mol^{-1}$

$2\ C_6H_5O(\bullet) \rightarrow 4,4'\text{-}HOC_6H_4C_6H_4OH$ $\quad \Delta H°_{298} = -60.6\ kcal\ mol^{-1}$

Formations of both the ether and biphenyl are substantially exothermic and equally likely on thermodynamic grounds. Combined with the heat of formation of $C_6H_5O(\bullet)$ [67], the obtained heats of formation are –28 and –38 kcal mol^{-1} for 4-$C_6H_5OC_6H_4OH$ and 4,4′-$HOC_6H_4C_6H_4OH$, respectively. It is expected that the other ether and biphenyl isomers have similar energetics. In contrast, formation of the peroxide is predicted to be slightly endothermic from the direct calculation suggesting that $C_6H_5OOC_6H_5$ not is one of the products from reaction (**52**).

To provide further information of "X" product mixtures were analysed using a GC-MS technique. The $(C_6H_5O)_2$ isomers have a molecular weight of 186 mass units. A mass 186 was found to be the major contribution of the obtained total ion chromatogram. The fragmentation pattern of each 186 mass ion showed a loss of the following three fragments: a 17 mass fragment (OH), a 28 mass fragment (CO), and a 29 mass fragment (CHO). These fragments are expected from phenolic compounds [68] and are consistent with the formation of the $(C_6H_5O)_2$ dimer. Authentic reference samples of 2,2′-biphenol, 4,4′-biphenol, and 4-phenoxyphenol were available and the response of the GC-MS system was tested for these compounds. From its retention time and fragmentation pattern the largest 186 mass product peak was identified as 4-phenoxy phenol. The results obtained using the GC-MS system are entirely consistent with the conclusions based from the analysis above that the major fate of phenoxy radicals in the experiments is self-reaction.

10.2 Fate of $C_6H_5O(\bullet)$ Radicals in Moderately Polluted Urban Atmosphere

The reaction of $C_6H_5O(\bullet)$ radicals with O_2 is extremely slow ($k_{C6H5O(\bullet)+O2} < 5 \times 10^{-21}$ cm^3 $molecule^{-1}$ s^{-1} at 296 K). In contrast to their behaviour towards O_2, $C_6H_5O(\bullet)$ radicals react rapidly with NO and NO_2 with rate constants of $(1.88 \pm 0.16) \times 10^{-12}$ and $(2.08 \pm 0.15) \times 10^{-12}$ cm^3 $molecule^{-1}$ s^{-1} at 296 K, see section 7.4 and Appendix F. In moderately polluted urban atmospheres the concentration of NO_x (NO + NO_2) is typically 1-10 ppb, i.e., 10^8-10^7 times less than that of O_2. From the present work the conclusion is that $C_6H_5O(\bullet)$ radicals react at least 4×10^8 times more rapidly with NO_x than with O_2. It then follows that under conditions typical of moderately polluted urban air, reaction of $C_6H_5O(\bullet)$ radicals with O_2 is not important. It seems likely that the fate of $C_6H_5O(\bullet)$ radicals in such environments will be reaction with NO_x which will presumably lead to the formation of nitroso- and nitro-phenols thereby sequestering NO_x and slowing down the reactions responsible for ozone formation. It would be interesting for a future study to investigate the existence of nitroso- and nitro-phenols products from oxidation of phenol under conditions containing NO_x.

Conclusion

During the period where my Ph.D. work was performed, CH_3OCH_3 (DME) and $CH_3OCH_2OCH_3$ (DMM) have been tested as an alternative diesel fuel and a diesel additive, respectively. Haldor Topsoe and Volvo are performing a full scale test experiment using DME as a diesel fuel in busses. There are still problems to solve if DME is to be a conventional alternative diesel fuel. Scientists at Ford Motor Company have tested DMM by adding 16% of DMM to a conventional diesel fuel. They observed a decrease of the particle mass from the tailpipe emissions of 36 ± 8% together with a decrease in the mean size of the particles to a diameter of 80 - 100 nm. Unfortunately the number density for both the diesel fuel and the DMM/diesel fuel blend is the same.

The major conclusion is: "it will take years before ethers will play a significant role as diesel fuels or diesel additives".

A substantial body of new results regarding the atmospheric chemistry of CH_3OCH_3, $CH_3OCH_2OCH_3$, $(CH_3O)_3CH$, 1,4-dioxane, 1,3,5-trioxane, cyclohexane, and $C_6H_5O(\bullet)$ radicals are obtained in this work. The compounds were followed from the initial atmospheric oxidation by OH radicals to the final degradation product. The results falls into mainly two parts. First, absolute rate constants and UV absorption spectra obtained at Risoe National Laboratory. Second, relative rate constants and product studies of the atmospheric degradation of the studied compounds are obtained at Ford Motor Company.

At Risoe first order rate constants were obtained for a series of reactions. First, H atom abstraction by reactions between organic compounds and F atoms or OH radicals. Second, reactions between alkyl radicals and O_2 forming alkyl peroxy radicals. Third, reactions between alkyl peroxy radicals and NO_x (NO or NO_2). Fourth, second order rate constants for self-reactions of alkyl and alkyl peroxy radicals. The atmospheric lifetime with respect to oxidation initiated by OH radicals for the studied ethers were determined to be ≤ 94 hours. This means that the studied ethers can be transported thousands of kilometres before they are oxidised. In the atmosphere the studied ether alkyl radicals react rapidly with O_2 with a lifetime less than 0.003 μs. A very interesting result is that the atmospheric fate of $C_6H_5O(\bullet)$ radicals is reaction with NO_x, instead of reaction with O_2. The lifetime with respect to reaction between $C_6H_5O(\bullet)$ radicals and NO_x is approximately 0.02 s (using $[NO_x]$ = 1ppb). Recently a rate constant of $(2.86 \pm 0.35) \times 10^{-13}$ cm^3 $molecule^{-1}$ s^{-1} for the reaction between $C_6H_5O(\bullet)$ radicals and O_3 has been reported [69]. This result indicate that there will be a competition for the $C_6H_5O(\bullet)$ radicals between NO_x and O_3. Further investigations of these phenoxy radical reactions are clearly needed. What are the chemical structure of the molecules formed by reaction between $C_6H_5O(\bullet)$ radical and O_3 or NO_x ? Can the reported rate constant for the reaction between $C_6H_5O(\bullet)$ radical and O_3 be confirmed ?

At Ford relative rate constants were measured for reactions between Cl atoms and a series of organic compounds. An interesting result is that reaction between Cl atoms and 2-chlorophenol is approximately 25 times less than the reactions between Cl atoms and 3-chlorophenol or 4-chlorophenol. Another surprising result obtained during the product studies is that the fate of $(c\text{-}C_4H_7O_2)O(\bullet)$ and $(c\text{-}C_3H_5O_3)O(\bullet)$ radicals are decomposition via ring opening. The fate of $c\text{-}C_6H_{11}O(\bullet)$ is a composition between decomposition via ring opening and reaction with oxygen forming a significant yield of the cyclohexanone even at low O_2 concentrations.

There are still lots of unsolved chemical problems related to the atmosphere and traffic pollution. An area that needs careful attention and that during my Ph.D. work caught my interest, is the atmospheric chemistry of aromatic compounds. Kinetic and mechanistic data concerning both gas phase and heterogeneous reactions need to be obtained and built into global atmospheric climate models.

References

1. Kwok, E. S. C.; Atkinson, R., *Atmos. Environ.*, **1995**, *29*, 1685-1695.
2. IPCC report *Climate Change 1994*.
3. IPCC report *Climate Change 1995*.
4. Danmarks Energifremtider, *Energiministeriet*, **1995**.
5. Roubi, M. A., *Chem. & Eng.*, **1995**, 44, 37.
6. Ellermann, T., *Risoe-M-2932*, **1991**.
7. Sehested, J., *Risoe-R-804(EN)*, **1995**.
8. Hansen, K. B.; Wilbrandt, R.; Pagsberg, P., *Rev. Sci. Instr.* **1979**, *50*, 1532.
9. Wallington, T. J.; Japar, S. M., *J. Atmos. Chem.*, **1989**, *9*, 399.
10. Rasmussen, O.L.; Bjergbakke, E.B., *Risoe-R-395* , **1984**.
11. Braun, W.; Herron, J. T.; Kahaner, D. K., *Int. J. Chem. Kinet.*, **1988**, *20*, 51.
12. Markert, F., **1993**, Ph.D. Thesis.
13. Seinfeld, J. H.; Pandis, S. N., *Atmospheric Chemistry and Physics*, **1998**.
12. Atkinson, R., *J. Phys. Chem. Ref. Data,* **1989**, Monograph.
15. Nielsen, O. J.; O´Farrel, D. J.; Treacy, J. J.; Sidebottom, H. W., *Environ. Sci. Technol.*, **1991**, *25*, 1098.
16. Nielsen, O. J.; Sidebottom, H. W.; Donlon, M, *J. Chem. Phys. Lett.*, **1991**, *178*, 163.
17. Markert, F.; Nielsen, O. J., *J. Chem. Phys. Lett.*, **1992**, *194*, 123.
18. Ravishankara, A. R.; Lovejoy, E. R., *J. Chem. Soc. Faraday Trans.*, **1994**, *90*, 2159.
19. Dorn, H.-P.; Brandenburger, U.; Brauers, T.; Ehhalt, D. H., *Geophys. Res. Lett.*, **1996**, *23*, 2537.
20. Hofzumahaus, A.; Aschmutat, U.; Hessling, M.; Holland, F.; Ehhalt, D.H., *Geophys. Res. Lett.*, **1996**, *23*, 2541.
21. Dagaut, P.; Liu, R.; Wallington, T. J.; Kurylo, M. J., *J. Phys. Chem.*, **1989**, *93*, 7838.
22. Porter, E.; Wenger, J.; Treacy, J.; Sidebottom, H.; Mellouki, A.; Téton, S.; LeBras, G., *J. Phys. Chem.*, **1997**, *101*, 5770-5775.
23. Perry, R. A.; Atkinson, R.; Pitts, J. N., *J. Chem. Phys.*, **1977**, 67, 611.
24. Tully, F. P.; Droege, A. T., *Int. J. Chem. Kinet.*, **1987**, 19, 251.
25. Wallington, T. J.; Lui, R.; Dagaut, P.; Kurylo, M. J., *Int. J. Chem. Kinet.*, **1988**, 20, 41.
26. Porter, E.; Wenger, J.; Treacy, J.; Sidebottom, H.; Mellouki, A.; Téton, S.; LeBras, G., *J. Phys. Chem.*, **1997**, 101, 5770-5775.
27. Dagaut, P.; Wallington, T. J.; Liu, R.; Kurylo, M. J., 22nd International Symposium on Combustion, **1988**, August, Seattle, 14-19.
28. Zabarnick, S.; Flemming, J. W.; Lin, M. C., *int, J. Chem. Kinet.*, **1988**, 20, 117.
29. Langer, S.; Ljungström, E.; Ellermann, T.; Nielsen, O.J.; Sehested, *Chem. Phys. Lett.* **1995**, *240*, 53.
30. Schuler, R. H.; Patterson, L. K., *Chem. Phys. Lett.*, **1974**, *27*, 369.
31. Porter, G.; Ward, B., *Proc. R. Soc. London A*, **1965**, *287*, 457.
32. Cercek, B.; Kongshaug, M., *J. Phys. Chem.*, **1970**, *74*, 4319.
33. Hassanzadeh, P.; Miller, J. H., *J. Phys. Chem.*, **1992**, *96*, 6570.
34. Engert, J. M.; Dick, B., *Appl. Phys. B*, **1996**, *63*, 531.
35. Miller, J. H.; Andrews, L.; Lund, P. A.; Schatz, P. N., *J. Chem. Phys.*, **1980**, *73*, 4932.

36. Ikeda, N.; Nakashima, N.; Yoshihara, K., *J. Am. Chem. Soc*, **1985**, *107*, 3381.

37. Tanaka, J., *Nippon Kagaku Zasshi*, **1958,** *79*, 1114.

38. Tabei, K.; Nagakura, S., *Bull. Chem. Soc. Jpn*., **1965**, *38*, 965.

39. Buth, R.; Hoyermann, K.; Seeba, J., *25th Symposium on Combustion*, The Combustion Institute, **1994**, 841.

40. Berho, F.; Lesclaux, R., *Chem. Phys. Lett.*, **1997**, *279*, 289.

41. Berho, F.; Caralp, F.; Rayez, M-T.; Lesclaux, R.; Ratajczak, E., *J. Phys. Chem. A*, **1998**, *102*, 1.

42. Kajii, Y.; Obi, K.; Nakashima, N.; Yoshihara, K., *J. Chem. Phys*. **1987**, 87, 5059.

43. Schuler, R.H.; Buzzard, G.K., *Int. J. Radiat. Phys. Chem.*, **1997**, 8, 563.

44. Sehested, K., private communication **1998.**

45. Maricq, M. M.; Szente, J. J. *J. Phys. Chem.* **1992**, *96*, 4925.

46. Lightfoot, P. D.; Cox, R. A.; Crowley, J. N.; Destriau, M.; Hayman, G. D.; Jenkin, M. E.; Moortgat, G. K.; Zabel, F. *Atmos. Environ.* **1992**, *26*, 1805.

47. Rowley, D. M.; Lightfoot, P. D.; Lesclaux, R.; Wallington, T. J., *J. Chem. Soc. Faraday Trans*., **1991**, *87*, 3221.

48. Hoyermann, K.; Nacke, F., *Twenty Sixth Int. Symp. on Comb*., Napoli, 28th July-2nd August, 1996.

49. Schuler, R H.; Patterson, L. K., *Chem. Phys. Lett*. **1974**, *27*, 369.

50. Mallard, W. G.; Westley, F.; Herron, J. T.; Hampson, R. F., *NIST Chemical Kinetics Database, Ver 6. 0, NIST Standard Reference Data, Gaithersburg, MD* **1994**.

51. Wu, D.; Bayes, K.D., I*nt. J. Chem. Kinet*, **1986**, 18, **547**.

52. Bjellqvist, B.; Reitberger, T.; K. Tek. Hoegsk., Stockholm, *Swed. Report (*1971), Issue INIS-mf-1104, 17 pp From: Nucl. Sci. Abstr. **1974**, 30(1), 120.

53. Braun, W.; Herron, J. T.; Kahaner, D. K., *Int. J. Chem. Kinet*., **1988,** 20, 51.

54. Park, J.; Lin, M. C., *J. Phys. Chem. A*, **1997**, *101*, 14.

55. Yu, T.; Lin, M. C., *J. Am. Chem. Soc*., **1993**, *115*, 4371.

56. Yu, T.; Lin, M. C., *J. Phys. Chem.*, **1994**, *98*, 2105.

57. Preidel, M.; Zellner, R., *Ber. Bunsen-Ges. Phys. Chem.*, **1989**, *93*, 1417.

58. Maricq, M. M.; Szente, J. J., *Chem. Phys. Lett.* **1992**, *96*, 4925.

59. Sehested, J., *Risoe-R-804(EN)*, **1995**, 63-69.

60. Sehested, J.; Nielsen, O. J.; Wallington, T. J. *Chem. Phys. Lett.* **1993**, *213*, 257.

61. Wallington, T. J.; Hurley, M. D., *Chem. Phys. Lett.*, **1992**, 189, 437.

62. Nese, C.; Schuchmann, M. N.; Steenken, S.; von Sonntag, C., *J. Chem. Soc. Perkin Trans 2* **1995,** 1037.

63. Aschmann, S. A.; Chew, A. A.; Arey, J.; Atkinson, R., *J. Phys. Chem.*, **1997**, *101*, 8042.

64. Takagi, H.; Washida, N.; Bandow, H.; Akimoto, H.; Okuda, M., *J. Phys. Chem*., **1981**, *85*, 2701.

65. Tuazon, E. C.; Atkinson, R., *Int. J. Chem. Kinet*., **1990**, 22, 1221.

66. Lightfoot, P. D.; Cox, R. A.; Crowley, J. N.; Destriau, M.; Hayman, G. D.; Jenkin, M. E.; Moortgat, G. K.; Zabel, F., *Atmos. Environ.* **1992**, *26*, 1805.

67. Atkinson, R.; Baulch, D. L.; Cox, R. A.; Hampson, R. F., Jr.; Kerr, J. A.; Troe, J., *J. Phys. Chem. Ref. Data* **1992**, 21, 1125.

68. Silverstein, R. M.; Bassler, G. C.; Morrill, T. C., "Spectrometric Identification of Organic Compounds", 5th Edition, **1991,** *John Wiley and Sons*, New York, NY.

69. Tao, Z.; Li Z., *Int. J. Chem. Kinet.*, **1999**, *31*, 65.

APPENDIX A

Jens Sehested, Knud Sehested, Jesper Platz, Helge Egsgaard, Ole J. Nielsen: ”Oxidation of Dimenthyl Ether: Absolute Rate Constant for the Self Reaction of CH_3OCH_2 Radicals, the Reaction of CH_3OCH_2 Radicals with O_2, and the Thermal Decomposition of CH_3OCH_2 Radicals”, Int. J. Chem. Kinet., 627, 29, 1997.

APPENDIX B

Timoty J. Wallington, Michael D. Hurley, James C. Ball, Ann M. Straccia, Jesper Platz, Lene Krogh Christensen, Jens Sehested, Ole J. Nielsen: ”Atmospheric Chemistry of Dimethoxymethane ($CH_3OCH_2OCH_3$): Kinetics and Mechanism of Its Reaction with OH Radicals and Fate of the Alkoxy Radicals $CH_3OCHO(\bullet)OCH_3$ and $CH_3OCH_2OCH_2O(\bullet)$”; J. Phys. Chem., 5302, 101, 1997.

APPENDIX C

Jesper Platz, Ole J. Nielsen, Trine Møgelberg, Jens Sehested, Timothy J. Wallington: ”Atmospheric Chemistry of 1,4-dioxane: Laboratory Studies”;, J. Chem. Soc., Fareday Trans., 2855, 93, 1997.

APPENDIX D

Jesper Platz, Lene K. Christensen, Ole J. Nielsen, Jens Sehested, Timothy J. Wallington, C. Sauer, Ian Barnes, Karl H. Becker, Rainer Vogt: ”Atmospheric Chemistry of 1,3,5-Trioxane: ”UV Spectra of c-$C_3H_5O_3$(•) and (c-$C_3H_5O_3$)O_2(•) Radicals, Kinetics of the Reactions of (c-$C_3H_5O_3$)O_2(•) Radicals with NO and NO_2, and Atmospheric Fate of the Alkoxy radical (c-$C_3H_5O_3$)O(•)”; J. Phys. Chem., 4829-4838, 102, 1997.

APPENDIX E

Timothy J. Wallington, Helge Egsgaard, Ole J. Nielsen, Jesper Platz, Jens Sehested, Thomas Stein: ”UV-visible spectrum of the phenyl radical and kinetics of its reaction with NO in the gas phase”; Chem. Phys. Lett., 363-370, 290, 1998.

APPENDIX F

Jesper Platz, Ole J. Nielsen, Jens Sehested, Timothy J. Wallington, Jim C. Ball, Mike D. Hurley, Ann M. Straccia, William F. Schneider: ”Atmospheric Chemistry of the Phenoxy Radical, $C_6H_5O(\bullet)$: UV Spectrum and Kinetics and Its Reaction with NO, NO_2, and O_2”; J. Phys. Chem. A, 7964-7974, 102, 1998.

APPENDIX G

Jesper Platz, Ole J. Nielsen, Jens Sehested, Timothy J. Wallington: ”Atmospheric Chemistry Trimethoxymethane, $(CH_3O)_3CH$; Laboratory Studies”; J. Phys. Chem., In press, 1998.

APPENDIX H

O. Sokolov, M.D. Hurley, T.J. Wallington, E.W. Kaiser, J. Platz, O.J. Nielsen, F. Berho, M.T. Rayez, R. Lesclaux: ”Kinetics and Mechanism of the Gas Phase Reaction of Cl atoms with Benzene”; J. Phys. Chem., In press, 1998.

APPENDIX I

Jesper Platz, Ole J. Nielsen, Jens Sehested, Timothy J. Wallington: ”Atmospheric Chemistry of Cyclohexane: ”UV Spectra of c-C_6H_{11}(•) and (c-C_6H_{11})O_2(•) Radicals, Kinetics of the Reactions of (c-C_6H_{11})O_2(•) Radicals with NO and NO_2, and Fate of the Alkoxy Radical (c-C_6H_{11})O(•)”; J. Phys. Chem., 1998. In press.

List of Publications

Papers

1. Sauer C. G., Barnes I., Becker K. H., Geiger H., Wallington T. J., Christensen L. K., Platz J., Nielsen O. J.: “Atmospheric chemistry of 1,3-dioxolane: Kinetic, mechanistic, and modeling study of OH radical initiated oxidation”; J. Phem. A, 5959-5966, 103, 1999.

2. T. N. N. Stein, L. K. Christensen, J. Platz, J. Sehested, O. J. Nielsen, T. J. Wallington: “Atmospheric Chemistry of $CF_3C(O)OCH_2CF_3$: UV Spectra and Kinetic Data for $CF_3C(O)OCH(\bullet)CF_3$ and $CF_3C(O)OCH(OO\bullet)CF_3$ Radicals, and Atmospheric Fate of $CF_3C(O)OCH(O\bullet)CF_3$ Radicals”; J. Phys. Chem. A, 5705-5713, 103, 1999.

3. Jesper Platz, Ole J. Nielsen, Jens Sehested, Timothy J. Wallington: “Atmospheric Chemistry of Cyclohexane: UV Spectra of $c\text{-}C_6H_5(\bullet)$ and $(c\text{-}C_6H_5)O_2(\bullet)$ Radicals, Kinetics of the Reactions of $(c\text{-}C_6H_5)O_2(\bullet)$ Radicals with NO and NO_2 and Fate of the Alkoxy Radical $(c\text{-}C_6H_5)O(\bullet)$”; J. Phys. Chem. A, 2688-2695, 103, 1999.

4. Jesper Platz, Ole J. Nielsen, Jens Sehested, Timothy J. Wallington: "Atmospheric Chemistry Trimethoxymethane, $(CH_3O)_3CH$; Laboratory Studies"; J. Phys. Chem. A, 2632-2640, 1999.

5. O. Sokolov, M. D. Hurley, T. J. Wallington, E. W. Kaiser, J. Platz, O. J. Nielsen, F. Berho, M. T. Rayez, R. Lesclaux: "Kinetics and Mechanism of the Gas Phase Reaction of Cl atoms with Benzene"; J. Phys. Chem. , 10671-10681, 102, 1998.

6. Jesper Platz, Ole J. Nielsen, Jens Sehested, Timothy J. Wallington, Jim C. Ball, Mike D. Hurley, Ann M. Straccia, William F. Schneider: "Atmospheric Chemistry of the Phenoxy Radical, $C_6H_5O(\bullet)$: UV Spectrum and Kinetics of Its Reaction with NO, NO_2 and O_2"; J. Phys. Chem. A, 7964-7974, 102, 1998.

7. Timothy J. Wallington, Helge Egsgaard, Ole J. Nielsen, Jesper Platz, Jens Sehested, Thomas Stein: "UV-visible spectrum of the phenyl radical and kinetics of its reaction with NO in the gas phase"; Chem. Phys. Lett., 363-370, 290, 1998.

8. Jesper Platz, Lene K. Christensen, Ole J. Nielsen, Jens Sehested, Timothy J. Wallington, C. Sauer, lan Barnes, Karl H. Beeker, Rainer Vogt: "Atmospheric Chemistry of 1,3,5-Trioxane: UV Spectra Of $C_3H_5O_3(\bullet)$ and $(C_3H_5O_3)O_2(\bullet)$ Radicals, Kinetics of the Reactions of $(C_3H_5O_3)O_2(\bullet)$ Radicals with NO and NO_2 and Atmospheric Fate of the Alkoxy radical $(C_3H_5O_3)O(\bullet)$ "; J. Phys. Chem., 4829-4838, 102, 1997.

9. Torben Nielsen, Jesper Platz, Kit Granby, Asger B. Hansen, Henrik Skov, Axel H. Egeløv: "Paticulate Orgainc Nitrates: Sampling and Night/Day Variation"; Atmos. Environ. 2601-2608, 14/15, 32, 1998.

10. Wallington T. J., Schneider W. F., Sehested J., Bilde M., Platz J., Nielsen O. J., Christensen L. K., Molina M. J., Molina L. T., Wooldridge P. W.; “Atmospheric chemistry of HFE-7100 ($C_4F_9OCH_3$): Reaction with OH radicals, UV spectra and kinetic data for $C_4F_9OCH_2$ center dot and $C_4F_9CH_2O_2$ center dot radicals, and the atmospheric fate of $C_4F_9OCH_2O$ center dot radicals”; J. Phys. Chem. A, 8264-8274, 101, 1997.

11. Timothy J. Wallington, A. Guschin, Jesper Platz, Thomas Stein, Jens Sehested, Ole J. Nielsen: "Atmospheric Chemistry of $CF_3CH(\bullet)OCH_2CF_3$: UV spectra and Kinetic Data for $CF_3CH(O\bullet)OCH_2CF_3$ and $CF_3CH(OO\bullet)OCH_2CF_3$ Radicals, Atmospheric Fate of the $CF_3CH(O\bullet)OCH_2CF_3$ Radicals"; J. Phys. Chem., 1152-1161, 102, 1997.

12. Jesper Platz, Ole J. Nielsen, Trine Møgelberg, Jens Sehested, Timothy J. Wallington:"Atmospheric Chemistry of 1,4-dioxane: Laboratory Studies"; J. Chem. Soc., Fareday Trans., 2855, 93, 1997.
13. Jens Sehested, Knud Sehested, Jesper Platz, Helge Egsgaard, Ole J. Nielsen: "Oxidation of Dimethyl Ether: Absolute Rate Constant for the Self Reaction of CH_3OCH_2 Radicals, the Reaction of CH_3OCH_2 Radicals with O_2 and the Thermal Decompotion of CH_3OCH_2 Radicals", Int. J. Chem. Kinet., 627, 29, 1997.

14. Timothy J. Wallington, Michael D. Hurley, James C. Ball, Ann M. Straccia, Jesper Platz, Lene Krogh Christensen, Jens Sehested, Ole J. Nielsen: "Atmospheric Chemistry of Dimethoxymethane ($CH_3OCH_2OCH_3$): Kinetics and Mechanism of Its Reaction with OH Radical and Fate of the Alkoxy Radicals $CH_3OCHO(\bullet)OCH_3$ and $CH_3OCH_2OCH_2O(\bullet)$"; J. Phys. Chem., 5302, 101, 1997.

15. Torben Nielsen, Ole Hertel, Kit Granby, Asger B. Hansen, Jesper Platz, Henrik Skov, Carsten S. Christensen, Axel H. Egeløv: "Comparison of measrements and modelling of ozone, other photochemical oxidants, precursors and atmospheric reaction products during a summer high pressure episode in Denmark; In Proc. of EUROTRAC Symposium16. Ed. By P.M. Borrel, T. Cvitas, K. Kelly, W Seiler, Computational Mechanics Publications, Southampton, Great Britain, 1996.

16. Henrik Skov, Carsten S. Christensen, Kit Granby, Axel H. Egeløv, Asger B. Hansen, Torben Nielsen, Jesper Platz: "Tropospheric ozone and other photochemical products measured at the TOR station at Ll. Valby, Denmark"; The oxidizing capacity of the troposphere. Abstracts of the 7th European Symp. on Physico-Chemical Behaviour of Atmospheric Pollutants. European Commision, 1996, p. 0-37.

17. Torben Nielsen, Ole Hertel, Carsten S. Christensen, Axel H. Egeløv, Kit Granby, Asger B. Hansen, Jesper Platz, Henrik Skov: "Evaluation of the Danish ACDEP model to simulate formation of tropospheric ozone, other photochemical oxidants and atmospheric reaction products"; The oxidizing capacity of the troposphere. Abstracts of the 7 th European Symp. on Physico-Chemical Behaviour of Atmospheric Pollutants. European Commision, 1996, p. 0-47.

18. Jesper Platz, Ole J. Nielsen, Jens Sehested, Timothy J. Wallington: "Atmospheric Chemistry of 1, 1, 1 -Trichloroethane: UV spectra and self-reaction Of CCl_3CH_2 and $CC1_3CH_2O_2$ radicals, kinetics of the reactions of the $CC1_3CH_2O_2$ radical with NO and NO_2, and the fate of the alkoxy radical $CC1_3CH_2O$"; J. Phys. Chem., 6570, 99, 1995.

19. Trine E. Møgelberg, Jesper Platz, Ole J. Nielsen, Jens Sehested, Timothy J.Wallington: "Atmospheric Chemistry of HFC-263fa: Spectrokinetic investigation of the $CF_3CHO_2(\bullet)CF_3$ radical, its reaction with NO and fate of the $CF_3CHO(\bullet)CF_3$ radical", J. Phys. Chem., 5373, 99,1995.

20. Edward Porter, Jesper Platz, Jack Treacy, Howard Sidebottom: "Reaction af OH radicals with Oxygen Containing Compounds"; To appear in proceedings of a joint Workshop LACTO/HALIPP, ECTUROTRAC/CDCH, Leipzig, Germany, september 1994.

21. Gorm V. Petersen, Jesper Platz, Claus Nielsen og Jesper Wengel: " Synthesis of Y-(N-Acetylpiperazino-2',3'-dideoxy-D-ribo-hexofuranosyI and -D-erythro-pentofuranosyl Thymine Nucleosides"; Jounal of Synthetic Organic Chemistry; 823, 8, 1994.

Presentations (Oral and Posters)

1. Jesper Platz, Jens Sehested, Ole J. Nielsen, Timothy J. Wallington, Jim C. Ball, Mike D. Hurley, Ann W. Straccia, William F. Scheider: "Atmospheric Chemisry of the phenoxy radical. UV spectrum and kinetics of the reaction with NO, NO_2 and O_2" (Poster); 15th International Symposium on Gas Kinetics, the University of the Basque Country (Bilbao), Spain, September 1998.

2. Jesper Platz, Jens Sehested, Ole J. Nielsen: "Atmospheric chemistry of cyclohexane, 1,4dioxane, 1,3,5-trioxane" (Poster); Annual Meeting of the Danish Chemical Society, Odense, Denmark, June 1997.
3. Jesper Platz, Trine E. Møgelberg, Ole J. Nielsen, Jens Sehested, Timothy J. Wallington, E. Kaiser: "Experimental study of CH_3OCH_3 in the gas phase" (Poster); NOSA/NORSAC symposium 1996, LO Højskolen, Denmark, 15-17 September 1996.

4. Jesper Platz, Trine E. Møgelberg, Ole J. Nielsen, Jens Sehested, Timothy J. Wallington: "Atmospheric Chemistry of 1,4-di- and 1,3,5-trioxane" (Oral); NOSA/NORSAC symposium 1996, LO Højskolen, Denmark, 15-17 September 1996.

5. Jens Sehested, Trine E. Møgelberg, Jesper Platz, Ole J. Nielsen, Helge Egsgaard, Timothy J. Wallington, Williarn E. Kaiser: "Dimethyl ether oxidation: Kinetics and mechanism of the $CH_3OCH_2 + O_2$ reaction" (Oral); 14th International Symposium on, Gas Kinetics, University of Leeds, Great Britain, September 1996.

6. Lene Krogh Kristensen, Merete Bilde, Trine E. Møgelberg, Jesper Platz, Jens Sehested, Timothy J. Wallington, Ole J. Nielsen: "Atmospheric chemistry of Acetic Anhydride" (Poster); 14th International Symposium- on, Gas Kinetics, University of Leeds, Great Britain, September 1996.

7. Jesper Platz, Jens Sehested, Knud Sehested, Helge Egsgaard, Ole J. Nielsen: "Reactions of Dimethylether at 296-666 K" (Poster); 14th International Symposium on Gas Kinetics, University of Leeds, Great Britain, September 1996.

8. Jesper Platz, Jens Sehested, Ole J. Nielsen: "Atmospheric chemistry of 1,4-dioxane" (Poster); Annual Meeting of the Danish Chemical Society, Odense, Denmark, June 1996.

9. Henrik Skov, Thomas Ellermann, Asger B. Hansen, Finn Palmgren, Torben Nielsen, Jesper Platz: "Automatic gas chromatography in atmospheric monitoring" (Oral); Workshop on Air Pollution Monitoring, Riso National Laboratory, Roskilde, Denmark, March 1996.

10. Torben Nielsen, Ole Hertel, Asger B. Hansen, Jesper Platz, Henrik Skov, Carsten S. Cristensen, Axel H. Egelov: "Chemical charecterization and modelling of ozone, other photochemical oxidants, precursors and atmospheric reaction products during a summer high pressure episode in Denmark (Poster); EUROTRAC, Garmisch-Partenkirchen, Gemany, March 1996.

11. Jesper Platz, Torben Nielsen: "PAN, PPN & PON *sampling, quantification and sources"* (Oral); Nordic Network Symposium on Experimental Atmospheric Chemistry, Karlslunde, Denmark, 17-19 November 1995.

12. Torben Nielsen, Jesper Platz, Kit Granby, Asger B. Hansen: "Day/night time variation of particulate organic nitrates" (Poster), 10th EUROTRAC-TOR Symposium, Agelonde, France, 17-19 October 1995.

13. Jesper Platz, Torben Nielsen: "ATMOSPHERIC ORGANIC NITRATES: Peroxyacetyl- and Particulate Organic Nitrates" (Oral); 6th Nordic Symposium on Organic Pollutants, Smygehus, Sweden, September 1995.

14. Merete Bilde, Jens Sehested, Trine E. Møgelberg, Ole J. Nielsen, Jesper Platz: "Surprising chemistry of halons" (Poster), Annual Meeting of the Danish Chemical Society, Odense, Denmark, June 1995.

15. Ole J. Nielsen, Trine E. Møgelberg, Jesper Platz, Jens Sehested, Timothy J. Wallington: "Atmospheric chemistry of HFC-236fa and HFC-272ca" (Poster); DCAR Annual Meeting, Eigtveds Pakhus, Copenhagen, Denmark, May 1995.

16. Ole J. Nielsen, Trine E. Møgelberg, Jesper Platz, Jens Sehested, Timothy J. Wallington: "Atmospheric chemistry of HFC-236fa and HFC-272ca" (Poster); Faraday Discussion on Atmospheric Chemistry, Norwich, England, 19-21 April 1995.

17. Jesper Platz, Jens Sehested, Ole J. Nielsen: "Atmospheric Chemistry Of $CC1_3CH_3$: Spectrokinetic investigation of the $CC1_3CH_2O_2$ radical, Its reaction with NO and NO_2 (Poster); Joint Workshop LACTOZ/11ALIPP, EC/EUROTRAC/CDCH, Leipzig, Germany, September 1994.

18. Jesper Platz, Jens Sehested, Ole J. Nielsen:"Atinospheric Chemistry Of $CC1_3CH_3$: Spectrokinetic investigation of he $CC1_3CH_2O_2$ radical, its reaction with NO and NO_2 (Poster); 13^{th} International Symposium on Gas Kinetics, University College Dublin, Ireland, September 1994.

19. Jesper Platz, Jens Sehested, Ole J. Nielsen: "The atmospheric degradation of 1,1,1-trichloroethane" (Oral); Nordic-Baltic meeting on Atmospheric Chemistry, Helsingør, Denmark, September 1994.

20. Jesper Platz, Jens Sehested, Ole J. Nielsen: "Atmosfærisk nedbrydning af 1,1,1-trichlorethan" (Poster); Odense University, Denmark, August 1994.

21. Jesper Platz, Jens Sehested, Ole J. Nielsen: “UV absorptions spectra and kinetics of the degradations products of Methylchloroform" (Poster); 3^{th} Danish Symposium in Analytical Chemistry, University of Copenhagen, Denmark, August 1994.

22. Jesper Platz, Jens Sehested, Ole J. Nielsen: "Atmospheric Chemistry of Methylchloroform" (Poster); Annual meeting of the Danish Chemical Society, Odense Universitet, Denmark, June 1994.

Bibliographic Data Sheet **Risø-R-1170(EN)**

Title and authors

Atmospheric Chemistry of Traffic Related Compounds
- Oxygenates and Aromatics -

Jesper Platz

ISBN	ISSN
87-550-2673-7 87-550-2674-5 (Internet)	0106-2840

Department or group	Date
Plant Biology and Biogeochemistry Department	January 2000

Groups own reg. number(s)	Project/contract No(s)

Pages	Tables	Illustrations	References
167	4	20	44

Abstract (max. 2000 characters)

The atmospheric chemistry of dimethylether, dimethoxymethane, trimethoxymethane, cyclohexane, 1,4-dioxane, 1,3,5-trioxane and phenol have been studied in this work.

The present thesis gives an extended summary of nine papers given in Appendix A to Appendix I. Sections 1 to 3 contains Abstract, Danish summery, and Motivation. Section 4 describes the pulse radiolysis technique used at Risoe National Laboratory and the FTIR Smog-chamber technique used at Ford Motor Company. Sections 5 to 8 present results of absolute rate constants and UV absorption spectra obtained at Risoe. Sections 9 to 12 present results of relative rate constants and atmospheric degradations studies performed at Ford. Section 13 gives a conclusion. Some of the sections are in the following further described.

Section 5 reports rate constants for reactions between OH radicals and $CH_3OCH_2OCH_3$, $(CH_3O)_3CH$, 1,4-dioxane, and 1,3,5-trioxane and they are measured to $(4.9 \pm 1.9) \times 10^{-12}$, $(6.0 \pm 0.4) \times 10^{-12}$, $(11.6 \pm 0.8) \times 10^{-12}$, $(6.0 \pm 1.0) \times 10^{-12}$ cm^3 $molecule^{-1}$ s^{-1}, respectively. The obtained rate constants are 210-348% higher than expected using the Structure-Reactivity Relationship model suggested by Atkinson

In section 6 UV absorption spectra of $(CH_3O)_2CHOCH_2(\bullet)$, $(CH_3O)_2CHOCH_2O_2(\bullet)$, c-$C_4H_7O_2(\bullet)$, (c-$C_4H_7O_2)O_2(\bullet)$, c-$C_3H_5O_3(\bullet)$, (c-$C_3H_5O_3)O_2(\bullet)$, c-$C_6H_{11}(\bullet)$, and c-$C_6H_{11}O_2(\bullet)$ radicals were recorded between (220-230) and (290-320) nm. They all show broad features with a typical maximum absorption cross section of approximately 6×10^{-18} cm^2 $molecule^{-1}$. UV absorption spectra of $C_6H_5(\bullet)$ and $C_6H_5O(\bullet)$ radicals were obtained between 220 - 575 nm and 220 - 400 nm, respectively. They both show a maximum absorption cross section of approximately 4×10^{-17} cm^2 $molecule^{-1}$ at approximately 245 nm.

In section 7 self-reactions and reactions with O_2 for $CH_3OCH_2(\bullet)$, $(CH_3O)_2CHOCH_2(\bullet)$, c-$C_4H_7O_2(\bullet)$, c-$C_3H_5O_3(\bullet)$, and c-$C_6H_{11}(\bullet)$ radicals were studied. Rate constants for the self-reactions are of the order of 3-4 $\times 10^{-11}$ cm^3 $molecule^{-1}$ s^{-1}. This is approximately a factor of 4 higher than rate constants for reactions between the alkyl radicals and O_2. The reaction between $C_6H_5O(\bullet)$ radicals and O_2 is slow with an upper limit of 5×10^{-21} cm^3 $molecule^{-1}$ s^{-1}. Reaction between the $C_6H_5(\bullet)$ radical and NO show a rate constant of 2×10^{-11} cm^3 $molecule^{-1}$ s^{-1} where as reactions $C_6H_5O(\bullet)$ radicals and NO or NO_2 show rate constants of 2×10^{-11} and 2×10^{-12} cm^3 $molecule^{-1}$ s^{-1}, respectively.

In section 8 self-reactions of $(CH_3O)_2CHOCH_2O_2(\bullet)$, (c-$C_4H_7O_2)O_2(\bullet)$, and (c-$C_3H_5O_3)O_2(\bullet)$ radicals give rate constants which are a factor of 3 lower than self-reactions obtained for the corresponding alkyl radicals. Rate constants for the reactions between these alkyl peroxy radicals and NO or NO_2, together with the reactions between the c-$C_6H_{11}O_2(\bullet)$ radical and NO or NO_2 were reported. In all cases rate constants for

NO_2 reactions are higher than the corresponding rate constants for NO reactions. Obtained rate constants were from $(9.5 \pm 1.5) \times 10^{-12}$ to $(1.3 \pm 0.3) \times 10^{-11}$ cm^3 $molecule^{-1}$ s^{-1}.

In section 9 a large number of relative rate constants with relation to experiments in the smog-chamber were reported.

In section 10 the atmospheric degradations of $CH_3OCH_2OCH_3$, $(CH_3O)_3CH$, c-C_6H_{12}, 1,4-dioxane, and 1,3,5-trioxane were studied. $CH_3OCH_2OCH_3$ give two major products, CH_3OCH_2OCHO and $CH_3OC(O)OCH_3$, arising from abstraction of H atoms placed at the primary and secondary carbon, respectively. $CH_3OC(O)OCH_3$ is the only product observed from $(CH_3O)_3CH$. The studies of 1,4-dioxane and 1,3,5-trioxane give only one product each $HC(O)OCH_2CH_2OCHO$ and $HC(O)OCH_2OCHO$, respectively.

Section 11 reports the atmospheric degradation of cyclohexane. The fate is competition between decomposition of the sixmembered ring and formation of cyclohexanone. The formation of cyclohexanone is a function of the O_2 concentration. At 1 atmosphere of air the yield of cyclohexanone is $39 \pm 3.9\%$ whereas $61 \pm 6.1\%$ of the oxidised cyclohexane decompose.

In section 12 the atmospheric fate of $C_6H_5O(\bullet)$ radical is reaction with NO or NO_2. The major product from the smog-chamber experiments is a $(C_6H_5O)_2$ compound. Using smog-chamber experiments, GC-MS, and quantum mechanical calculations of the structure of $(C_6H_5O)_2$ give that the formed $(C_6H_5O)_2$ is determined to be 4-phenoxyphenol.

Descriptors INIS/EDB

AIR POLLUTION; ALKOXY RADICALS; ALKYL RADICALS; ATMOSPHERIC CHEMISTRY; CHEMICAL REACTION KINETICS; CHEMICAL REACTION YIELD; CYCLOHEXANE; DECOMPOSITION; DIOXANE; FUEL ADDITIVES; FUEL SUBSTITUTION; HYDROXYL RADICALS; METHYL ETHER; METHYLAL; NITRIC OXIDE; NITROGEN DIOXIDE; OXYGEN; PEROXY RADICALS; PHENOL; PHENOXY RADICALS; PHENYL RADICALS; TRIOXANES; ULTRAVIOLET SPECTRA; VEHICLES

Available on request from Information Service Department, Risø National Laboratory,
(Afdelingen for Informationsservice, Forskningscenter Risø), P.O.Box 49, DK-4000 Roskilde, Denmark.
Telephone +45 4677 4004, Telefax +45 4677 4013